The Pennsylvania State University

The Graduate School

Civil and Environmental Engineering

The Comparison of Two Acid Mine Drainage Sites in Central Pennsylvania: Field Site Characterizations and Batch Reactor Experiments

A Thesis in

Environmental Engineering

by

Melanie Anne Lucas

Submitted in Partial Fulfillment
of the Requirements
for the Degree of

Master of Science

May 2008

The thesis of Melanie Anne Lucas was reviewed and approved* by the following:

William D. Burgos
Associate Professor of Environmental Engineering
Thesis Advisor

John M. Regan
Assistant Professor of Environmental Engineering

Peter J. Heaney
Professor of Geosciences

Peggy Johnson
Professor of Civil Engineering
Head of the Department of Civil and Environmental Engineering

*Signatures are on file in the Graduate School

ABSTRACT

Biological oxidation of iron(II) in acid mine drainage (AMD) and the subsequent precipitation of iron(III) occurs unaided at Gum Boot Mine in McKean County, Pennsylvania but it is not observed at a large number of AMD sites across the state. To improve passive AMD treatment methods through a better understanding of biological iron(II) oxidation, the Pennsylvania Department of Environmental Protection (PA DEP) selected this and a similar AMD site (Fridays-2 Mine in Clearfield County, PA) for chemical, microbial, and kinetic characterization of the observed abiotic and biological oxidation processes.

Sampling transects were established to identify any spatial trends over the iron mounds at each mine. Water chemistry measurements were conducted on mine drainage waters during several sampling events at each mine site. Solids were collected for subsequent SEM and molecular analyses. Iron sediments collected from the sampling locations of highest and lowest activities of iron(II) oxidation (Gum Boot "fastest", Fridays-2 "slowest", and Fridays-2 "fastest") were incubated in batch reactors under different gas mix compositions of O_2, CO_2, and N_2. The batch reactor results were then used to calculate the abiotic and biological iron(II) oxidation rates of the sediments to determine if field trends were observed in controlled laboratory conditions. These results were also used to examine the effects of pO_2 and pCO_2 on iron(II) oxidation rates. Lastly, the results of the batch reactor experiments were used to model the iron(II) oxidation kinetics of the sediments with *STELLA* computer program and the combined model for abiotic and biological iron(II) oxidation proposed by Kirby et al. (1999).

Water chemistry results indicate similarities between the emergent AMD at Gum Boot and Fridays-2 Mines, with no observed seasonal trends in iron(II) concentrations, pH, temperature, and DO at either mine site. Iron(II) was quickly removed in the first 10 meters of flow over the iron mound at Gum Boot Mine; however, most iron(II) was still present in solution at Fridays-2 Mine immediately before the AMD mixed with Fridays Run. Given the distance of AMD flow and measured rates of AMD emergence, the residence time over the iron mound at Fridays-2 Mine was much shorter than the residence time at Gum Boot. No nutrient limitations were observed at either Gum Boot or Fridays-2 Mine.

Microbial characterization of the mine sites included SEM images of sediments, population counts of iron(II) oxidizing bacteria (IOB), and phylogenetic analyses of IOB communities, in addition to batch reactor experiments with glucose additions to examine the contribution of heterotrophic vs. autotrophic IOB at Gum Boot and Fridays-2 Mines. SEM images and phylogenetic analysis reveal greater morphological and genetic diversity in sediments collected from Gum Boot AMD emergence than from Fridays-2 AMD emergence. Additionally, sediments at each mine site from the sampling locations with the largest numbers of IOB and the largest rates of iron(II) oxidation had the greatest phylum-level similarities. Lastly, though batch reactor experiments with glucose additions did not show any change in observed iron(II) oxidation rates, phylogenetic analyses indicated heterotrophs were the dominant IOB present at the sampling locations with the highest levels of iron(II) oxidation activity.

Batch reactor iron(II) oxidation rates were observed to increase with O_2 concentrations of 21%. However, IOB numbers increased during each batch reactor experiment, with the largest increases observed at O_2 concentrations > 10%. There were no noticeable effects of CO_2 concentration on abiotic or biological iron(II) oxidation rates. Fridays-2 reactors generally had higher abiotic rates of iron(II) oxidation and were capable of achieving biological iron(II) oxidation rates that equaled or exceeded the rates observed in the Gum Boot reactors.

The Kirby et al. (1999) iron(II) oxidation model was successfully modified in *STELLA* for application to the batch reactor results of this study. Observed iron(II) oxidation rates were less than the rates predicted by the default *STELLA* model as well as rates published by other previous studies. Additionally, the pO_2 of the gas mix did affect the model performance and fit to the batch reactor data. Lastly, the biological rate constant, k_{bio}, for iron(II) oxidation may be dependent on the bacterial communities composition and certain environmental factors of an AMD site.

The results of this study indicate that both Gum Boot and Fridays-2 Mines are equally capable of efficient oxidative precipitation of iron(II) from acid mine drainage. Biological iron(II) oxidation was observed at both mine sites and with both batch reactor sediments. However, the shorter residence time at Fridays-2 Mine did not allow enough time for the hydrolysis and precipitation of iron(III) before the AMD mixed with Fridays Run. In conclusion, future remediation strategies at Fridays-2 Mine should focus on increasing the AMD residence time to encourage optimal conditions for biological iron(II) oxidation promote iron(III) precipitation.

TABLE OF CONTENTS

LIST OF FIGURES

LIST OF TABLES

ACKNOWLEDGEMENTS

I would like to thank my master's committee members for their patience and guidance through my education. Special thanks are given to Dr. Carl Kirby for supplying the *STELLA* program code and assisting with the batch reactor model development. Additionally, I would like to thank John Senko, Gengxin Zhang, Tetyana Peretyazhko, Mary Ann Bruns, Pauline Wanjugi, Jon Smoyer, and Brent Means for their contributions to this study. Lastly, I would like to thank my family and my loving husband, Bill, for their endless belief in and support of my life and goals.

1 INTRODUCTION

The United States (US) has long relied upon coal mining to supply fuel for homes and industrial applications. Today, the largest coal producers in the US are Wyoming, West Virginia, Kentucky, and Pennsylvania (PA DEP, 2003). Unfortunately, these states are also the most impacted by acid mine drainage (AMD) that forms in both operating and abandoned mines and drains to nearby streams and watersheds.

Anthracite and bituminous coal mining has detrimentally affected lands and surface waters in Pennsylvania. The Pennsylvania Department of Environmental Protection estimates that at least 2,400 miles of streams in the state are impacted by AMD. Additionally, the largest amount of abandoned mine lands in the country are found in Pennsylvania, with over 250,000 acres in 45 of the 67 counties (Rossman et al., 1997).

AMD is created when metal sulfides (primarily iron sulfide), often found alongside rich coal seams, react with water to produce sulfuric acid and dissolved ferrous iron. Through this process, other trace metals such as aluminum and manganese are also dissolved and transported to surface waters. Upon mixing with more neutral aerated surface waters, the metals quickly oxidize and precipitate out of solution; the precipitation of ferric (oxyhydr)oxides produces additional acidity that further lowers the pH of the system. The precipitation of ferric (oxyhydr)oxides also coats stream bottoms and significantly harms the benthic community.

Common AMD treatment methods involve chemical or biological remediation strategies to remove the metals (specifically iron, aluminum, and manganese) and raise the pH to between 6 and 9 prior to mixing with surface waters. For chemical treatment, the AMD typically is mixed with or flows through limestone beds to dissolve the limestone and add alkalinity to the water. However, because iron oxidizes and precipitates quickly in the presence of oxygen, the limestone is quickly coated with metal precipitates that limit its neutralizing capacity and effectiveness.

Biological treatment utilizes bacteria that obtain energy for growth from the oxidation of iron(II) to iron(III). Aerobic and anaerobic wetlands and other biological systems attempt create optimal biogeochemical conditions for the oxidation and precipitation of iron from the AMD before it passes through limestone beds or channels. This spatial separation of metals removal and alkalinity addition has the potential to greatly reduce AMD treatment maintenance and costs.

One mine that heavily impacts the receiving watershed with AMD is Gum Boot Mine in McKean County, Pennsylvania (Figure **1-1**). Gum Boot Mine, first opened in 1879 as part of the Buffalo Coal Company, was mined for several decades (Planet Smethport, 2008) with the coal being mined likely from the Brookville or Clarion coal seams (Figure **1-2**). Early mining methods usually involved digging the mine up-dip, allowing for the natural drainage of water that had flowed through the overburden material above the mine. It is unknown exactly when Gum Boot Mine was abandoned and left unreclaimed; however, the mine has at least 10 drainage sites that have been feeding metal-rich AMD to Gum Boot Run for decades.

Figure **1-1**: Location of experimental field sites Gum Boot Mine, located in McKean County (41.652 °N, 78.526 °W), and Fridays-2 Mine (41.244 °N, 78.535 °W), located in Clearfield County. Coal from Gum Boot was mined from the Brookville or Clarion seams, and mine drainage flow enters the East Branch Clarion River watershed. Fridays-2 coal was mined from the Lower Kittanning seam and drainage enters the Bennett Branch watershed.

Draining to Gum Boot Run and on to the East Branch Clarion River, AMD site GB5 (Figure **1-3**) experiences a loss of approximately 23 mg/L of iron(II) over 127 m of flow with most of the loss within the first 15 m. The AMD emerges at the top of a kill zone and flows in sheets over hardened iron sediments; about 18 m from emergence the flow disappears belowground and reemerges another 30 m downhill (Figure **1-4**). The rapid loss of iron at low-pH at this site suggests the possibility of biological iron(II) oxidation and subsequent precipitation of iron(III) hydroxides. If true, this AMD site could serve as a model for the enhancement of similar sites for biological iron(II) oxidation and the spatial separation of iron removal (via oxidative precipitation) from alkalinity addition (via conveyance through limestone) for cost-effective AMD treatment.

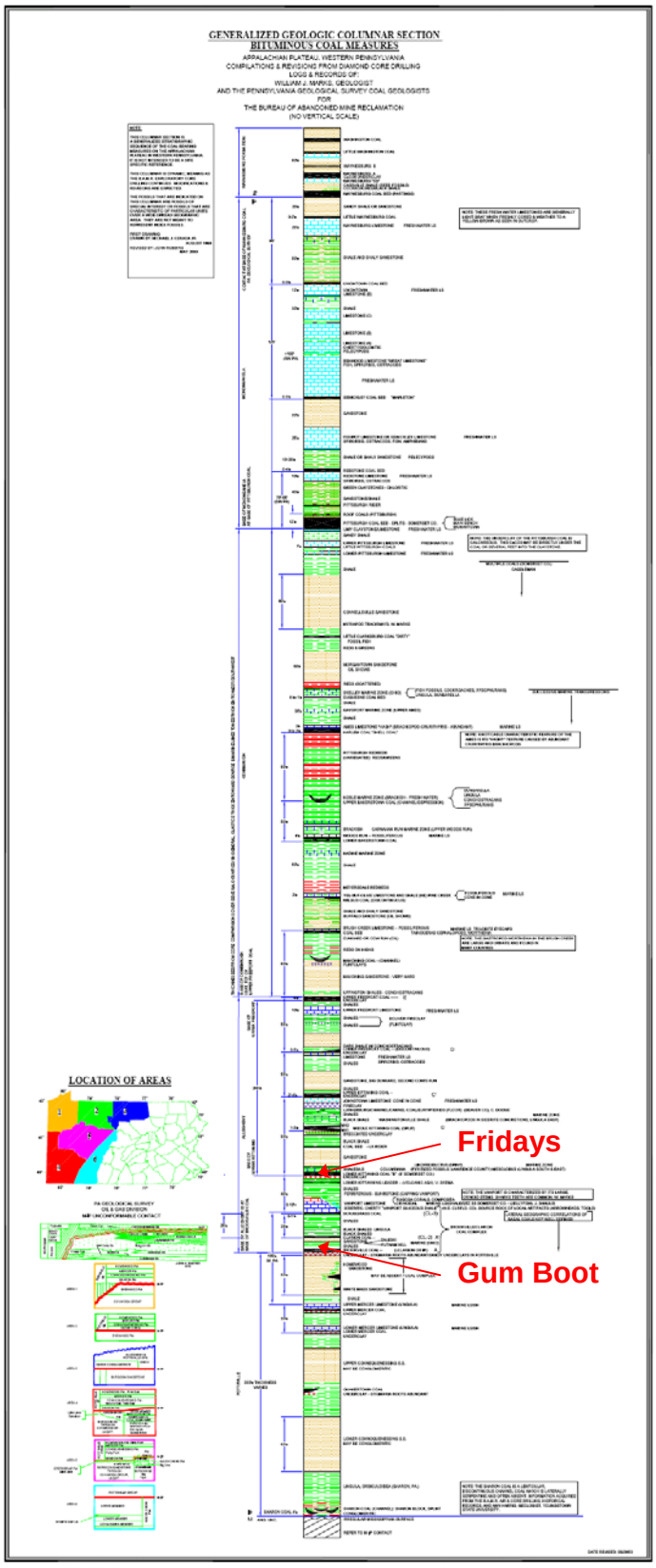

Figure **1-2**: Generalized geologic stratigraphy for bituminous coal fields in western Pennsylvania. Coal seams mined at Gum Boot and Fridays-2 sites are labeled accordingly.

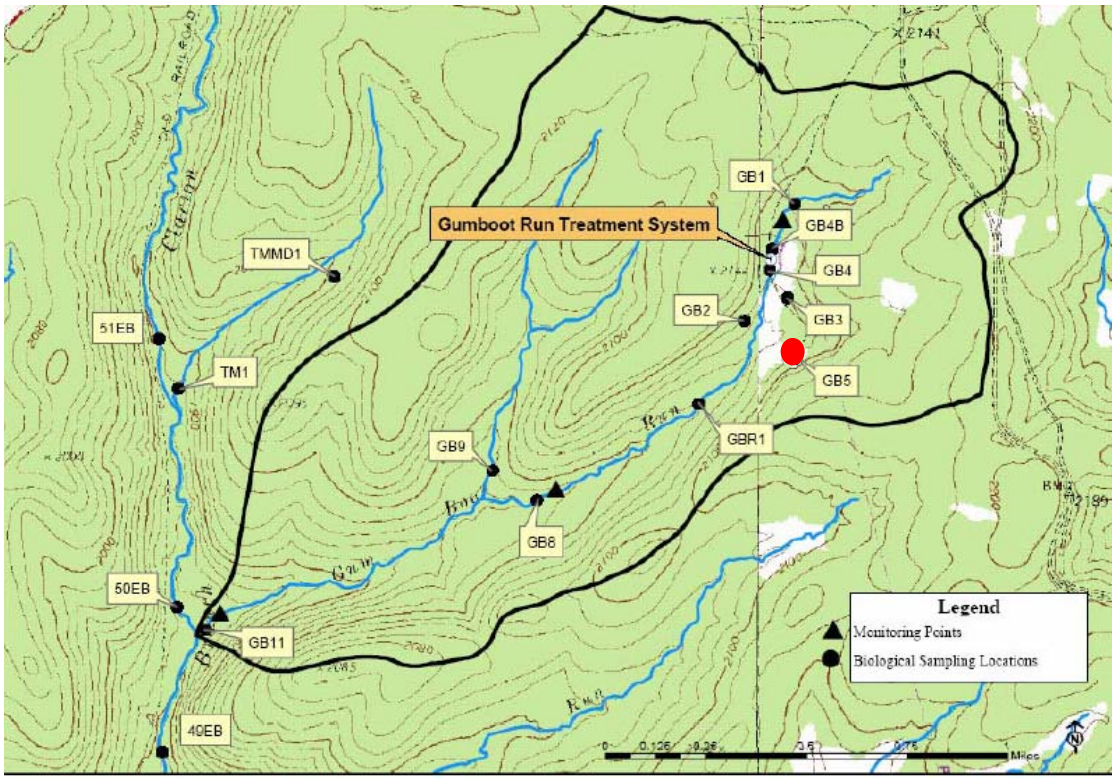

Figure **1-3**: Map of the Gum Boot Run Watershed in McKean County, Pennsylvania (PA DEP 2005). The acid mine drainage at site #5 (GB5) experiences naturally occurring biological iron(II) oxidation prior to mixing with Gum Boot Run. GB5 is designated by a red circle.

To characterize the iron(II) oxidation occurring at Gum Boot Mine, another mine similar in geology and water chemistry was selected for comparison: Fridays Mine in Clearfield County, Pennsylvania (see Figure 1-1). Coal mining began in the middle to late 1800's from the Kittanning coal seam (PA DEP, 2006) and has overburden similar to Gum Boot Mine (see Figure 1-2). The two AMD sites at Fridays Mine (FRI1 and FRI2) drain to Fridays Run, then Tyler Run, and on into the Bennett Branch watershed (Figure **1-5**) (PADEP, 2006).

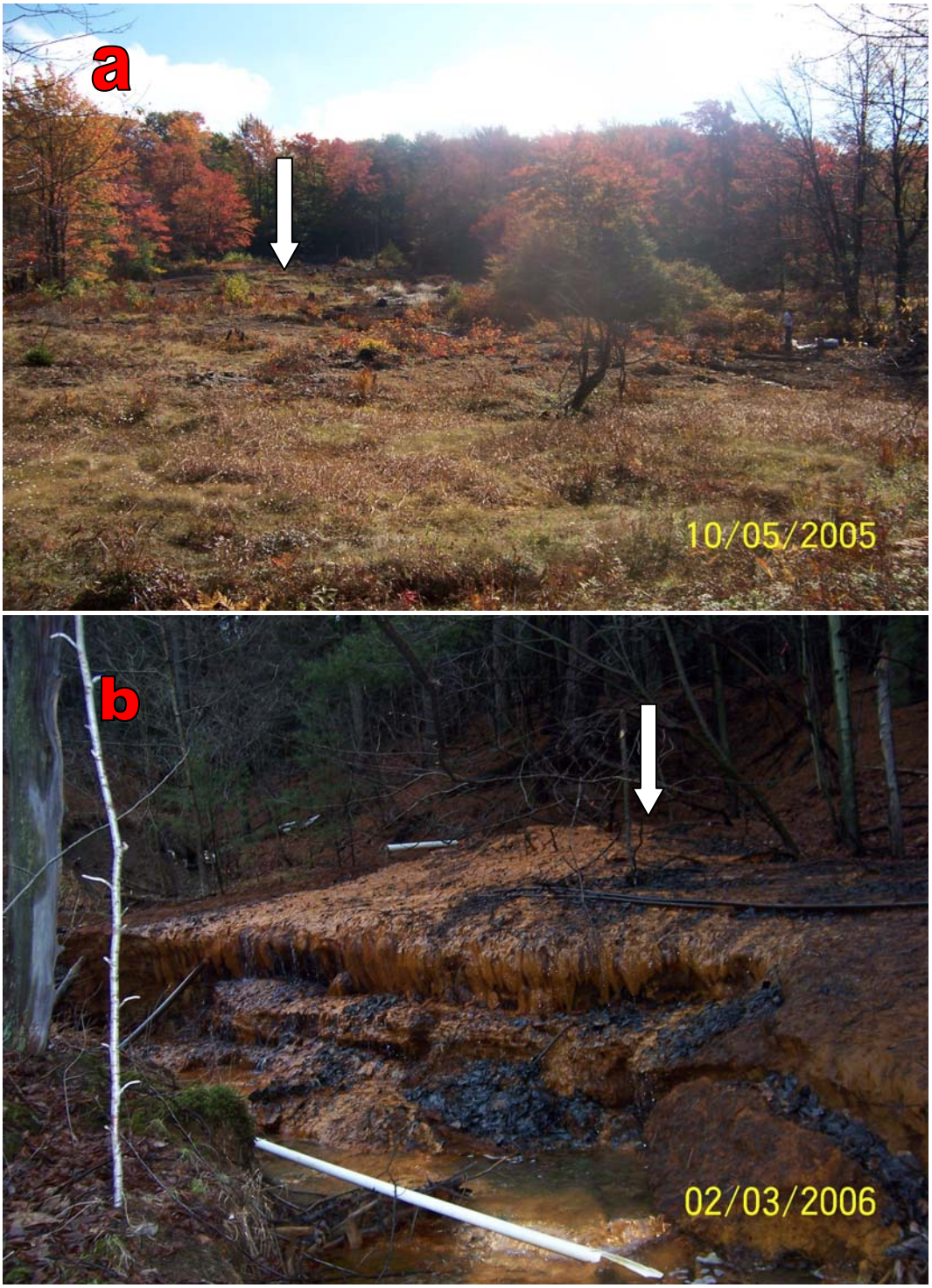

Figure **1-4**: Pictures of field sites a) Gum Boot Mine and b) Fridays-2 Mine. The mine drainage at Gum Boot travels downhill from the upper left to the lower right before mixing with a creek. The mine drainage at Fridays-2 travels over the iron mound and mixes with the creek in the foreground. White arrows indicate points of mine drainage emergence.

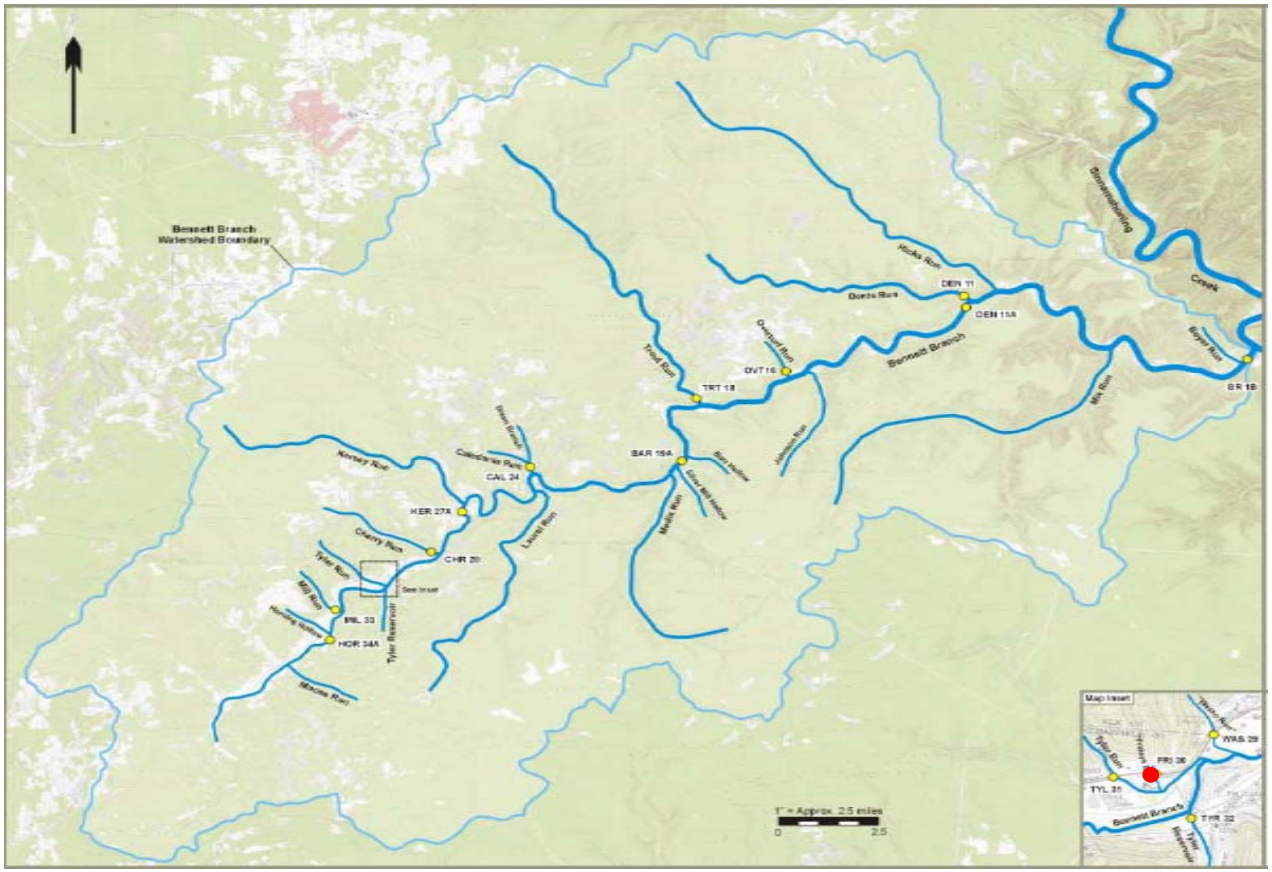

Figure **1-5**: Map of the Bennett Branch watershed in Clearfield County, Pennsylvania (Growing Greener, 2003). The red circle represents the Fridays Mine drainage locations. The light blue line indicates watershed borders.

Fridays-2 site (FRI2) was chosen by the PA DEP for this study because its flow characteristics were initially thought to be similar to those at Gum Boot Mine. AMD emerges at the top of a hill and flows in sheets over hardened iron sediments (see Figure 1-4). However, this site has little iron(II) removal before the AMD mixes with the creek, losing about 10 mg/L or less of iron(II) in 10 m of flow from emergence. While Gum Boot is surrounded by deciduous trees and Fridays-2 AMD sites are surrounded by deciduous and coniferous trees, the Fridays site gets less sunlight during the day due to shading.

The purpose of this study was to compare two similar AMD sites in order to identify what conditions favor biological iron(II) oxidation at the Gum Boot Run drainage site GB5. Both sites were analyzed with respect to site characteristics and water chemistry. Sediments collected from each mine site were returned to the laboratory for incubation in batch reactor experiments to evaluate the iron(II) oxidation kinetics. Incubation experiments were conducted in the dark while reactors were continuously stirred and flushed with one of several pre-selected gas mixes of oxygen, carbon dioxide, and nitrogen. Reactors were sampled at least once daily for iron(II), pH, and other measurements to determine the rates of abiotic and biological iron(II) oxidation of each mine site. The results from the batch reactors were then modeled to determine the iron(II) oxidation kinetics of each AMD site and compare the rate constants from this study with published rate constants for abiotic and biological iron(II) oxidation.

Current treatment methods for AMD could be greatly improved by incorporating biological iron(II) oxidation in the removal of iron prior to alkalinity additions to raise

system pH. This spatial separation could reduce or eliminate the armoring effect of iron hydroxide precipitates on limestone treatment beds. Additionally, maintenance and design costs could decrease significantly since biological oxidation would utilize existing landscape and reduce the amount of labor and materials needed to maintain the neutralizing capacity of limestone treatment methods. If this study can determine what factors affect the rate of oxidation at Gumboot Mine, other AMD sites and treatment systems could be adapted for similar site conditions to encourage natural biological iron(II) oxidation.

2 OBJECTIVES

Acid mine drainage (AMD) is an enormous problem for surface water quality in the Appalachian region of the eastern United States. Numerous treatment methods have focused on the neutralization of AMD with limestone through combined iron(II) oxidation and alkalinity additions to raise the pH and promote precipitation of iron(III) and other trace metals. However, iron(III) precipitates can quickly coat treatment system surfaces, "armoring" the limestone against further dissolution and neutralizing capacity. If biological oxidation could be used to remove iron from AMD prior to alkalinity additions, current treatment methods could be greatly improved through increased efficiency and reduced maintenance costs.

This study attempted to characterize both Gum Boot and Fridays-2 Mine sites in order to address the following list of objectives:

1. The first objective was to determine if biological iron(II) oxidation was actively occurring at either Gum Boot or Fridays-2 Mines.
2. The second objective was to evaluate the mine water chemistry and site characteristics to determine if environmental conditions were responsible for the slower rates of iron(II) removal at the Fridays-2 AMD system.
3. The third objective was to measure the biological iron(II) oxidation rates for sediments collected from each mine site. The results of experiments conducted under various concentrations of O_2 and CO_2 were used to evaluate the effects of

O_2 and CO_2 on biological iron(II) oxidation as well as determine the potential rates of iron removal at both Gum Boot and Fridays-2 Mines.

4. The fourth objective was to model the kinetics of low-pH iron(II) oxidation in the laboratory-scale batch reaction experiments.

In addition, as part of a larger collaborative project examining Gum Boot and Fridays-2 Mines, the iron(II) oxidizing bacterial communities at both mines were examined for differences in community composition and species dominance.

3 LITERATURE REVIEW

3.1 The History of Coal Mining

Coal mining in the United States (US) began in the Appalachian Mountain basin in the mid 1700's primarily to support the Colonial iron industry. However, mining later served to provide fuel for the Industrial Revolution as well as both World Wars (PA DEP, 2003). The expansive distribution of coalfields throughout the eastern US helped the mining industry develop quickly and successfully as mining company-owned towns sprung up anywhere coal seams could be accessed (Figure **3-1**). By 1900, approximately 30 million tons of coal were mined annually in four mountain states (Zinc et al., 2005).

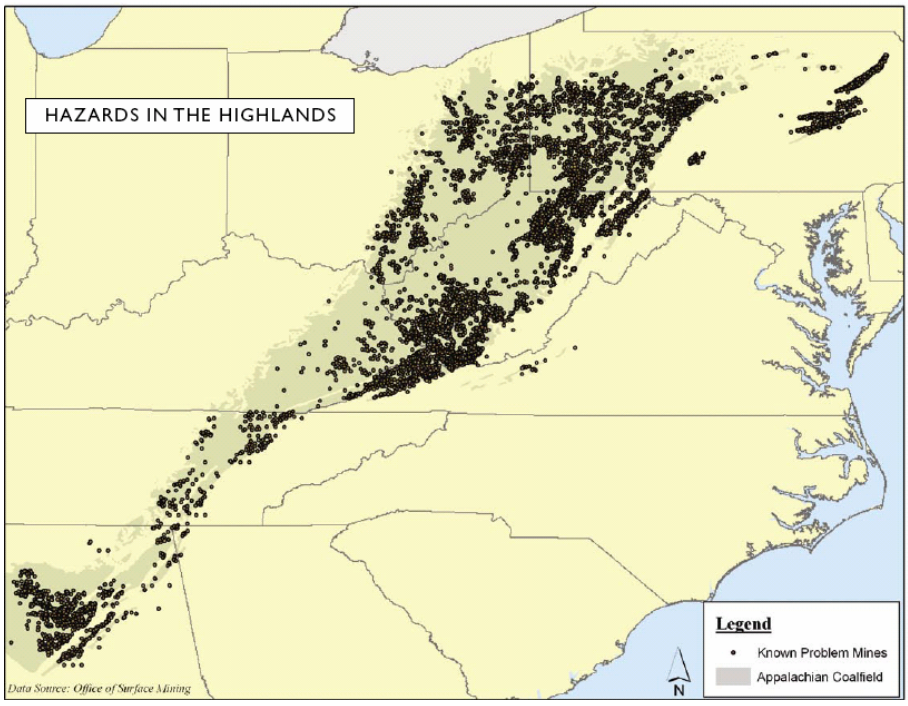

Figure **3-1**: Location of Appalachian coalfields and mines known to have acid mine drainage problems (Zinc et al., 2005).

The Appalachian coalfields are dominated by the softer bituminous coal that spans across eight states: Alabama, Kentucky, Maryland, Ohio, Pennsylvania, Tennessee, Virginia, and West Virginia (Figure **3-2**). Generally, harder anthracite coal is only found in small pockets in northeastern Pennsylvania (Figure **3-3**). Analysis of drainage from 140 abandoned mines in Pennsylvania resulted in a pH range of 2.7 – 7.3, with higher iron, acidity, hardness, and sulfate in AMD from bituminous coal mines than from anthracite coal mines (Cravotta, 2008a; Cravotta, 2008b). By 1900, Pennsylvania was a US leader in coal production and, in 1917, a US single-state coal production record of 217 million tons of coal was mined from Pennsylvania (Taylor et al., 2003). In 1995, 8.7 million tons of anthracite and 60.8 million tons of bituminous were mined in Pennsylvania alone. Additionally, coal mining supplies 60 percent of the fuel for electric power generation in Pennsylvania (PA DEP, 2003).

The two main types of mining techniques are surface mining and underground mining; which technique will be employed is usually determined by technology and location of the coal seams. Surface mining involves removing the top layers of vegetation and soil to expose the coal seams before blasting to loosen the rocks; common methods include 1) contour strip mining, 2) area strip mining, 3) open-pit mining, and 4) auger core mining (Encyclopaedia Britannica, 2007). Underground mining involves using tunnels and roadways to access and extract deeper coal seams. Typical underground mining techniques include 1) room-and-pillar, 2) longwall, 3) shortwall, and 4) thick-seam (Encyclopaedia Britannica, 2007). With early mining methods, typically gravity was used instead of pumping to remove collected water from the tunnels of deep mines; this gravity draining was referred to as digging the mine “up-dip” (J. Smoyer, personal communication).

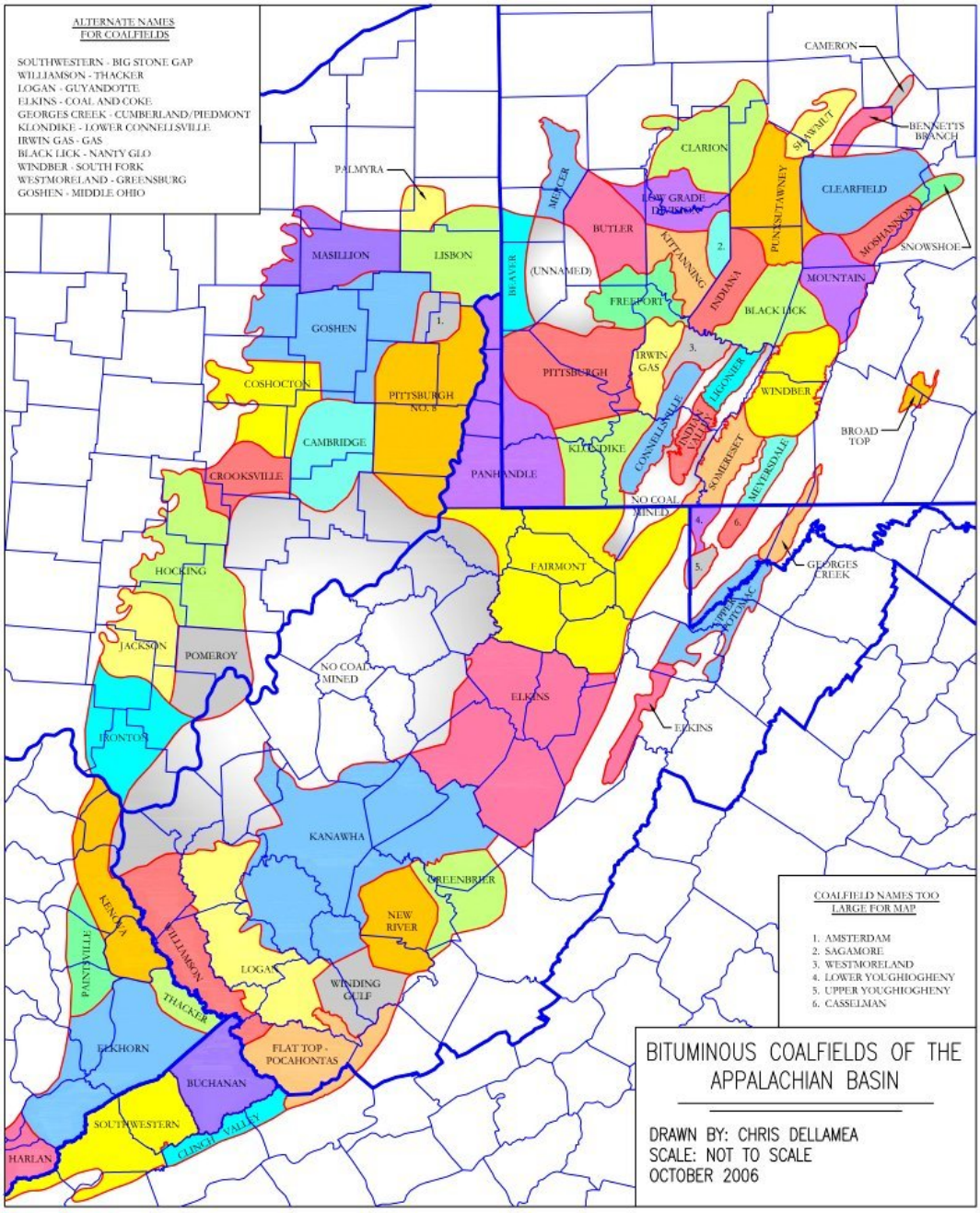

Figure **3-2**: Identification and location of the bituminous coalfields of the Appalachian Basin. (Dellamea, 2006).

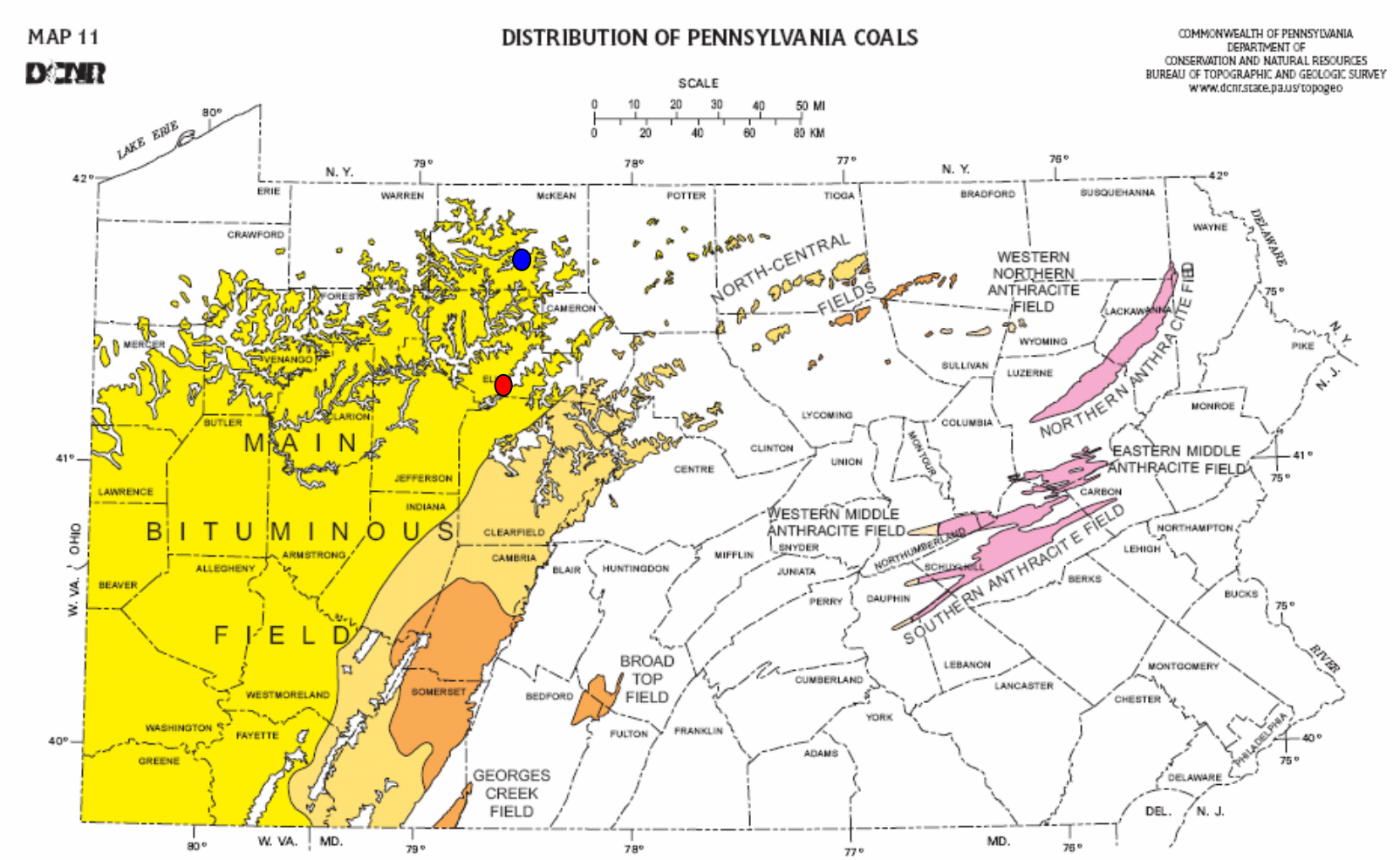

Figure **3-3**: Bituminous and anthracite coal fields of Pennsylvania (DCNR, 1992). Shades of yellow and orange represent types of bituminous coal while pink regions designate anthracite coal fields. The approximate locations of Gum Boot and Fridays-2 Mines are marked by the blue and red circles, respectively.

With the onset of WWI, the coal mining industry boomed as a result of the need for fuel throughout Europe (Zinc et al., 2005). Following the war and especially during the Great Depression of 1929, demands decreased and prices of coal dropped. Coal mining picked up again during WWII but declined after the war as Europe began to meet its own coal needs (Zinc et al., 2005).

Over a century of coal mining has left the US scarred and impacted by the abandoned mines and mine lands. Herlihy et al. (1990) reported that over 6,200 m of streams within the Appalachian region are impacted by drainage from abandoned mines and mine lands. According to the Pennsylvania Department of Environmental Protection, at least 2,400 miles of streams are impacted by AMD in this state alone (Rossman et al., 1997). For at least decades to come, the nation will continue to work towards the abatement of AMD and the restoration of streams and watersheds to their pristine conditions.

3.2 Generation of Acid Mine Drainage

Acid mine drainage (AMD) is formed when iron sulfide minerals (e.g., pyrite) are exposed to oxygen and water, which frequently occurs in non-flooded abandoned deep mines. This process produces acidity which can leach other major and trace metals from the surrounding minerals. AMD then exits the mine and drains to nearby surface waters. The following sections will examine the biogeochemistry of these steps in more detail.

3.2.1 Pyrite Oxidation

The generation of AMD begins with the exposure of pyrite, FeS_2, to oxygen and water draining through coal mines and their overburden. Upon contact with oxygen, sulfide in the pyrite is oxidized to sulfate following Eq. **3.1** (Singer and Stumm, 1970), leading to the subsequent destruction of the mineral. Pyrite can also be oxidized by iron(III) (Eq. **3.2**), generating large amounts of acidity (Sung and Morgan, 1980; Wiersma and Rimstidt, 1984; Rimstidt, 2004). Wiersma and Rimstidt (1984) also demonstrated that this form of pyrite oxidation is very rapid and oxidation rates increase with increasing temperatures, with measured first-order rate constants of 1.0×10^{-4} to 2.7×10^{-4} 1/s.

$$FeS_2\,(s) + 3.5\,O_2\,(aq) + H_2O \rightarrow Fe^{2+} + 2SO_4^{2-} + 2H^+ \qquad \textbf{3.1}$$

$$FeS_2\,(s) + 14\,Fe^{3+} + 8H_2O \rightarrow 15Fe^{2+} + 2SO_4^{2-} + 16H^+ \qquad \textbf{3.2}$$

At pH values above 4, pyrite oxidation occurs through reactions with both iron(III) and dissolved oxygen (DO); however, the effect of DO has been shown to increase as pH values approach neutral (Williamson and Rimstidt, 1994). Since iron(III) solubility increases with decreasing pH, the rate of pyrite oxidation is dominated by reaction with iron(III) at pH values below 4 (Figure **3-4**). Once pyrite has been exposed to oxygen, autocatalytic pyrite oxidation by iron(III) will proceed indefinitely (Rimstidt, 2004).

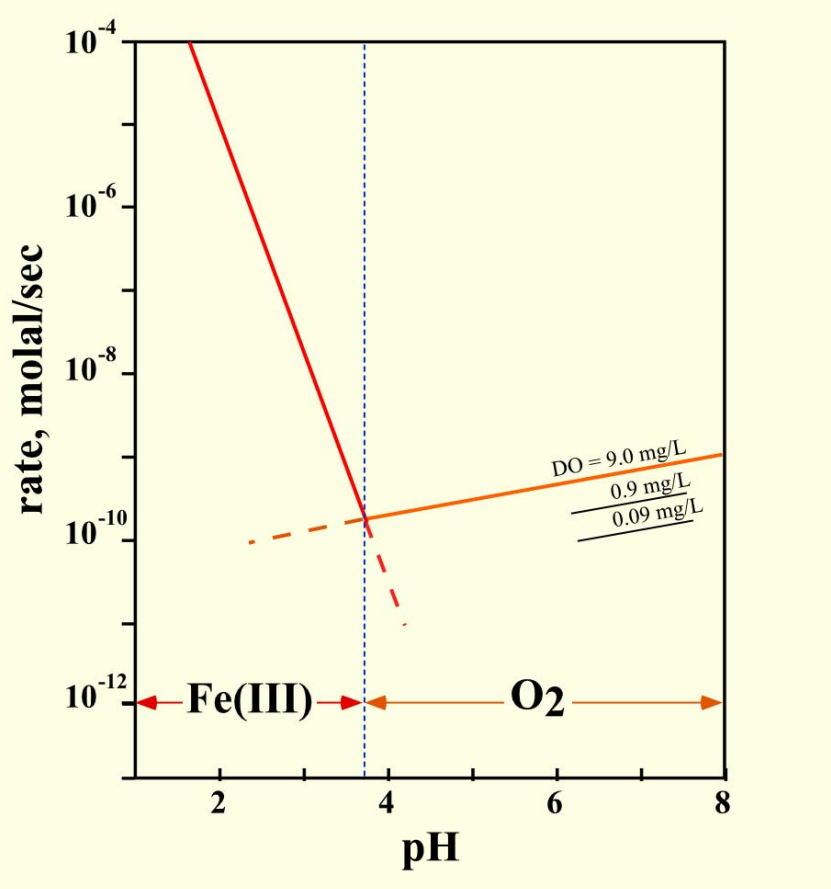

Figure **3-4**: Rates of pyrite oxidation by iron(III) and dissolved oxygen (DO). At pH values above about 4.0, pyrite oxidation is dominated by reaction with oxygen. As pH decreases below 4.0, iron(III) becomes increasingly soluble and pyrite oxidation occurs primarily through reaction with iron(III) (Rimstidt, 2004).

3.2.2 Abiotic Iron(II) Oxidation

Following pyrite oxidation, aqueous iron(II) can be rapidly oxidized to iron(III) in the presence of oxygen (Eq. **3.3**). Singer and Stumm (1970) demonstrated that at pH values below about 3.5, the abiotic rate of iron(II) oxidation is relatively constant and independent of pH. However, as pH values increase above 3.5, the abiotic rate of iron(II) oxidation quickly increases and becomes pH dependent. Once oxidized, iron(III) quickly hydrolyzes to

produce iron(III) hydroxides (Eq. **3.4**) and additional acidity. These iron(III) hydroxides are very insoluble at higher pH values and precipitate almost immediately upon mixing with more-neutral surface waters. Unfortunately, given the typical pH (2.7-4.0) and DO (< 2 mg/L) of Pennsylvania coal mine drainage (Cravotta, 2008a; Cravotta, 2008b), little to no abiotic iron(II) oxidation occurs before the AMD mixes with surface waters.

$$Fe^{2+} + 0.25\ O_2\ (aq) + H^+ \rightarrow Fe^{3+} + 0.5\ H_2O \qquad \textbf{3.3}$$

$$Fe^{3+} + 3H_2O \rightarrow Fe(OH)_3\ (s) + 3H^+ \qquad \textbf{3.4}$$

3.2.2.1 Homogeneous Iron(II) Oxidation

Homogeneous iron(II) oxidation involves the oxidation of dissolved iron(II) species such as Fe^{2+}, $FeOH^+$, or $Fe(OH)_2$ (Stumm and Morgan, 1996). At pH values below ~4, the rate of homogeneous oxidation is independent of pH because the concentration of Fe^{2+} dominates (Figure **3-5**); at pH greater than ~5, $Fe(OH)_2$ is far more easily oxidized than the other two species and thus determines the oxidation rate (Morgan and Lahav, 2007). For solutions between pH 5 and 8, the concentration of $Fe(OH)_2$ increases quickly as does the rate of oxidation. Above pH of ~8, iron(II) species concentrations no longer vary with pH so the iron(II) oxidation rate is pH independent (Morgan and Lahav, 2007).

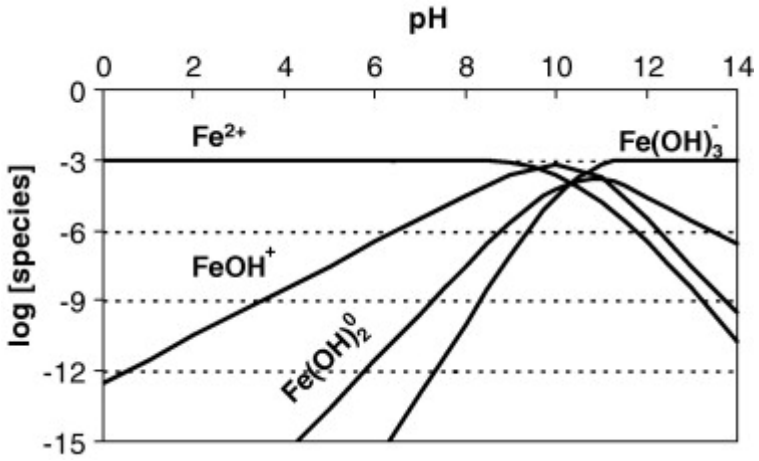

Figure **3-5**: Log species-pH diagram of soluble ferrous hydroxide species at infinite dilution (Morgan and Lahav, 2007).

A first order rate law for homogeneous iron(II) oxidation was first proposed by Stumm and Lee (1961) and later recast to the final version by Stumm and Morgan (1981) (Eq. **3.5**). Oxygen can be cast as either partial pressure or as dissolved concentration; pH dependence can be cast as either OH^- or H^+. Liang et al. (1993) found that at low partial pressures of oxygen, the homogeneous oxidation rate was zero order with respect to iron(II) concentrations. Another study demonstrated that the oxidation rate increases as either temperature increases or ionic strength decreases (Sung and Morgan, 1980). Published rate constants for homogeneous oxidation range from $8.0 \pm 2.5 \times 10^{13}$ $M^{-2}atm^{-1}min^{-1}$ (Stumm and Lee, 1961) to $3.3 \pm 0.7 \times 10^{16}$ $M^{-3}min^{-1}$ (Sung and Morgan, 1980).

$$\frac{d[Fe(II)]}{dt} = -k_1 [Fe(II)] [O_2] [OH^-]^2 \qquad \textbf{3.5}$$

3.2.2.2 Heterogeneous Iron(II) Oxidation

Heterogeneous iron(II) oxidation, involving either sorbed Fe^{2+} species or sorbed O_2, has been less studied but is of increasing interest due to the potential of catalytic effects by

iron(III) solid species (Dempsey et al., 2001). Studies have shown that iron(III) oxy-hydroxide catalyzes the abiotic oxidation of adsorbed iron(II) (Tamura and Nagayama, 1976; Sung and Morgan, 1980). These authors found that as the concentration of H^+ increased (or as pH decreased) the concentration of sorbed iron(II) decreased, resulting in a second order heterogeneous rate equation (Eq. **3.6**). Published rate constants for heterogeneous oxidation range from 6.0×10^{-9} mg/L-s (Dempsey et al., 2001) to 2.6×10^{-8} mg/L-s (Tamura and Nagayama, 1976; Sung and Morgan, 1980).

$$\frac{d[Fe(II)]}{dt} = \frac{k_2 [Fe(III)] [Fe(II)] [O_2]}{[H^+]} \qquad \textbf{3.6}$$

3.2.3 Effects on Surface Waters and Fauna

If the iron is not removed prior to the AMD mixing with more neutral surface waters, it will quickly oxidize and precipitate out of solution, generating additional acidity in the process. Other trace metals that may be present in large quantities, like aluminum and manganese, oxidize and coprecipitate with iron. These fine metal precipitates can then coat the stream and lake beds of the receiving waters.

Because of the detrimental impact mine drainage has on watersheds across the world, numerous studies have been done to determine the extent of the damage to aquatic ecosystems. DeNicola and Stapleton (2002) conducted a study to examine the effects of metal precipitates separate from aqueous effects of AMD. The authors determined that coating the substrata did not significantly affect macroinvertebrate or periphyton density or composition; impacts to aquatic benthic communities may instead be caused by other dissolved constituents of the AMD. Another study conducted macroinvertebrate surveys on

20 stations within an AMD-impacted watershed in Virginia and found that 6 stations had no organisms; another 8 stations had total abundances of only one to nine macroinvertebrates (Cherry et al., 2001).

Similar surveys were conducted in the watersheds of both Gum Boot Mine and Fridays-2 Mine. Macroinvertebrate surveys were conducted on Gum Boot Run with three sampling locations at the headwaters, downstream of most of the discharges, and at the mouth of the stream. The downstream location was severely impacted with only a third to a half the taxa diversity and a third to a quarter the total organism abundance seen at the other two sampling locations (PA DEP, 2005). Evaluations on the Bennett Branch Watershed (receiving Fridays-2 Mine drainage) rated the waters as very poor to marginal quality with very low fish and macroinvertebrate diversity and abundance (Growing Greener, 2003; Civil and Environmental Consultants, Inc., 2006).

3.3 Acid Mine Drainage Treatment Methods

Most treatment methods of acidic mine drainage involve the addition of alkalinity to raise the pH of the water and promote the oxidation and precipitation of iron and other trace metals. Treatment systems range from chemical methods like active treatment plants and anoxic limestone drains to biological methods like aerobic and anaerobic wetlands. The following sections will discuss in detail the designs, benefits, and problems of the most common AMD treatment methods used today.

3.3.1 Land Reclamation

As a result of the long history of coal miningin the US, the Land and Water Reclamation Fund was established in 1967 to provide funding to address abandoned mine land problems. The abandoned mine portion of the Fund was called Operation Scarlift and only achieved limited success. Operation Scarlift projects included development of watershed studies, surface mine reclamation, mine sealing, and construction of AMD chemical treatment plants (Lehigh Earth Observatory, 2008).

Congress then formed the National Mine Land Reclamation Center (NMLRC) in 1988. The organization was set to the task of addressing four main problems related to active and abandoned coal mines: 1) acid mine drainage, 2) prime farmland restoration, 3) subsidence control, and 4) groundwater degradation (National Mine Land Reclamation Center, 2008). The largest of these problems remains the treatment or abatement of acid mine drainage.

An amendment to the federal Surface Mine Control and Reclamation Act (SMCRA) in 1990 allowed states to designate 10 percent of their Abandoned Mine Land Trust grant for addressing relevant issues. States, like Pennsylvania, could then develop their own programs for dealing with the effects of AMD. For example, in 1992, Pennsylvania established the 10 Percent Set Aside Program and the first treatment systems were constructed in 1997. Next the federal Office of Surface Mining created the Appalachian Clean Streams Initiative (ACSI) in 1997 to provide additional funding to states for addressing AMD problems in the Appalachian basin (Lehigh Earth Observatory, 2008).

3.3.2 Active Treatment Methods

Conventional active AMD treatment systems involve neutralizing the water with alkaline chemicals such as limestone, lime, sodium hydroxide, sodium carbonate, or magnesia (Gazea et al., 1996). This alkalinity addition raises the pH of the AMD, promoting metal oxidation and precipitation. Similar to drinking and waste water treatment, active methods usually require construction and installation of a plant with agitated reactors, precipitators, clarifiers, and thickeners. Unfortunately, these treatment plants also necessitate additional expenses for reagents, operation, and maintenance for as long as AMD treatment is required. Lastly, the precipitation of large amounts of trace metals leads to problems with the transportation and disposal of these metal-rich solids (Gazea et al., 1996).

3.3.3 Passive Treatment Methods

To reduce the costs and maintenance of treating acid mine drainage, passive treatment methods have become preferable to active methods. The most common types of passive treatment include the use of aerobic wetlands, anaerobic compost reactors, limestone drains or channels, or any combination of these three systems (Gazea et al., 1996; Cravotta and Trahan, 1999, Ziemkiewicz et al., 2003) (Figure **3-6**). Aerobic wetlands are used for net alkaline waters and promote oxidation and hydrolysis reactions to precipitate metals (Gazea et al., 1996; Ziemkiewicz et al., 2003). Net acidic AMD high in dissolved oxygen (DO) or iron can be treated with anaerobic wetlands or compost reactors; these systems utilize anaerobic bacterial activity to reduce sulfate, precipitate sparingly soluble metal sulfides, and generate alkalinity (Gazea et al., 1996; Ziemkiewicz et al., 2003). Both aerobic and

anaerobic systems often contain limestone in the substrate for increased alkalinity production. The need for larger tracts of land and for the periodic addition of organic substrates are a few of the disadvantages of these two methods.

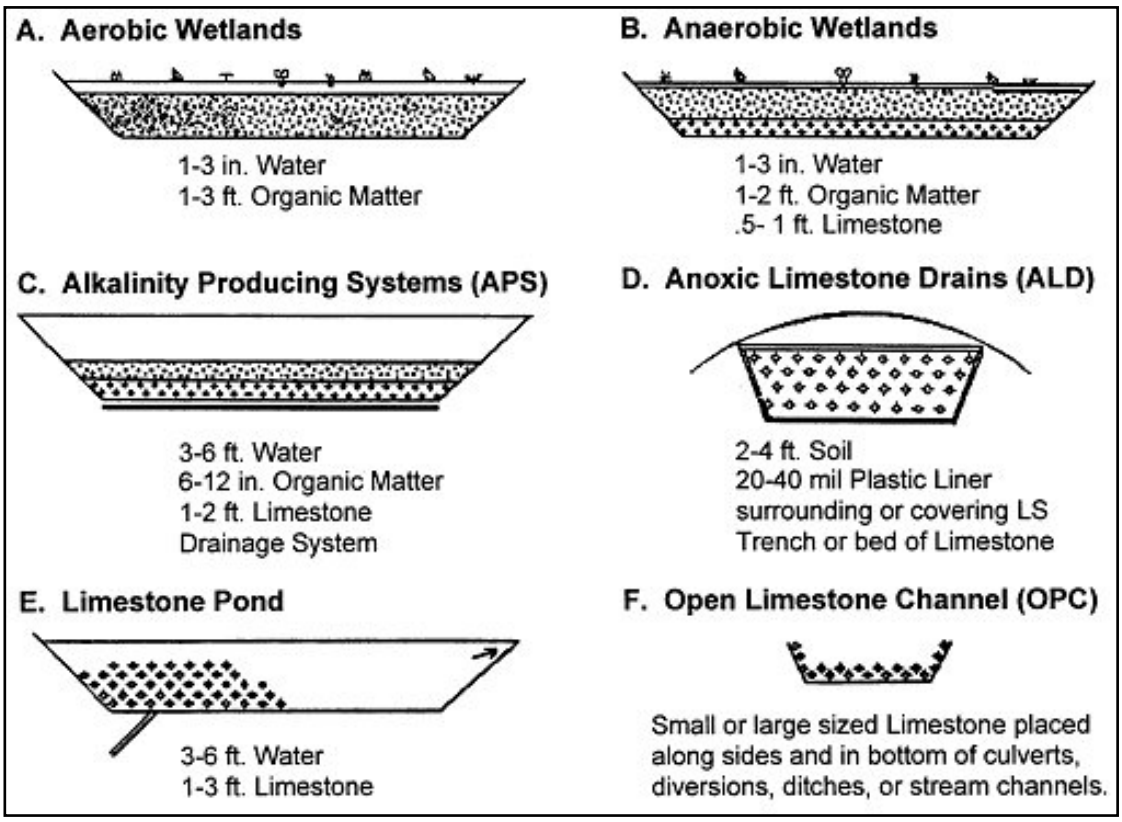

Figure **3-6**: Schematic diagram of passive remediation methods for treatment of AMD (Skousen, 1995).

Other common methods of passive AMD treatment involve alkalinity production by directing AMD through limestone beds or channels. Anoxic limestone drains (ALD) are used for net acidic AMD with low concentrations of dissolved oxygen (DO), iron, and aluminum (Gazea et al., 1996; Ziemkiewicz et al., 2003). Frequently, passive treatment systems utilize limestone beds in combination with other methods, such as wetlands or

following successive alkalinity producing systems (SAPS) that reduce DO through anaerobic activity. Unfortunately, limestone treatment systems usually require both long residence times due to slow dissolution of limestone and maintenance of the limestone beds to prevent armoring by iron(III) precipitates; treatment efficiency is also highly dependent on the influent AMD quality (Cravotta and Trahan, 1999).

3.4 Biological Iron(II) Oxidation

Singer and Stumm (1970) demonstrated that of all the potential catalysts they studied, microorganisms appeared to have the greatest effect in increasing the rate of iron(II) oxidation, in some cases by a factor of more than 10^6. At pH values less than 4.0, biological iron(II) oxidation has been shown to dominate over abiotic oxidation (Figure **3-7**) (Kirby et al., 1999; Rimstidt, 2004). Many studies have attempted to describe and identify the microbial communities found at acidic and circumneutral-pH mine drainage sites (Noike et al. 1983; Bond et al., 2000; Baker and Banfield, 2003; Johnson et al., 2005). Though *Acidothiobacillus ferrooxidans* (formerly known as *Thiobacillus ferrooxidans*) and *Leptospirillum ferrooxidans* are the most well-known of the the iron(II) oxidizing bacteria (IOB), mine drainage sites support a wide range of iron-oxidizing chemolithotrophs as well as heterotrophs (Johnson, 1998).

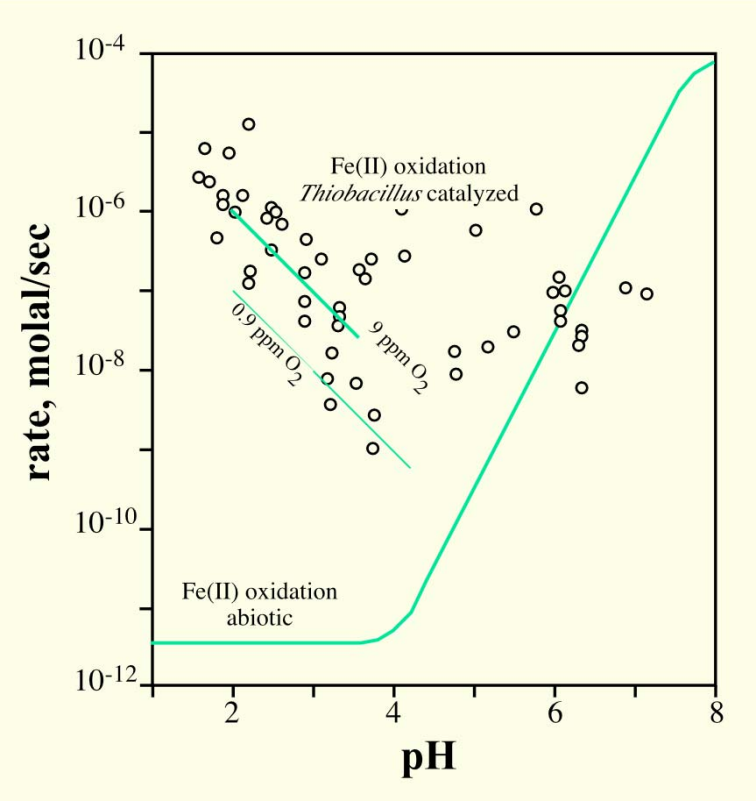

Figure **3-7**: Biological and abiotic rates of iron(II) oxidation of acid mine drainage (Rimstidt, 2004). Open circles represent observed in-situ rates of combined biological and abiotic iron(II) oxidation.

3.4.1 Iron(II) Oxidizing Microorganisms

The most well known IOB include the chemolithotrophs *Acidothiobacillus ferrooxidans* and *Leptospirillum ferrooxidans*. *A. ferrooxidans* was originally described in 1922 and later reclassified in 2000; this IOB is a rod-shaped chemolithoautotroph with optimum activity at pH 2.5 and at 30-35 °C (Kelly and Wood, 2000). The organism *L. ferrooxidans* was first identified in 1972 as a small, curved rod-shaped bacterium; it is aerobic and mesophilic with optimum activity at pH 2.5-3.0 (Hippe, 2000).

However, in addition to these two model organisms described, other acidophilic bacteria and archea have been discovered and identified. Chemolithotrophic bacteria such as additional *Acidithiobacillus* spp. and obligately heterotrophic bacteria such as *Acidiphilium* spp. have been isolated from AMD environments (Johnson et al., 2001). However, current isolation techniques for IOB were designed based on the model organisms *A. ferrooxidans* and *L. ferrooxidans* due to the relative ease in culturing these organisms; thus, scientists have probably only identified a portion of the overall distribution of iron(II) oxidizing bacteria. As analytical and isolation techniques improve, other previously unidentified organisms will certainly be discovered (Johnson, 1995; Johnson et al., 2005).

3.4.1.1 Circumneutral pH Iron(II) Oxidizers

The presence of carbonate rocks in the overburden of abandoned mines can result in more circumneutral mine drainage water that is still high in iron(II) and other trace metals. Numerous studies have identified microorganisms that successfully oxidize iron(II) in these higher pH mine waters. *Gallionella* spp. are microaerophilic chemolithoautotrophic IOB that prefer neutral to slightly acidic environments with relatively low levels of oxygen (0.1-1.0 mg/L) and high concentrations of carbon dioxide (Sogaard et al., 2001); these bacteria form distinctive helical stalks of exopolymers (Vatter and Wolfe, 1956). *Leptothrix* spp. are another sheath-forming chemolithotrophic bacterium capable of oxidizing both iron(II) and manganese(II). These bacteria typically grow in environments rich in organic material, at temperatures between 10-35 °C and pH of 6.5-7.5 (Spring et al., 1996). Other microorganisms isolated from circumneutral AMD sites include species from the genera

Acidobacterium, *Acidiphilium*, *Acidothiobacillus*, and *Ferrimicrobium* (Hallberg and Johnson, 2005).

3.4.2 Cellular Mechanisms for Biological Iron(II) Oxidation

To determine the cellular mechanisms for biological iron(II) oxidation, the model organism for most studies has been *A. ferrooxidans*. In 1998, Nemati et al. described the oxidizing system for *A. ferrooxidans* as a short chain of three electron carriers incorporated into the cellular membrane (Figure **3-8**). The electrons flow from the iron(II) ions in solution around the outer membrane to a copper-containing protein, rusticyanin, within the cellular membrane. From rusticyanin, the electrons pass to an adjacent cytoplasmic cytochrome c. Once reduced, cytochrome c transfers the electrons to an inner membrane-integrated cytochrome a. Finally, the electrons are released from cytochrome a to the intercellular space to be utilized in the reduction of oxygen to water. This transfer of electrons generates a proton motive force across the cell membrane which is then used to generate energy for the cell in the form of adenosine triphosphate (ATP) (Madigan and Martinko, 2006; Nemati et al., 1998). Additionally, the initial oxidation of iron(II) results in the oxidized form iron(III) that, depending on external pH, may hydrolyze and form precipitates on the bacterial cellular surfaces.

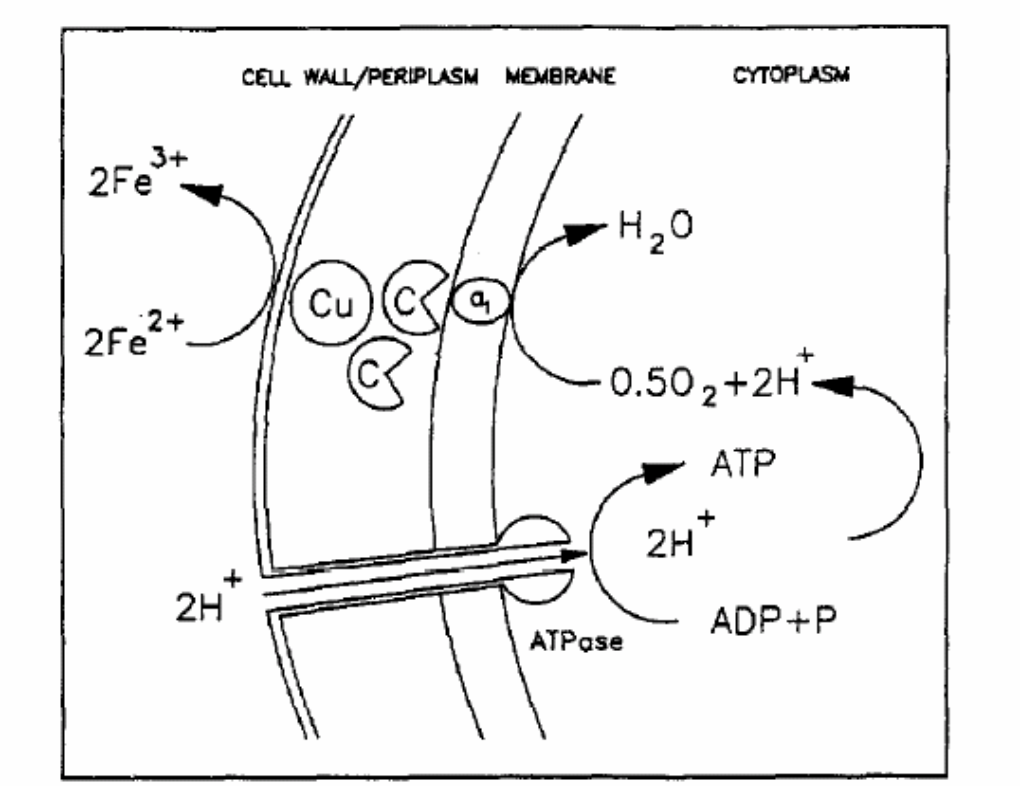

Figure **3-8**: The proposed electron transport chain for iron(II) oxidation by A. ferrooxidans (Nemati et al., 1998). Cu refers to Rusticyanin; c, cytochrome c; and a_1, cytochrome a_1. ADP/ATP = adenosine di/triphosphate.

3.4.3 Optimal Conditions for Biological Iron(II) Oxidation

Optimal conditions for both growth and energy acquisition for IOB certainly vary with species but, overall, the organisms must be capable of thriving in slightly to extremely harsh environments. Oxygen and carbon must be both present in adequate amounts and accessible to microorganisms. Other limiting nutrients such as N, P, etc. must also be present for growth to occur. Numerous studies have utilized the model organisms *A. ferrooxidans* and *L. ferrooxidans* to examine the effects of various environmental conditions on biological iron(II) oxidation.

Both optimal and maximum temperatures for biological iron(II) oxidation have been shown to be pH-dependent, with temperatures decreasing as pH decreases (Nemati et al., 1998). A study by Malhotra et al. (2002) examined the optimal conditions for the bio-oxidation of iron(II) in flask culture experiments with *A. ferrooxidans*. The authors found efficient bio-oxidation of iron(II) in the temperature range of 20-44 °C and the pH range of 1.8-2.2. These values were supported with work by Mousavi et al. (2006; 2007) that reported an optimal temperature of 33 °C for growth and an optimal pH range of 2-2.3 for both growth and iron(II) bio-oxidation with *A. ferrooxidans*.

Obligate aerobic autotrophs, like *A. ferrooxidans* and *L. ferrooxidans*, require both carbon dioxide and oxygen for growth. It has been shown that biological iron(II) oxidation by *A. ferrooxidans* can be uncoupled from cellular growth at limited CO_2 concentrations (Kelly and Jones, 1978). In a literature review by Nemati et al. (1998), CO_2 concentrations for maximum growth with *A. ferrooxidans* ranged from 5-8% sparge volume; however, a study by MacDonald and Clark (1970) demonstrated no effect of CO_2 on the growth rate of *A. ferrooxidans* at concentrations from 0.035 – 10%. Other studies examining the effects of oxygen concentrations on growth have reported no oxygen limitation on growth at atmospheric conditions; however, DO has been shown to limit growth at concentrations of 0.29 mg/L or less (Nemati et al., 1998). Smith et al. (1988) proposed an overall stoichiometric relationship for bacterial iron(II) oxidation and biomass synthesis (represented by $C_5H_7O_2N$) by *A. ferrooxidans* at pH 2 with a typical electron transfer efficiency of 30% (Eq. **3.7**).

$$Fe^{2+} + 0.224\ O_2 + 0.0045\ CO_{2(g)} + 0.0011\ HCO_3^- + H^+ + 0.0011 NH_4 \rightarrow Fe^{3+} + 0.0011\ C_5H_7O_2N + 0.4989\ H_2O \quad \textbf{3.7}$$

Specific elements may be required by living organisms for cellular growth (i.e. nitrogen and phosphorus) while other elements may be necessary for metabolic activity (Madigan and Martinko, 2006). Magnesium is one element of interest since it has been shown to be necessary for autotrophic carbon fixation (Zajic, 1969; Malhotra et al., 2002). Efficient bio-oxidation of iron(II) can occur at the minimum concentration of 3 mg/L Mg^{2+} with no effect of the Mg concentration on the rate of bio-oxidation above this value (Malhotra et al., 2002; Mousavi et al., 2006).

Numerous authors have published rates of laboratory biological iron(II) oxidation from laboratory-based experiments; however, the bioreactor experimental design and conditions are usually not consistent between studies. Reactor configurations range from chemostats with freely suspended cells to packed beds with cells immobilized within the bed matrix. Kinetic data for free and immobilized cells of *A. ferrooxidans* are presented in Table **3-1**, modified from Nemati et al. (1988). The iron(II) oxidation rates in bed bioreactors using immobilized IOB are higher than rates observed in chemostats or rotating biological contactors (RBC). Rates also appear to increase as temperature or volumetric loading of iron(II) increases within the reactor. Multiple studies conducted within the optimal conditions for growth and metabolic activity resulted in a range of oxidation rates spanning several orders of magnitude. Thus, biological iron(II) oxidation of acidic mine drainage is very sensitive to environmental conditions.

Table **3-1**: Kinetic data for iron(II) oxidation with different laboratory bioreactor configurations using free and immobilized cells of *Acidobacillus ferrooxidans*. RBC = Rotating Biological Contactor.

Study	Reactor Configuration	pH	Temp. (°C)	Volumetric Loading Rate (kg/m3-hr)	Oxidation Rate (kg/m3-hr)
MacDonald and Clark (1970)	Chemostat Free cells	2.2	28	0.49	0.42
Smith et al. (1988)	Chemostat Free cells	1.8-2.1	30	0.23	0.21
Halfmeier et al. (1993a, 1993b)	Chemostat Free cells	1.3	30	1.07	0.77
Grishin and Tuovinen (1988)	Packed bed	1.3-1.5	23	8.1-59.1	3.3-52.6
Halfmeier et al. (1993a, 1993b)	Packed bed	1.8	30	5.04	3.6
Nemati and Webb (1996)	Packed bed	1.8-2.0	30	60.0	34.2
Jensen and Webb (1994)	Trickle bed	2.3	28-30	8.0	4.4
Grishin and Tuovinen (1989)	Fluidized bed	1.3-1.5	23	2.69	1.58
Olem and Unz (1977)	RBC	2.6-3.2	9-12	0.35	0.34
Nakamura et al. (1986)	RBC	1.0-2.6	10-40	0.89	0.78

3.5 Models for Field and Laboratory Iron(II) Oxidation

While numerous studies have attempted to measure the oxidation rate of iron(II) in natural settings, very few have focused on developing an all-inclusive rate law to describe these systems. Stumm and Morgan (1981) published a rate law for abiotic homogeneous iron oxidation of AMD (see Eq. 3.5). Pesic et al. (1989) proposed a rate equation to calculate the biological contribution to iron(II) oxidation at pH values above 2.2 (Eq. **3.8**), where the rate coefficient is in units of $L^3/mg\text{-}mol^2\text{-}s$, C_{bact} is the concentration of bacteria in mg/L dry weight, and R is the universal gas constant. However, neither of these papers addressed the overall reaction where both biotic and abiotic processes were considered.

$$\frac{d[Fe(II)]}{dt} = -1.62 \times 10^{11} C_{bact} [Fe(II)] [H^+] pO_2 e^{-(58.77 / RT)} \qquad \textbf{3.8}$$

Kirby et al. (1999) proposed a single unified rate law to describe the iron(II) oxidation that occurs in natural systems such as aerobic wetlands. The authors combined the rate laws of Stumm and Morgan (1981) (abiotic rate) and Pesic et al. (1989) (biologic rate) to get one overall equation (Eq. **3.9**). This rate equation was then verified against field data using iron, pH, temperature, DO, and flow rate measurements from several flow-through treatment ponds. Outflow concentrations of iron(II) were accurately predicted for most of the ponds using the Kirby et al. model. The authors found that at pH values above 5, oxidation was dominated by abiotic reactions while biological iron(II) oxidation processes dominated at pH values less than 5.

$$\text{Overall Rate} = -\frac{d[Fe(II)]}{dt} = r_{abiotic} + r_{biol} \qquad \textbf{3.9}$$

4 MATERIALS AND METHODS

4.1 Field Site Characterization

At both Gum Boot Mine and Fridays Mine, sampling transects were delineated to analyze aqueous and solid chemistry from the AMD emergence to the point of mixing with the free stone creek.

4.1.1 Sampling locations

Seven sampling locations were selected along the 150 meter Gum Boot transect, beginning at the mine pool and ending immediately at the free stone creek (Figure **4-1**). About 18 meters downhill from emergence, the AMD flows below ground and reemerges 30 meters later. The last sampling location was located directly at the mixing point with the creek. At Fridays Mine, AMD travels approximately 10 meters from the emergence point to the free stone creek and four sampling locations were selected along the transect, with one additional upstream and downstream location (Figure **4-2**).

4.1.2 Field Measurements

DO, pH, temperature, and conductivity were measured at each sampling location along each transect. DO was measured using a Thermo Orion 810A dissolved oxygen meter; temperature and pH were measured with a Beckman Φ255 pH/Temp/mV meter; and conductivity was measured using a Thermo Orion 105A+ basic conductivity/salinity meter. All meters were calibrated in the laboratory prior to sampling except for the pH

meter which was calibrated in both the laboratory and field using standard buffer solutions of pH 4.01 and 7.0.

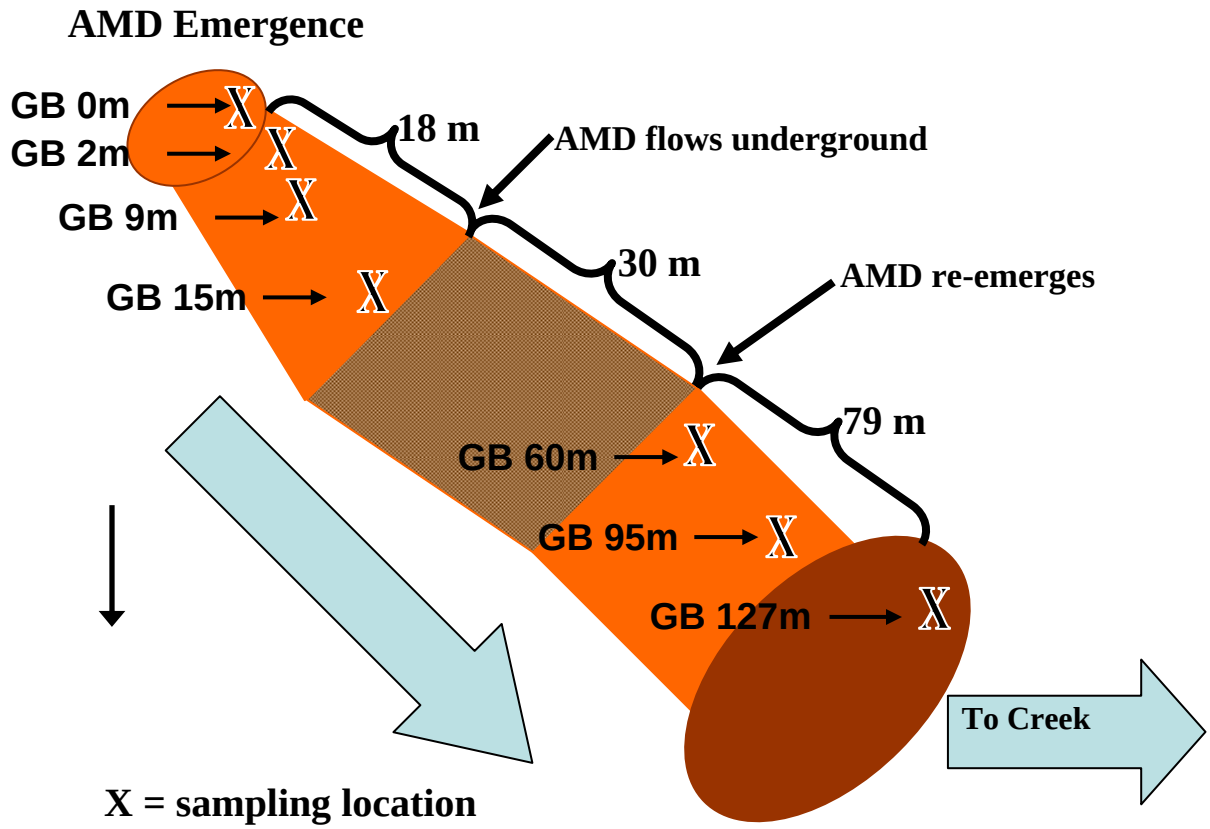

Figure **4-1**: Diagram of the acid mine drainage (AMD) from Gum Boot Mine. Blue arrows represent direction of flow. X symbols represent sampling location, and sample identifications were designated as GB 15m for samples collected 15 m downstream of AMD emergence at Gum Boot Mine. Diagram is not to scale.

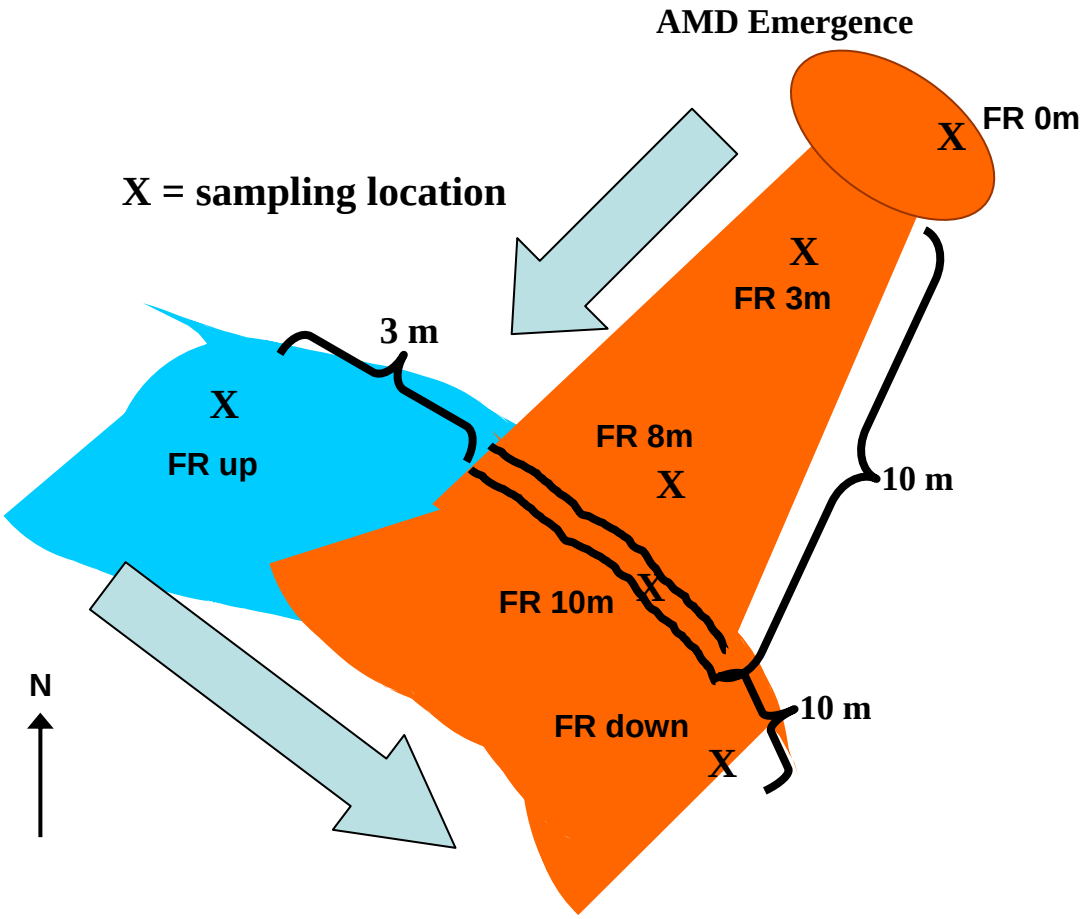

Figure **4-2**: Diagram of the acid mine drainage (AMD) from Fridays-2 Mine. Blue arrows represent direction of flow. X symbols represent sampling locations, and sample identifications were designated as FR 3m for samples collected 3 m downstream of AMD emergence. Fridays Run sampling locations upstream and downstream of AMD emergence are designated as FR up and FR down, respectively. Thick black lines 10 m downstream of AMD emergence represent steep stream banks. Diagram is not to scale.

4.1.3 Water Sample Collection and Preservation

Water samples were collected at each sampling location with pre-sterilized syringes and stored in 50 mL centrifuge tubes. All samples for iron, ion chromatography, total organic carbon (TOC), total nitrogen (TN), and metals were filtered with 0.45 μm

filters either in the field or immediately upon return to the laboratory. Samples for iron were acidified for preservation at a ratio of 1:2 with 1.0 N hydrochloric acid. Metals samples were acidified 1% (v/v) with concentrated nitric acid, and TOC/TN samples 1% (v/v) with concentrated sulfuric acid. Samples then were transported on wet ice to the laboratory and refrigerated at 4 °C.

4.1.4 Solid Sample Collection

Soil samples were collected for DNA analysis, SEM characterization, and batch reactor incubations. Using spatulas sterilized in the field with ethanol and flame, all solid samples were collected from the top 5 cm of sediment. Samples collected for DNA analysis were placed in 15 mL pre-sterilized centrifuge tubes, transported on dry ice to the laboratory, and then stored at -80 °C. SEM solids were also placed in 15 mL centrifuge tubes and 2-4% (v/v) of concentrated gluteraldehyde was added for preservation. Autoclaved mason jars (15 minutes at 123 °C, 16 psi) were used to store batch reactor solids until later use in sediment incubations. Both SEM and batch reactor solids were also transported on wet ice to the laboratory for storage at 4 °C.

4.1.5 Flow Measurements

The flow rate of Fridays Mine AMD was measured in July 2006 by digging a depression in the iron mound along the main path of flow. Using a stopwatch and an 18

gallon container, flow was measured by the time needed to fully fill the container. Replicate samples were taken to increase measurement precision.

A cutthroat flume (Baski) was used to measure the flow rate at Gum Boot Mine also in July 2006. A wedge was dug adjacent to the pool of AMD emergence and the flume was placed. Front and back height measurements were collected and compared to a standardized table to obtain the flow rate.

4.2 Laboratory Analyses

Samples collected in the field were analyzed in the laboratory within the proper storage time. For each sampling event, the analyses included aqueous iron, anions, total organic carbon (TOC), total nitrogen (TN), and trace metals. Analysis methods are described in detail in the following sections.

4.2.1 Aqueous Iron Measurements

Ferrous and ferric iron concentrations were determined within 48 hours using a modification of the 1,10-phenanthroline assay. Tamura et al. (1974) demonstrated that 1,10-phenanthroline forms a colorimetric complex with ferrous iron. The ultraviolet light absorbance at a wavelength of 510 nm is proportional to the intensity of the color complex and, thus, the concentration of ferrous iron in the sample.

To measure soluble ferrous iron, 0.05 mL of 0.45 μm filtered sample was placed in a 1.5 mL microcentrifuge tube along with 0.05 mL of 0.5M hydrochloric acid. Then,

0.65 mL of 0.6% hydrochloric acid was added and each tube was closed and inverted to mix. The next step was the addition of 0.048 mL of 0.73M ammonium fluoride to each tube, followed by mixing. After exactly 2 minutes, 0.1 mL of 1,10-phenanthroline (100 mg in 100 mL MilliQ water) was added and the tubes were again inverted to mix. Lastly, 0.1 mL ammonium acetate buffer (25g in 15mL water with 70 mL acetic acid) was added and each tube was mixed again. The treated samples were emptied into spectrophotometric cuvettes for measurement on a Shimadzu – UV-visible Spectrophotometer UV-1601 at a wavelength of 510 nm.

Ferrous ammonium sulfate was added to 0.5M hydrochloric acid and diluted to prepare standard solutions of 0.025, 0.1, 0.25, 0.5, and 1.0mM ferrous iron. These standard solutions and two samples of 0.5M hydrochloric acid were treated following the same procedures listed above. The two 0.5M hydrochloric acid samples were used to zero the spectrophotometer against any background absorbance from the reagents used in the assay. The standards were used to create a curve to calculate the concentration of ferrous iron in the original sample from the absorbance reading on the spectrophotometer.

Total dissolved iron was also measured with the 1,10-phenanthroline assay but ferric iron was first reduced to ferrous iron with 0.5M hydroxylamine hydrochloric acid. To prevent reoxidation of the ferrous iron, 0.5 mL of sample was placed in a microcentrifuge tube with 0.5 mL of 0.5M hydroxylamine hydrochloric acid and incubated overnight in an anaerobic chamber. Ferrous iron was then measured as done above using 0.1mL of the diluted sample. Ferric iron was calculated as the difference between the total iron and ferrous iron measurements.

4.2.2 Dissolved Total Organic Carbon and Total Nitrogen

For determination of TOC and TN, samples were run on a Shimadzu TOC-VCSN Total Organic Carbon Analyzer and Shimadzu TNM-1 Total Nitrogen Measuring Unit, respectively. Zero-moisture compressed air was used as the carrier gas and a Shimadzu ASI-V autosampler collected the samples. A 1000 mg/L potassium hydrogen phthalate stock solution (2.125 g dried for 3 hours at 105°C, then mixed with 1L MilliQ water) was used to prepare TOC standards of 10 mg/L and 50 mg/L. A 1000 mg/L potassium nitrate stock solution (7.219 g dried for 3 hours at 105C, then mixed with 1L MilliQ water) was diluted for the 10 mg/L and 20 mg/L TN standards.

TOC and TN standards were prepared using above-mentioned stock solutions and run on the TOC analyzer to create calibration curves. Curves were generated through autodilution and any curves with an R^2 value of less than 99.0% were discarded and rerun. Samples were then run using both of the newly created calibration curves for each measurement. TOC and TN concentrations were automatically calculated during sampling by the TOC analyzer.

4.2.3 Dissolved Trace Metals

Samples intended for metals analysis were filtered with 0.45 μm filters, acidified with concentrated nitric acid prior to storage, and analyzed within 6 months of collection. The metal cations Al, Ba, Ca, Cr, Cu, Fe, K, Mg, Mn, Na, Pb, Si, Sr, and Ti were run on a Leeman Labs PS3000UV inductively coupled plasma atomic emission spectrophotometer

(ICP-AES). The detection limit for most of the cations was between 0.02 and 0.05 mg/L. High quality standards were also analyzed with each run.

4.2.4 Ion Chromatography

Anion analysis was conducted on a DX-100 Ion Chromatograph (IC) with an IonPac AS4A-SC column and an AS40 autosampler. Sample detection and integration were performed using PeakNet software, version 5.1. The anions analyzed in this study included Cl^-, NO_2^-, NO_3^-, and SO_4^{2-}. Samples were filtered with 0.45 μm filters and stored unacidified at 4 °C until further analysis. Because sulfate concentrations in the samples were above the detection range of the IC, replicates were run using different dilution ratios. Chloride, nitrite, and nitrate were analyzed at full concentration while sulfate samples were diluted 1:5 with deionized water.

4.2.5 Microbial Population Counts

IOB were enumerated by Senko et al. (in press) using a plate counting technique described by Johnson (1995). The medium contained 1.8 g/L ammonium sulfate ($(NH_4)_2SO_4$), 0.5 g/L magnesium sulfate ($MgSO_4 \cdot 7H_2O$), and 0.25 g/L tryptic soy broth and was adjusted to pH 3.5 with 1.0 N sulfuric acid. Agarose (20 g/L) was used as a solidifying agent and ferrous sulfate (25 mM) was provided as an electron donor. To avoid growth inhibition of IOB by hydrolysis products of the agarose, plates were prepared with two layers of medium. Before pouring, the underlayer was inoculated

(2.5% volume/volume) with the acidophilic organoheterotrophic bacterium *Acidophilium organovorum* (cultivated on the medium described above with galactose as an electron donor and carbon source); the overlayer received no inoculum before pouring. Hydrolysis products were minimized by the inclusion of *A. organovorum*. Samples were suspended in an agarose-free medium (approximately 0.2 g sediment/ 5 mL medium), homogenized by vortexing, serially diluted, and spread on solidified plates. IOB colony forming units (CFU/g DW sediment) were indicated by the formation of red-orange colonies.

4.2.6 Scanning Electron Microscopy

Scanning electron microscopy (SEM) samples were prepared following a previously published procedure (Zhang et al., 2007). Cell-mineral suspensions were fixed in anoxic 2.5% glutaraldehyde and placed on a glass cover slip; mineral particles were then allowed to settle onto the cover slip for 15 min. An ethanol series was used to gradually dehydrate the cover slips, which were then finished with critical point drying (CPD). Except CPD, all sample preparation was performed in an anoxic glovebag to minimize the exposure of samples to O_2. After mounting onto a SEM stub, cover slips were Au coated for observation using a Zeiss Supra 35 FEG-VP SEM and an accelerating voltage of 10 to 15 kV. To achieve the best image resolution, a short working distance (6 -10 mm) and low beam current (30 - 40 mA) were used. For energy dispersive spectroscopy (EDS) analysis, a longer working distance (8.0 mm) and higher beam

current (50 - 70 mA) were used. Special thanks to Dr. Gengxin Zhang for microscopy work.

4.3 Experimental Methods

Iron sediments were collected from field sites and incubated to compare biological iron(II) oxidation kinetics of Gum Boot Mine and Fridays-2 Mine. One liter batch reactors used for the incubations were continuously fed a pre-selected gas mix of oxygen, carbon dioxide, and nitrogen. The reactors were run in the dark at room temperature for 21 days with an iron(II) spike once every 7 days. To look at the potential effects of heterotrophic bacteria, the breathing air gas mix was replicated in an experiment using glucose at starting concentrations of about 50 mg/L (Marchand and Silverstein, 2003). Glucose was used as the carbon source instead of other substrates to prevent volatilization of organic acids under the low pH conditions of the batch reactors.

4.3.1 Synthetic Acid Mine Drainage

A synthetic acid mine drainage (SAMD) was used as the media for the sediment incubations. The SAMD was modified from the 9K media developed by Silverman and Lundgren (1964) and developed to represent typical AMD from the western Pennsylvania bituminous coal fields (Table **4-1**). Components were added one at a time to continuously stirred deionized water. After pH was adjusted to about 3.1, the media was

0.45 μm filter sterilized with 0.45 μm Nalgene disposable bottle top filters into autoclaved pyrex bottles and stored at 4 °C until later use.

Table **4-1**: Composition of the synthetic acid mine drainage (SAMD) used for the batch reactor sediment incubations, given as final concentrations.

Component	mM
$Al_2(SO_4)_3 \cdot 17H_20$	0.5
$CaSO_4 \cdot 2H_20$	5.0
$MgSO_4 \cdot 7H_20$	4.0
$MnSO_4 \cdot H_20$	0.4
Na_2SO_4	1.0
$(NH_4)_2FeSO_4 \cdot 6H_20$	0.1
$FeSO_4 \cdot 7H_20$	4.5
KH_2PO_4	0.07*

*This component was added only in gas mix 5 (breathing air) as a control experiment.

4.3.2 Batch Reactor Design

Iron sediments were incubated in continuously stirred batch reactors while the headspace of each reactor was constantly purged with a specific gas mix (Figure **4-3**). The batch reactors were made from one-liter high density polyethylene bottles and designed to allow for the removal and addition of liquids at any time by inserting a stopper and septum into the lid of each (Figure **4-4**). Using stir bars and stir plates, the reactors were stirred at 60 rpm to create a well mixed solution without suspending large amounts of sediment solids.

Figure **4-3**: Picture of batch reactors in a laboratory fume hood. The third stir plate is located in the back right of the hood. The gas mix is fed through a main line on the left to the three teal-colored aquarium manifolds and then to the reactors. Aluminum foil was removed from one of the reactors for illustration purposes.

Three lengths of PVC tubing were inserted through holes in the black stoppers; one length into the headspace for premixed air entering the reactor, one length into the headspace for air leaving the reactor, and one length into the SAMD for sampling. The air-in tube was placed close to the liquid-air interface and the air-out tube was placed as close to the reactor lid as possible, to spatially separate the intake and outtake ports and allow for complete flushing of the headspace. While the SAMD in the reactors was assumed to be completely mixed, the sampling port was placed slightly above the sediment-liquid interface to avoid removing solids during sampling and, thus, changing the sediment to liquid ratio.

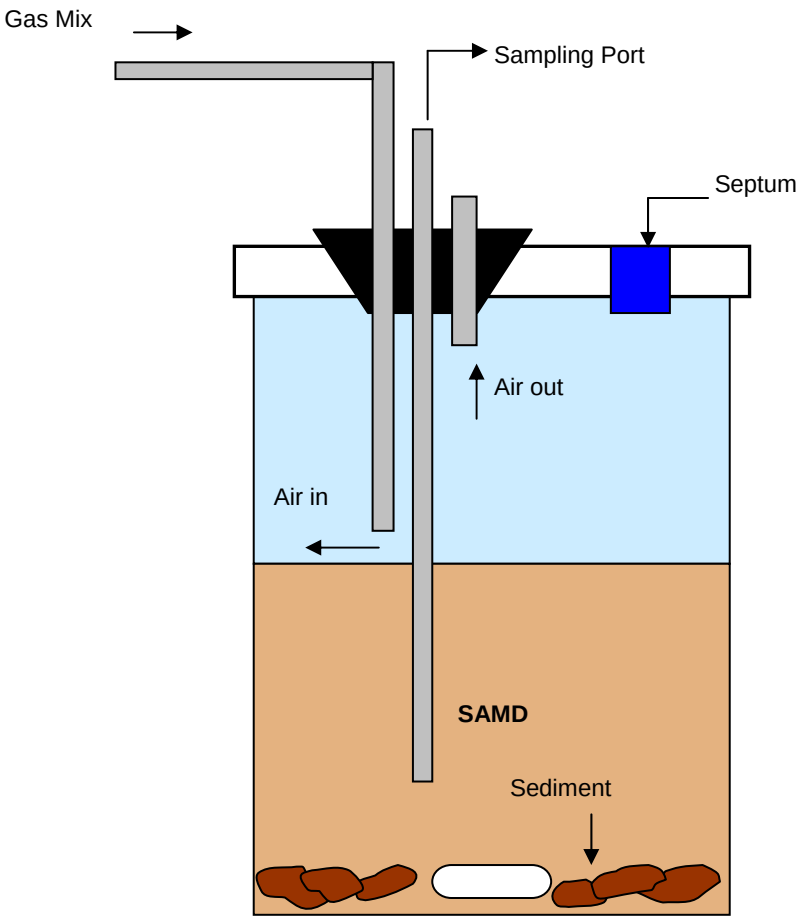

Figure **4-4**: Diagram of experimental reactor setup. Reactors were continuously stirred by stir bar and headspace air was constantly purged at positive pressure. SAMD is the synthetic acid mine drainage media used for the incubations.

4.3.3 Gas Mix Selection and Verification

Specific gas mix compositions were used to purge the reactor headspaces to allow for the comparison of iron(II) oxidation kinetics at varying partial pressures of oxygen and carbon dioxide (Table **4-2**). Standard grade oxygen, carbon dioxide, and nitrogen gases were mixed at predetermined ratios using an in-line Aalborg mixing system, with a Command Module and three AFC Mass Flow Controllers. The gas mix was fed from the

mixing system through a main feed line to three aquarium manifolds that allowed the manual on-off switching of gas flow. These manifolds then delivered the gas mix to each batch reactor through the air-in tube mentioned above.

Table **4-2**: Composition of gas mixes used for sediment incubations. Values are reported as percentages of total gas volume. Gas mixes 3 and 5 both used breathing air for headspace purging. However, gas mix 5 also incorporated glucose additions to examine the possible contribution of heterotrophic iron(II) oxidizing bacteria.

Gas Mix #	Oxygen (%)	Carbon Dioxide (%)	Nitrogen (%)
1	0.7	1.1	98.2
2	1.5	7.3	91.2
3	21	0.035	78
4	10	1	89
5	21 + Glucose	0.035	78
6	---	5	95

Gas mixes were selected to evaluate a wide range of conditions at the field site. AMD often emerges with low DO and high dissolved carbon concentrations. Personal communication (B. Means) has verified the Dissolved Inorganic Carbon concentration at Fridays-2 Mine can be as high as the equivalent of 5% atmospheric carbon dioxide. Oxygen concentrations were varied from near-zero values to saturated values (atmospheric breathing air); carbon dioxide was varied from the breathing air value of 0.035% to values of 7.3 %. Experiments conducted under the highest carbon dioxide partial pressure were shown to yield maximum growth of *A. ferrooxidans* (Nemati et al., 1998). The balance of each mix was filled by nitrogen gas.

Each gas mix was verified for composition using an SRI 310C Gas Chromatograph (GC), with a 3 inch molecular sieve 5A column and a low-gain thermal conductivity detector (TCD). With argon as the carrier gas, the GC was set at 70 °C and 20 psi head pressure for operation; gas-tight locking syringes were used to obtain and inject the gas mix sample into the sampling port on the GC. Standards from cylinders or atmospheric air were run periodically to determine calibration curves for each gas type. All samples and standards were run on the low TCD setting and analyzed using PeakSimple software version 3.29.

4.3.4 Sediment Selection

Iron sediments were collected from the field sites in July of 2006 for use in the batch reactor incubation experiments. Sediments were selected from the results of previous work by Dr. John Senko (Figure **4-5**). Colony forming units (CFU) of IOB were determined with enumeration methods described in a preceding section and normalized per g of dry weight (DW) sediment; first-order rate constants (k, 1/day) were obtained from preliminary sediment incubations conducted in 100 mL serum bottles with breathing air and synthetic acid mine drainage (SAMD; described above). CFU counts and the field rates of iron(II) oxidation were then used to select for Gum Boot's "fastest", Fridays-2 "slowest", and Fridays-2 "fastest" iron oxidizing sediments.

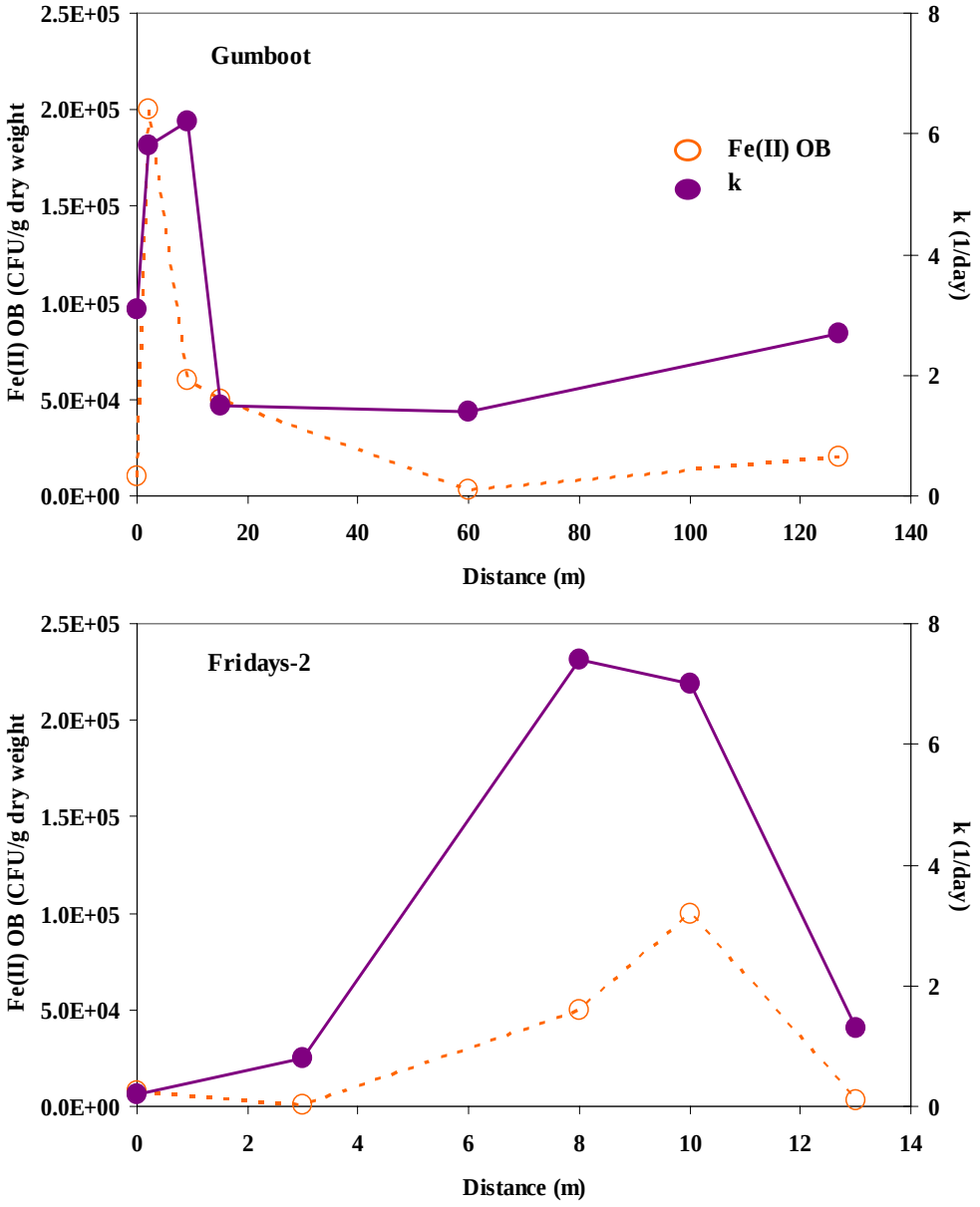

Figure **4-5**: Fe(II) oxidizing bacteria colony forming units (CFU) and first order rate constants for sediments collected from A) Gum Boot Mine and B) Fridays-2 Mine. Units of bacterial counts reported as CFU/g dry weight (DW) sediment. Orange (open) and purple (closed) circles represent the CFU counts and k values, respectively.

4.3.5 Reactor Preparation and Construction

Prior to construction, all reactor components and materials were autoclaved for 15 minutes at 123 °C and 16 psi. The small septum was placed in the lid, all tubing was inserted in the large stoppers, and the stir bars were placed in the reactors bottles prior to autoclaving. Additionally, any glassware and tubing that would be used in the construction of the reactors were autoclaved.

Previously prepared SAMD was connected to the gas mix and allowed to bubble for about 2 hours before the reactors were started. Meanwhile, 25 g of wet sediment was weighed out into the appropriate batch reactors and 5 mL of concentrated formaldehyde was added to any killed control reactors (final 1% v/v). Two live and two killed reactors were run per sediment for each gas mix experiment. Additional experimental controls are discussed in later sections.

Once the reactors and SAMD were both ready, the reactors were constructed using sterile methods. 500 mL of SAMD was siphoned by tubing to a graduated cylinder and then gently poured into a reactor; all transfers of SAMD were conducted with little aeration in order to maintain equilibrium with the selected gas mix. The reactor was immediately sealed with a lid and stopper, placed on a stir plate, and connected to the gas flow.

After all batch reactors were assembled and attached to gas flow, four reactors were removed at a time to obtain a starting mass weight. Tubing was disconnected from the aquarium manifolds but left intact with the stoppers. Reactors were then reconnected

to the gas mix and covered with aluminum foil to prevent the potential contribution of phototrophic bacteria to the iron(II) oxidation rates.

4.3.6 Sampling

Immediately upon construction (time=0) and at least once daily, the reactors were sampled for iron(II) and pH measurements. At each sampling event, the time, date, and room temperature were recorded. An approximately 1 mL sample was removed from each reactor by connecting a syringe to the sampling port tubing. Measurement of additional analytes, other than IC analysis of anions, required the removal of larger quantities of SAMD. IC, TOC/TN, and metals analyses followed the appropriate methods described in previous sections. A Thermo Orion 810A basic dissolved oxygen meter was used to measure DO by sampling 10 mL from a batch reactor and transferring it, with minimal aeration, to a centrifuge tube.

Iron(II) was measured by the ferrozine method (Stookey, 1970; Lovley and Phillips, 1987). Samples were centrifuged for 2 minutes at 13,400 rpm to remove any solid iron phases from solution. The sample was then diluted with 0.5 M hydrochloric acid and 20 µL was pipetted into a spectrophotometer cuvette; 1 mL of ferrozine reagent (1 g/L ferrozine dissolved in 50 mM HEPES buffer that was adjusted to pH 6.8-7.0) was added to each cuvette. Standards were also measured using the same technique to construct a calibration curve.

The iron(II) samples were measured spectrophotometrically using the absorbance values at a wavelength of 562 nm. Absorbance values were measured on a Shimadzu –

UV-visible Spectrophotometer UV-1601. Blanks using 0.5 M hydrochloric acid instead of sample were run for each sampling event to zero the machine.

Using the phenol-sulfuric acid method described by Huang and Forsberg (1990), glucose concentrations were measured daily during gas mix 5 (breathing air + glucose); 1 mL samples were mixed with 1 mL of 5% phenol. Five mL of sulfuric acid was added and samples were allowed to stand for 10 minutes and then sit for 10-20 minutes in a water bath (20-30 °C). Samples were transferred to spectrophotometer cuvettes and absorbance at 490 nm was measured as described above.

At each sampling event, pH was measured on a Thermo Orion 550A advanced pH/conductivity meter. The meter was calibrated each time using 4.01 and 7.0 pH standard buffers. A VWR Symphony glass semi-micro pH electrode was used to reduce the amount of sample needed for measurement to about 0.75 mL. If a pH adjustment was needed to keep the reactors above pH 2.5, sodium hydroxide (0.1 or 0.5 M) was added as necessary through the septum in the lid.

4.3.7 Additions of Iron and Glucose

To obtain longer time series and multiple rate values, two additions of iron(II) were added to the batch reactors after weeks 1 and 2 of each experiment. Once the reactors were sampled, they were weighed to determine the amount of mass lost; this weight was used to estimate the loss due to sampling and evaporation (assuming 1 g = 1 mL). Ferrous sulfate was dissolved in deionized water and added to the reactors to bring each concentration back to the original starting value; Luer Loc 0.45 μm syringe filters

were used to filter-sterilize the solution. Glucose additions were also conducted at the same time using similar methods for preparation and filtration. To bring the concentrations close to the starting measurements, glucose was dissolved in deionized water and filter-sterilized before adding to the reactors.

4.3.8 Experimental Controls

Several controls were run along side the experimental reactors to examine the impact of certain variables upon the iron(II) oxidation rates of the different sediments. Four different treatments were analyzed in the control experiments: 1) Killed controls, to look at abiotic rates; 2) iron-free SAMD incubations, to determine if iron(II) is released from or sorbed to the sediments over time; 3) phosphorus-free SAMD reactors, to examine the potential for nutrient limitation; and 4) SAMD incubations with no sediments, to check for cross-contamination of reactors during the experiments. All controls were run under identical conditions to the experimental reactors except for the iron-free SAMD incubations.

4.3.8.1 Killed Controls

Killed controls were run with each experiment to obtain the rates for non-biological iron(II) oxidation for the three sediments and five different gas mixes. To evaluate the effects of various eradication methods for killed control reactors, Dr. John Senko conducted short term iron(II) oxidation experiments. Iron(II) and pH (Figure **4-6**)

were measured frequently over 2 days in reactors sterilized with either 1% v/v formaldehyde, 0.1% v/v azide, or autoclaving (30 minutes at 123 °C and 16 psi). Results show that autoclaving increases the iron(II) concentration of the solution while azide increases the pH. However, since formaldehyde does not noticeably alter either analyte it was used as the sterilization method for all killed control reactors.

4.3.8.2 Iron-free Synthetic Acid Mine Drainage Incubations

A separate experiment was conducted with the sediments in small 50 mL serum bottles using iron-free SAMD. Approximately 1 g of sediment was placed in an autoclaved (15 minutes at 123 °C and 16 psi) serum bottle and 20 mL of iron-free SAMD was added to each bottle. The reactors remained open to the atmosphere and were shaken by hand periodically to distribute and aerate the sediments. Iron(II) and pH were measured every couple of days using the methods described in previous sections.

4.3.8.3 Phosphorus-free Synthetic Acid Mine Drainage Incubations

To demonstrate the iron(II) oxidizing bacteria were not phosphorus-limited in the reactors, experiment #5 (breathing air + glucose) used SAMD with phosphorus for the incubations. Two reactors had GB 2m sediments but used P-free SAMD; the other reactors (including two GB 2m live reactors) were incubated in SAMD containing about 0.07 mM final concentration phosphorus. Both pairs of GB 2m reactors also received the weekly iron(II) and glucose spikes.

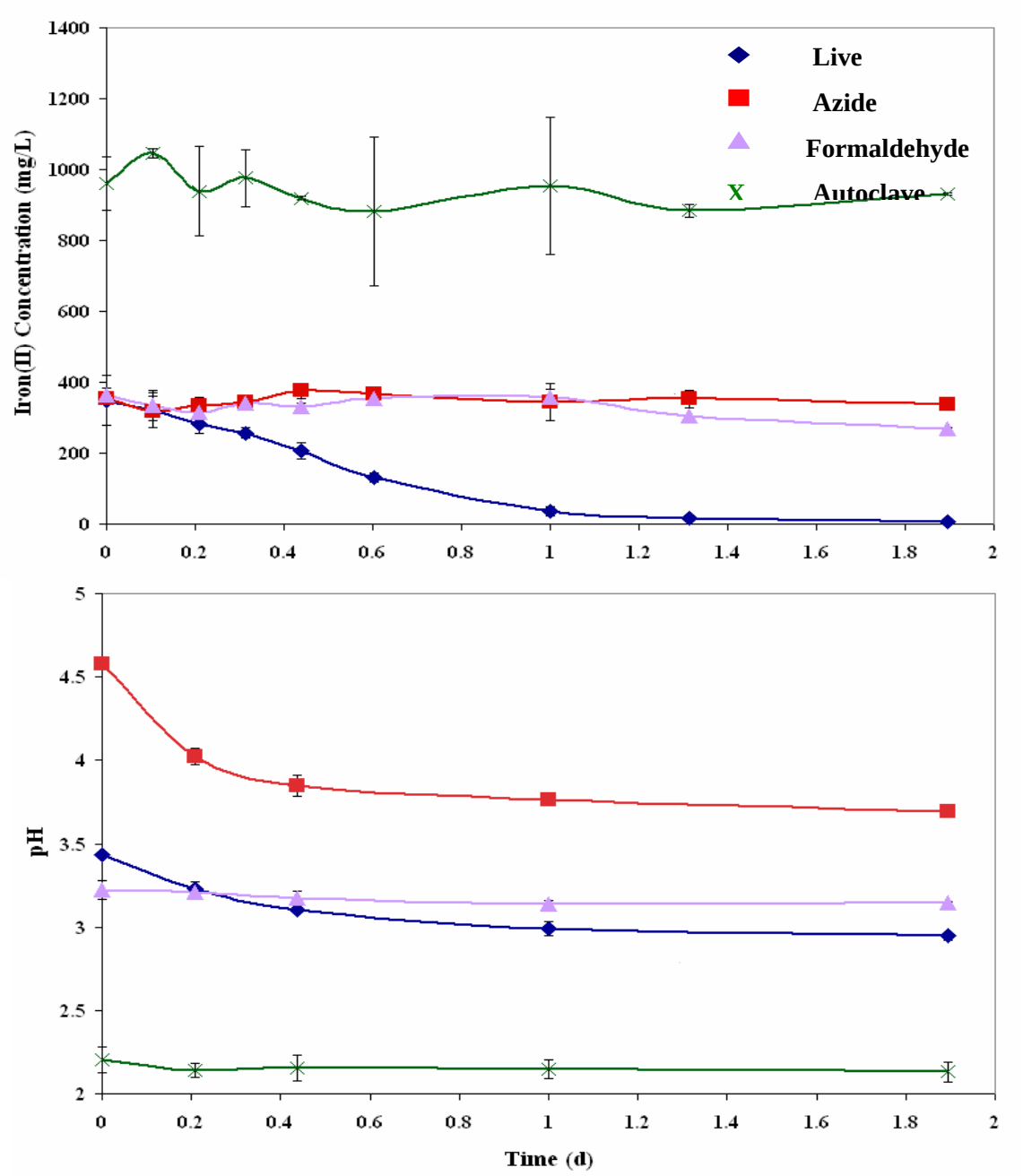

Figure **4-6**: Comparison of procedures to create a "killed" control, using GB 2m sediments and breathing air. Procedures include sodium azide (0.1% v:v), formaldehyde (1% v:v), and autoclaving (30 minutes at 123 °C and 16 psi).

4.3.8.4 Incubations with No Sediments

To demonstrate that the positive pressure of the reactor headspace helped to minimize or eliminate cross-contamination of microbial populations, experiment #5 (breathing air + glucose) had two reactors that contained SAMD with phosphorus but no sediments. Iron(II), pH, and glucose were measured at each sampling event. However, these control reactors were not subjected to the weekly spikes of iron and glucose. Upon completion, final samples were plated along with all other reactor samples to measure colony forming units (CFU/g DW sediment) of iron(II) oxidizing bacteria.

4.3.9 Reactor Breakdown

Upon completion of each experiment, the reactors were sampled for iron(II) and pH before being weighed for final volumes. Next, 10 mL aliquots were placed in pre-sterilized 15 mL centrifuge tubes and frozen at 80 °C for later DNA analysis. About 10-20 mL of each reactor's final slurry was collected and transferred to pre-sterilized 50 mL centrifuge tubes; these samples were then plated to determine the CFU counts of IOB. Lastly, liquid and solid samples were collected upon reactor breakdown for later analyses such as metals, TOC, or X-ray diffraction (XRD).

4.4 Iron(II) Oxidation Data Modeling

The results from the batch reactor experiments were input into *STELLA* computer program to model the iron(II) oxidation kinetics using the combined iron(II) oxidation

model proposed by Kirby et al. (1999). The combined oxidation model was originally designed for a flow-through system and was first modified for the constant-volume batch reactors in this study. Soluble iron(II) concentrations and pH measurements for each sampling time were used directly in the model. DO concentrations were calculated using Henry's Law and both DO and temperature were held constant for the duration of the experiments (Table **4-3**). The biological kinetic rate constant, k_{bio}, and the IOB concentrations, C_{bact}, were varied between model runs to examine the effects of decreased biological iron(II) oxidation rates and IOB numbers on model performance and fit. All other parameters were held identical to the values used in the original STELLA model by Kirby et al. (1999) and the model was run using an iteration time of 0.5 d.

Table **4-3**: Variable parameter inputs for the computer program STELLA to model the batch reactor iron(II) oxidation results used in the Kirby et al. (1999) model for abiotic and biological iron(II) oxidation. Iron(II) and pH measurements for each gas mix experiment were input directly into STELLA for use in the model. All other parameters were identical to those used by Kirby et al. (1999).

Gas Mix	**DO (mg/L)***	**Temp. (°C)**	**k_{bio} (L^3/mg-mol^2-s)**	**C_{bact} (mg DW/L)**
1	0.291	25	1.02×10^9	15
(0.7% O_2, 1.1%			1.02×10^8	15
CO_2, 98.2% N_2)			1.02×10^8	1.5
2	0.624	25	1.02×10^9	15
(1.5% O_2, 7.3%			1.02×10^8	15
CO_2, 91.2% N_2)			1.02×10^8	1.5
3	8.74	25	1.02×10^9	15
(breathing air)			1.02×10^8	15
			1.02×10^8	1.5

* DO (mg/L) was calculated from the pO_2 of the gas mixes using Henry's constant (k_H) for O_2 and the equation [pO_2 (atm) = k_H (1.3×10^{-3} mol/L-atm) x [DO] (mol/L) x (3200 mg O_2/mol)].

5 RESULTS

5.1 Field Water Chemistry Data

The mine sites were sampled six times each between October 2005 and July 2007. Gum Boot Mine was sampled 10/2005, 02/2006, 05/2006, 07/2006, 10/2006, and 05/2007. Fridays-2 Mine was sampled 02/2006, 05/2006, 07/2006, 10/2006, 05/2007, and 07/2007. At both mine sites, no seasonal trends were observed with the emergent mine drainage chemistry during the monitoring period of this study. The emergent mine drainage chemistry was similar between Gum Boot and Fridays-2 except for dissolved iron(II) concentrations (Figure **5-1**) with 0.11-0.80 mM at Gum Boot and about 1.0 mM at Fridays-2. Iron(II) is almost completely removed (average of dissolved 0.43 ± 0.25 mM Fe(II)) from the AMD before it mixes with Gum Boot Run. However, AMD at Fridays has an average of 0.58 mM of dissolved iron(II) when it joins Fridays Run.

Measurements for pH, temperature, and dissolved oxygen (DO) in the emergent AMD displayed no obvious seasonal trends. At Gum Boot, the pH dropped and the temperature and DO rose quickly in the first several meters of flow across the iron mound. At Fridays-2, there were no rapid changes in water chemistry within the 10 meters of flow. The largest changes occurred near FR 10m, where the mine drainage dropped over steep ledges right before mixing with the creek.

Dissolved TOC and TN measurements also did not display any obvious seasonal trends or large changes along the AMD path of flow (Figure **5-2**). TOC values were

relatively similar between the two mine sites, ranging between 0.5 and 3.0 mg C/L for most of the sampling events. However, TN concentrations at Fridays-2 Mine were almost twice as high as concentrations measured at Gum Boot Mine.

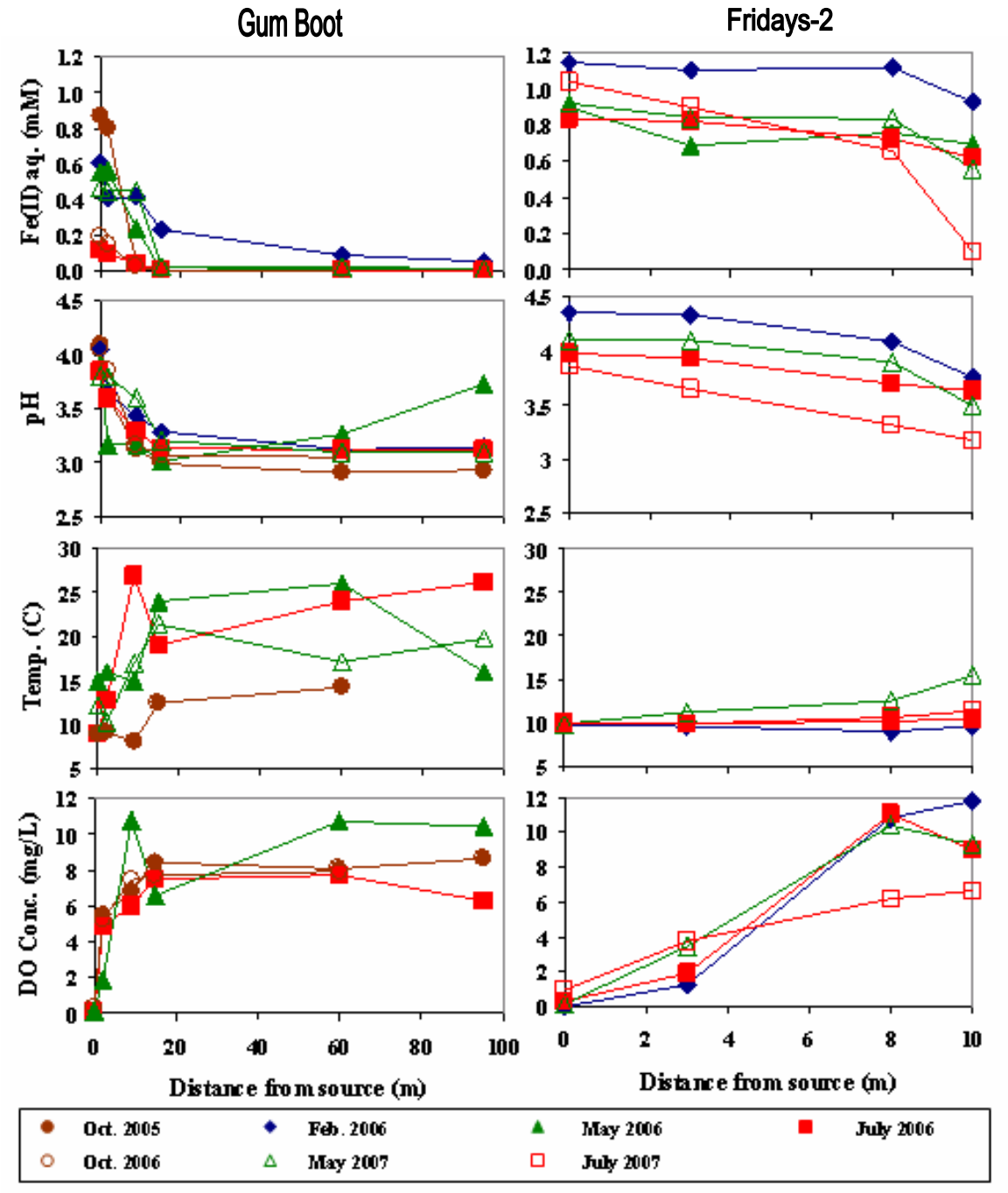

Figure **5-1**: Field chemistry measurements for Gum Boot Mine and Fridays-2 Mine as a function of sampling event.

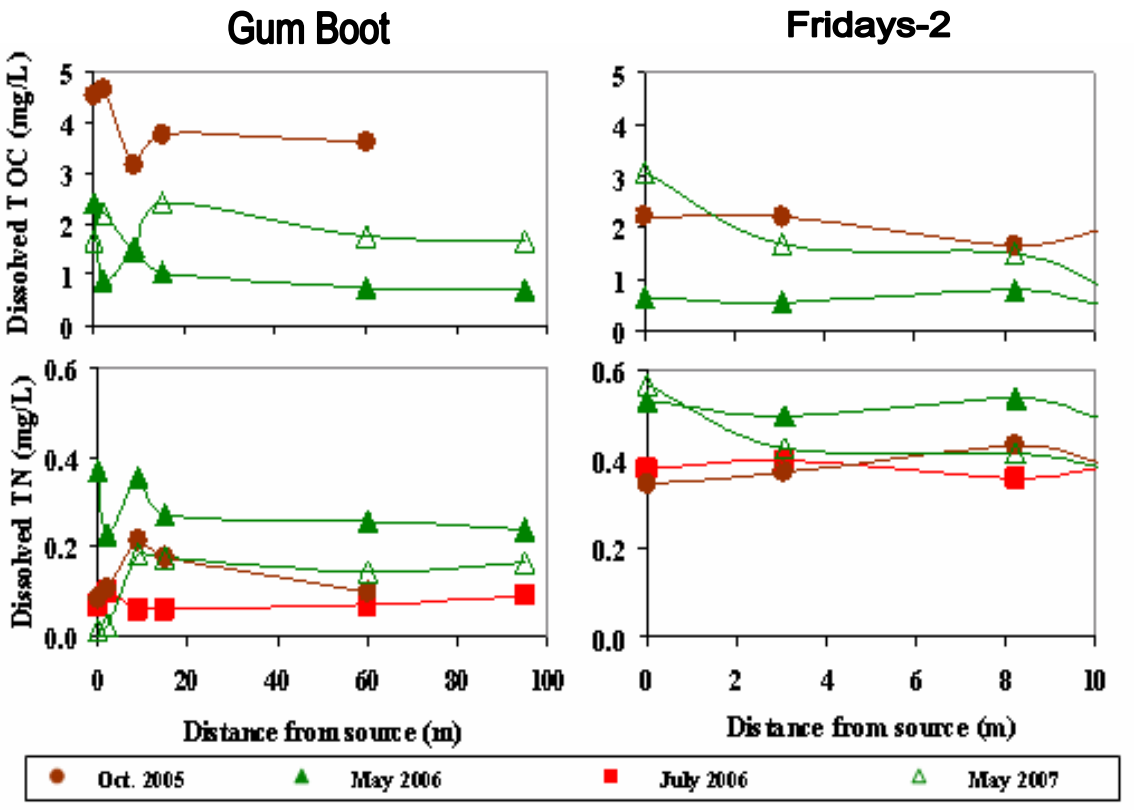

Figure **5-2**: Dissolved total organic carbon (TOC) and total nitrogen (TN) measurements for Gum Boot Mine (on the left) and Fridays-2 Mine (on the right) as a function of sampling event.

Trace metal samples were collected four times at each mine site and analyzed by ICP-AES analysis. Major components at Gum Boot included Ca, Fe, K, Mg, Mn, and Si all at concentrations of 2 mg/L or higher (Table **5-1**). The last sampling location at 127 meters was taken at the mixing zone with Gum Boot Run; thus, those values are not included when analyzing data for trends along the flow path across the iron mound. Fe was the only element that experienced an observable change in concentration from AMD emergence to mixing with the creek, dropping from an average of 22.5 mg/L to 0.28 mg/L along the path of flow.

Table **5-1**: Elemental composition of Gum Boot water samples collected along the flow path as determined by ICP-AES analysis. All values are given in mg/L.

		Distance along flow path (m)						
Element	**Sample Date**	**0**	**2**	**9**	**15**	**60**	**95**	**127**
Al	May 2006	0.71	0.67	0.65	0.71	1.1	1.2	1.5
	July 2006	0.60	0.65	0.63	0.81	0.81	0.83	0.08
	October 2006	1.2	1.2	1.2	1.4	1.5	---	0.56
	May 2007	< 0.05	< 0.05	0.13	0.31	0.5	0.72	< 0.05
Ba	May 2006	< 0.02	0.02	0.02	0.02	0.02	0.03	0.03
	July 2006	< 0.02	0.02	0.02	0.02	0.03	0.03	0.03
	October 2006	< 0.02	< 0.02	< 0.02	0.02	0.02	---	0.03
	May 2007	1.2	1.0	0.91	1.2	1.5	1.2	0.59
Ca	May 2006	11	9.7	9.8	10	9.8	9.7	12
	July 2006	10	10	10	9	10	10	6.6
	October 2006	10	10	10	10	10	---	5.8
	May 2007	9.3	9.1	9.0	9.8	9.0	8.7	6.3
Fe	May 2006	23	21	12	2.8	0.66	0.28	3.0
	July 2006	23	21	7.7	0.49	0.36	0.42	0.95
	October 2006	24	21	10	0.55	0.45	---	0.57
	May 2007	20	19	16	1.7	0.23	0.15	0.13
K	May 2006	2.8	2.8	2.8	3.1	3.0	3.2	1.8
	July 2006	2.8	3.1	2.8	2.9	3.0	3.2	0.7
	October 2006	2.9	2.7	7	2.7	2.9	---	0.9
	May 2007	2.4	2.6	2.6	3.8	3.4	0.15	0.2
Mg	May 2006	5.9	5.6	5.6	5.9	5.5	5.4	6.1
	July 2006	5.6	5.9	5.6	5.3	5.5	5.4	1.7
	October 2006	5.4	5.4	5.4	5.2	5.3	---	1.4
	May 2007	5.3	5.2	5.1	5.3	4.8	4.7	2.0
Mn	May 2006	2.3	2.2	2.3	2.4	2.2	2.2	6.0
	July 2006	2.2	2.3	2.3	2.1	2.2	2.1	0.71
	October 2006	2.1	2.1	2.1	2.0	2.1	---	0.54
	May 2007	1.9	1.9	1.9	1.9	1.7	1.7	0.83
Na	May 2006	0.5	0.7	0.6	0.9	0.8	0.7	0.7
	July 2006	0.4	0.5	0.4	0.4	0.5	0.5	0.2
	October 2006	1.3	1.4	1.3	1.1	1.3	---	0.9
	May 2007	5.9	5.2	5.2	5.9	5.9	6.9	3.8
Si	May 2006	11	9.1	9.6	10	13	13	6.5
	July 2006	8.7	9.0	9.4	9.5	10	11	3.2
	October 2006	9.7	9.6	8.5	8.9	9.1	---	3.6
	May 2007	8.6	8.5	8.5	9.2	8.5	8.9	3.4
Sr	May 2006	0.03	0.03	0.03	0.03	0.03	0.03	0.04
	July 2006	0.03	0.03	0.03	0.03	0.03	0.03	0.02
	October 2006	0.03	0.03	0.03	0.03	0.04	---	0.02
	May 2007	0.04	0.04	0.04	0.04	0.04	0.04	0.03

The major metal components at Fridays-2 Mine included Al, Ca, Fe, K, Mg, Na, and Si at concentrations of 2 mg/L or higher (Table **5-2**). Concentrations of these elements were all larger than those measured for Gum Boot Mine, specifically Al. Excluding the first and last sampling points (at -3 meters and 20 meters) which were collected from Fridays Run upstream (-3m) and downstream (10m) of the AMD stream mixing zone, there were no observable changes in elemental composition along the AMD flow path. Total dissolved Fe dropped slightly from emergence to mixing with the creek, with an average emergent concentration of 48.3 mg/L and an average of 38.5 mg/L just before mixing with Fridays Run.

Anion concentrations for Gum Boot Mine water samples measured by Ion Chromatography (IC) analysis did display some trends along the AMD flow path from emergence to Gum Boot Run (Table **5-3**). Measurements for chloride, nitrite (when detected), and nitrate all increased slightly from emergence to mixing. The trend for sulfate concentrations varied for the different sampling events. In February and May of 2006, sulfate concentrations did not display large changes along the flow path. However, for the other three sampling events, sulfate measurements increased greatly from emergence to mixing with Gum Boot Run. Some dilution effect may have been experienced at GB 127m where the Gum Boot Mine drainage mixes with a larger volume of water in Gum Boot Run.

Table **5-2**: Elemental composition of Fridays-2 water samples collected along the flow path as determined by ICP-AES analysis. All values are given in mg/L.

		Distance along flow path (m)					
Element	**Sample Date**	**-3**	**0**	**3**	**8**	**10**	**20**
Al	May 2006	0.06	22	22	23	23	7.6
	July 2006	0.1	21	21	21	21	17
	October 2006	0.95	22	21	22	21	21
	May 2007	---	17	17	18	17	---
Ba	May 2006	< 0.02	< 0.02	< 0.02	< 0.02	< 0.02	< 0.02
	July 2006	0.02	< 0.02	< 0.02	< 0.02	< 0.02	< 0.02
	October 2006	0.02	< 0.02	< 0.02	< 0.02	< 0.02	< 0.02
	May 2007	---	0.53	0.58	0.70	0.57	---
Ca	May 2006	10	63	63	64	64	29
	July 2006	14	55	57	55	55	48
	October 2006	15	60	60	61	59	58
	May 2007	---	61	62	62	59	---
Fe	May 2006	0.27	51	49	47	44	14
	July 2006	1.06	55	44	39	38	25
	October 2006	2.8	45	43	40	32	25
	May 2007	---	42	42	42	40	---
K	May 2006	0.7	3.5	3.2	3.4	3.3	1.6
	July 2006	1.0	3.3	3.2	3.3	3.3	2.9
	October 2006	1.1	3.5	3.3	3.3	3.3	3.2
	May 2007	---	3.4	3.4	3.4	3.6	---
Mg	May 2006	2.8	23	22	23	23	10
	July 2006	3.9	20	21	20	20	17
	October 2006	4.3	22	21	22	21	20
	May 2007	---	22	22	22	21	---
Mn	May 2006	0.01	1.4	1.4	1.4	1.4	0.51
	July 2006	0.36	1.2	1.3	1.2	1.2	1.1
	October 2006	0.32	1.3	1.3	1.3	1.3	1.2
	May 2007	---	1.2	1.2	1.2	1.2	---
Na	May 2006	1.6	15	16	15	15	6
	July 2006	2.1	15	14	15	15	12
	October 2006	3.9	16	15	16	16	15
	May 2007	---	19	19	20	20	---
Si	May 2006	4.3	28	29	23	22	13
	July 2006	4.0	20	20	20	20	17
	October 2006	5.0	22	21	21	21	21
	May 2007	---	19	19	19	19	---
Sr	May 2006	0.06	1.2	1.2	1.2	1.2	0.45
	July 2006	0.11	1.1	1.1	1.1	1.1	0.88
	October 2006	0.13	1.1	1.1	1.1	1.1	1.0
	May 2007	---	1.0	1.0	1.1	1.0	---

Table **5-3**: Anion concentrations of Gum Boot mine drainage samples collected along the flow path as determined by IC analysis. All values are reported as mM. ND=Not Detected.

		Distance along flow path (m)						
Anion	**Sample Date**	**0**	**2**	**9**	**15**	**60**	**95**	**127**
Chloride	May 2006	0.028	0.028	0.038	0.030	0.031	0.031	0.052
	July 2006	0.056	0.115	0.142	0.157	0.148	0.161	0.115
	May 2007	0.072	0.070	0.061	0.107	0.097	0.087	0.081
Nitrite	May 2006	0.082	0.080	0.083	0.082	0.070	0.077	0.081
	July 2006	ND	ND	ND	ND	ND	ND	ND
	May 2007	ND	ND	ND	ND	ND	ND	ND
Nitrate	May 2006	0.027	0.025	0.066	0.036	0.017	0.020	0.039
	July 2006	0.021	0.002	0.015	0.024	0.056	0.049	0.028
	May 2007	0.022	0.048	0.011	0.052	0.068	0.071	0.006
Sulfate	Oct. 2005	0.990	1.230	1.220	1.140	1.180	---	0.590
	Feb. 2006	0.801	0.767	0.836	0767	0.767	0.662	0.574
	May 2006	0.845	0.807	0.655	0.708	0.605	1.030	0.532
	July 2006	0.347	2.760	3.043	3.919	4.678	3.230	3.291
	May 2007	0.667	0.734	0.679	0.994	1.046	1.101	0.292

Fewer changes in anion concentrations along the AMD flow path were apparent for Fridays-2 Mine water samples (Table **5-4**). Chloride, nitriate, and nitrate concentrations did not change much from AMD emergence to mixing with Fridays Run. Except for one sampling event, sulfate concentrations increased by at least 1mM along the flow path. The samples for FR -3m and FR 20m were collected from Fridays Run to represent conditions before and after mixing with the AMD and, thus, were excluded from the flow path for trend analysis.

Water chemistry measurements of the AMD at Gum Boot and Fridays-2 were compared to previous studies conducted as part of remediation efforts. However, studies found in the literature only measured emergent mine drainage chemistry at either mine site and did not sample the AMD along the flow paths. A study conducted by the

Pennsylvania DEP (2006) found values for flow, pH, Al, Fe, Mn, and SO_4^{2-} to be similar to those measured in this study (Table **5-5**). Additionally, no large changes in mine drainage quality at Gum Boot were observed for the entire monitoring period of 11 years.

Table **5-4**: Anion concentrations of Fridays-2 mine drainage samples collected along the flow path as determined by IC analysis. All values are reported as mM. ND=Not Detected.

		Distance along flow path (m)					
Anion	**Sample Date**	**-3**	**0**	**3**	**8**	**10**	**20**
Chloride	May 2006	0.030	0.009	0.005	0.006	0.005	0.010
	July 2006	0.024	0.545	0.358	0.059	0.038	0.140
	May 2007	---	0.088	0.089	0.078	0.090	---
	July 2007	---	0.009	0.012	0.012	0.015	---
Nitrite	July 2006	0.031	ND	ND	ND	ND	ND
	May 2007	ND	ND	ND	ND	ND	ND
	July 2007	---	0.014	0.021	0.026	0.019	---
Nitrate	May 2006	0.077	0.088	0.028	0.032	0.024	0.069
	July 2006	0.038	0.042	0.008	0.020	0.035	0.026
	May 2007	---	0.020	0.017	0.021	0.023	---
	July 2007	---	0.003	0.008	0.011	0.008	---
Sulfate	Feb. 2006	0.493	3.961	3.927	4.216	4.063	14
	May 2006	2.578	2.633	1.465	3.956	4.212	25
	July 2006	0.040	0.188	4.016	4.237	4.425	25
	May 2007	---	2.858	2.505	3.976	3.999	---
	July 2007	---	4.172	4.927	5.712	5.643	---

Fridays-2 Mine emergent water chemistry values measured in this study were similar to values reported by previous surveys conducted by Growing Greener (2003) and Civil and Environmental Consultants, Inc. (2006) (Table **5-6**). Measurements for Al, Fe, and $SO4^{-2}$ reported by Growing Greener (2003) were slightly higher than measurements from the other studies for Fridays-2 Mine. However, mine drainage measurements at Fridays-2 did not display any major changes during the 5 years of monitoring.

Table **5-5**: Emergent water chemistry for Gum Boot Mine AMD discharge site #5. Values in the table include: Average ± SD; (minimum – maximum); and the number of samples, N. The values for the PADEP study were reported as averages but the number of samples, standard deviations, and ranges were not given.

Date	Flow (gpm)	Temp. (°C)	DO (mg/L)	Conductivity (µS/cm)	pH	Al (mg/L)	Fe (mg/L)	Mn (mg/L)	SO_4^{-2} (mg/L)
10/2005 – 05/2007	3.4	11.3 ± 2.9	0.2 ± 0.1	226	4.0 ± 0.1	0.8 ± 0.2	22.5 ± 1.7	2.3 ± 0.3	84.4 ± 9.5
This study	N=1	(8.9-15.0)	(0.1-0.3)	N=1	(3.8-4.1)	(0.60-1.2)	(20.0-24.0)	(1.9-2.8)	(76.9-95.0)
		N=4	N=4		N=6	N=5	N=4	N=6	N=3
1996 – 12/2004	4	---	---	---	3.9	1.2	24.2	2.5	105.9
PADEP, 2006									

Table **5-6**: Emergent water chemistry for Fridays Mine AMD discharge site #2. Values in the table include Average ± SD, (minimum – maximum), and the number of samples N.

Date	Flow (gpm)	Temp. (°C)	DO (mg/L)	Conductivity (µS/cm)	pH	Al (mg/L)	Fe (mg/L)	Mn (mg/L)	SO_4^{-2} (mg/L)
02/2006 – 07/2007	36	9.8 ± 0.1	0.36 ± 0.43	772 ± 1	4.1 ± 0.2	20.0 ± 2.4	45.2 ± 3.4	1.3 ± 0.1	316.3 ± 90.3
This study	N=1	(9.7-10.0)	(0-0.97)	(771-772)	(3.9-4.4)	(17-22)	(42-51)	(1.2-1.4)	(252.5-380.2)
		N=4	N=4	N=2	N=4	N=6	N=6	N=6	N=2
01/2002 – 05/2003	37 ± 15	10 ± 1	---	986 ± 87	3.8 ± 0.2	25.6 ± 2.6	51.8 ± 6.5	1.4 ± 0.1	519 ± 68
Growing Greener, 2003	(10-55)	(9-11)		(892-1110)	(3.6-4.1)	(22.3-28.9)	(46.3-64.5)	(1.3-1.6)	(438-619)
	N=6	N=6		N=6	N=6	N=6	N=6	N=6	N=6
10/2004 – 07/2006	35 ± 18	---	---	---	4.2 ± 0.4	20.6 ± 4.1	46.1 ± 17.0	1.3 ± 0.3	448 ± 79
CEC, 2006	(24-100)				(3.7-4.5)	(14.3-29.4)	(31.1-104)	(0.3-2.42)	(304.4-597.9)
	N=17				N=10	N=19	N=19	N=19	N=19

5.2 Microbial Characterization

Culture-based techniques were used to enumerate the number of IOB in the different sediment samples following procedures developed by Johnson (2005). Overall, the greatest activity appeared to occur between 2 m and 10 m from emergence at both Gum Boot and Friday-2 Mines (Figure **4-5**).

5.2.1 Population Counts

Counts of colony forming units (CFU) were conducted on sediments collected July 2006 and intended for use in the batch reactor experiments (Table **5-7**). Both initial and final killed batch reactor samples yielded zero CFU counts and, thus, only live reactor sample data is shown. Measurements for all three sediments were within the same order of magnitude, averaging about 3.5×10^4 CFU/g DW. Even though previous work indicated larger numbers of iron(II) oxidizing bacteria (IOB) at the FR 10m sampling location (Senko et al., in press), CFU measurements were almost identical for both Fridays-2 sediments. Overall, there was no difference in the number of culturable IOB among the three sediments (Figure **5-15**).

Table **5-7**: Initial population counts (as colony forming units per g dry weight sediment) of iron(II) oxidizing bacteria (IOB) for sediments collected from both field sites in July 2006.

Sediment	CFU/g DW (S.D.)
GB 2m	4.1×10^4 (2.2×10^4)
FR 3m	1.4×10^4 (3.7×10^3)
FR 10m	5.1×10^4 (9.4×10^3)

5.2.2 Scanning Electron Microscropy

Sediment samples were collected in the field, immediately preserved with gluteraldehyde, and then carefully prepared to retain biologic features. Scanning electron microscopy was used to obtain detailed images of sediments collected from both mine sites (Figure **5-3**). Among aggregates of unidentified cocci bacteria and iron precipitates, GB 0m sediments had helical stalks typically indicative of *Gallionella* spp. bacteria (Vatter and Wolfe, 1956). Both cocci bacteria and rigid hollow sheaths typical of *Leptothrix* spp. (Hashimoto et a., 2007) were also visible in GB 9m sediments. In sediments collected at GB 15m, iron precipitate-coated cocci bacteria were found among larger aggregates.

SEM images of sediments collected from Fridays-2 sampling locations revealed less morphological diversity in the types of microorganisms (see Figure 5-3). FR 3m sediments had large clusters of unidentified cocci bacteria. Images of FR 10m sediments also displayed cocci bacteria that appeared to be covered in iron precipitates. The abundance of microorganisms was similar in the SEM images of both mine sites.

However, morphological diversity was greater among the microorganisms found in Gum Boot Mine sediments.

5.2.3 Phylogenetic Characterization of the Bacterial Communities

In a collaborative study by Senko et al. (in press), nucleic-acid based characterization of the bacterial communities at Gum Boot and Fridays-2 Mine sites was conducted to evaluate the phylogenetic diversity of the two AMD systems (see Appendix E for methods). At both Gum Boot and Fridays-2, the AMD emergence sampling locations (GB 0m and FR 0m) had the lowest phylum-level diversity while the stream samples (GB 127m and Fridays Run upstream and downstream) displayed the highest diversity (Figure **5-4**). Sampling locations with the highest rates of iron(II) oxidation (GB 2m and FR 10m) had similar banding patterns, suggesting similar community structure. However, phylum-level assignments of genetic sequences revealed the same phyla but different community compositions at the sampling locations GB 2m and FR 10m. The heterotrophic Actinobacterial and Gammaproteobacterial IOB were prevalent on both iron mounds, suggesting these organisms were predominantly responsible for the biological iron(II) oxidative precipitation.

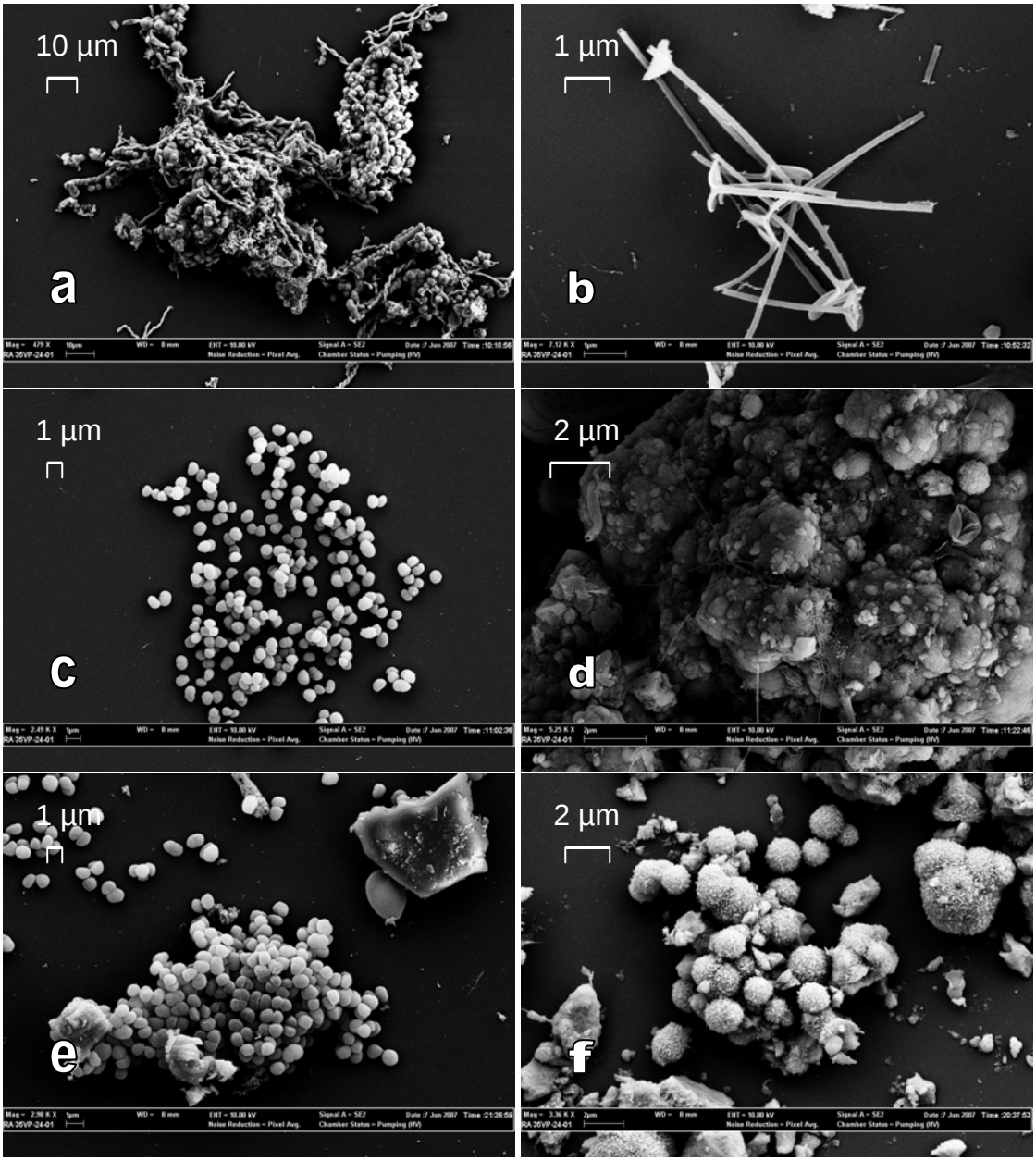

Figure **5-3**: SEM images of field sediment samples: a) Gum Boot 0m; b) Gum Boot 9m; c) Gum Boot 9m; d) Gum Boot 15m; e) Fridays-2 3m; and f) Fridays-2 10m. Images courtesy of Dr. G. Zhang.

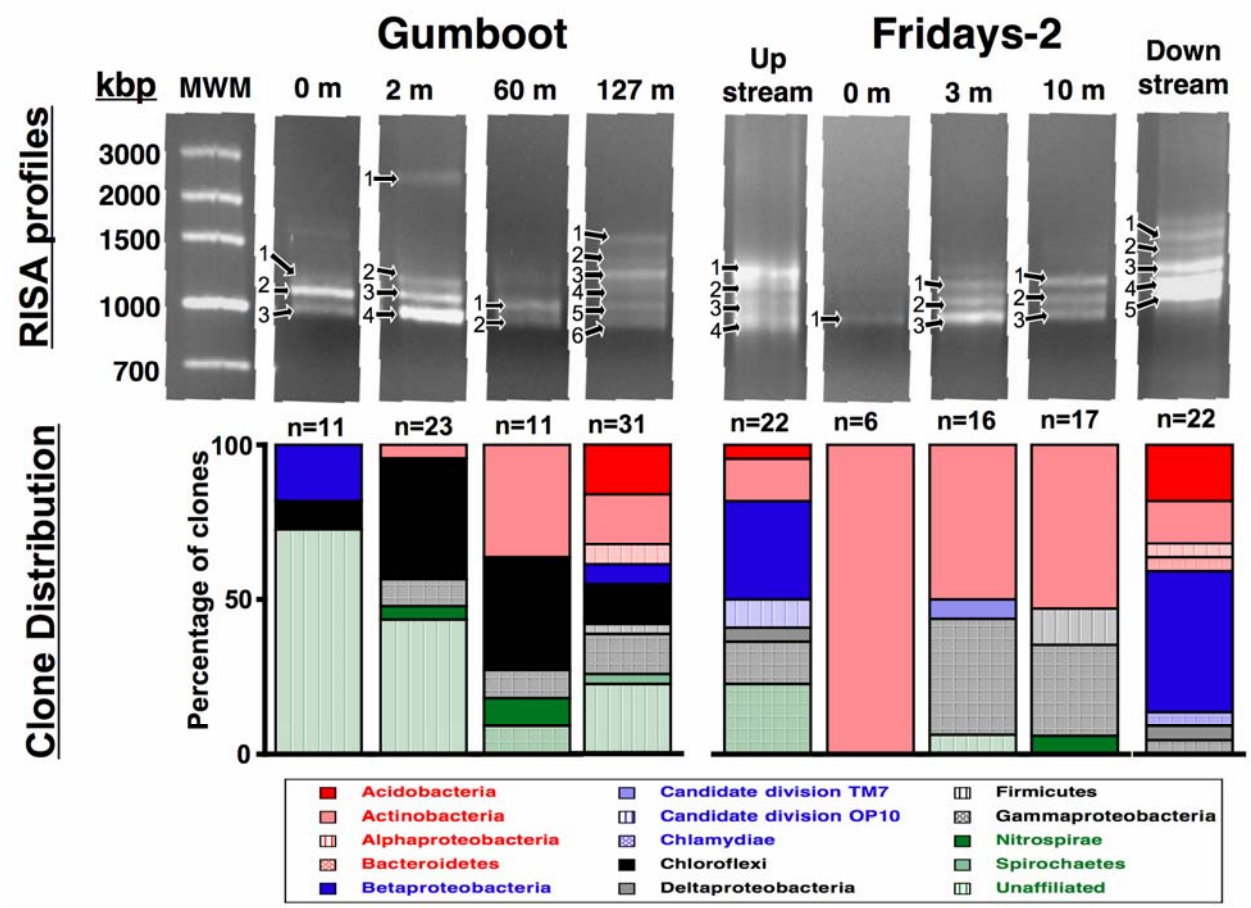

Figure **5-4**: Ribosomal intragenic spacer analysis (RISA) (top panels) and phylum-level distribution of 16S rDNA sequences observed in the close libraries recovered from the RISA gel (bottom panel) of microbial communities present at discrete sampling points in the Gum Boot and Fridays-2 Mine systems. "Unaffiliated" sequences are those that could not be assigned to an established bacterial phylum with ≥ 80% confidence using Ribosomal Database Project II's classifier function. n indicates the number of clones in each 16S rDNA clone library (Senko et al., in press).

5.3 Batch Reactor Experimental Results

To examine the kinetics of iron(II) oxidation at Gum Boot Mine and Fridays-2 Mine, iron sediments collected from each mine site were incubated in synthetic acid mine drainage while exposed to one of several pre-determined gas mixes. Iron(II)

concentrations and pH were measured daily throughout the experiments. At one week intervals, iron(II) was reintroduced to the batch reactors in the form of concentrated iron(II) spikes. Additionally, several control reactors were run simultaneously with the experimental reactors to examine the effects of individual variables.

5.3.1 Solution Chemistry

The iron(II) and pH results of the batch reactor experiments for live and killed control reactors are presented in Figure **5-5** to Figure **5-10**. All three sediments were used for gas mixes 1 through 4. However, since no large differences were observed between FR 3m and FR 10m sediments, only FR 10m and GB 2m sediments were used in the experiments with gas mixes 5 and 6. See Table **4-2** for the composition of each gas mixture.

There were very few differences between the soluble iron(II) results for live FR 3m and FR 10m sediments (Figure **5-11**). However, variations between Gum Boot and Fridays live reactors were observed. Fridays sediments appeared capable of sustained iron(II) oxidation with O_2 concentrations as low as 0.7%. Unable to maintain iron(II) oxidation under 0.7% O_2, iron(II) was more efficiently removed in Gum Boot sediments maintained under 1.5% O_2. Almost no variation in iron(II) oxidation was observed between the three sediments at O_2 concentrations of 10% or greater. With the exception of gas mixes 1 and 6, the greatest variation in the removal of soluble iron(II) between sediments occurred during the second iron(II) addition.

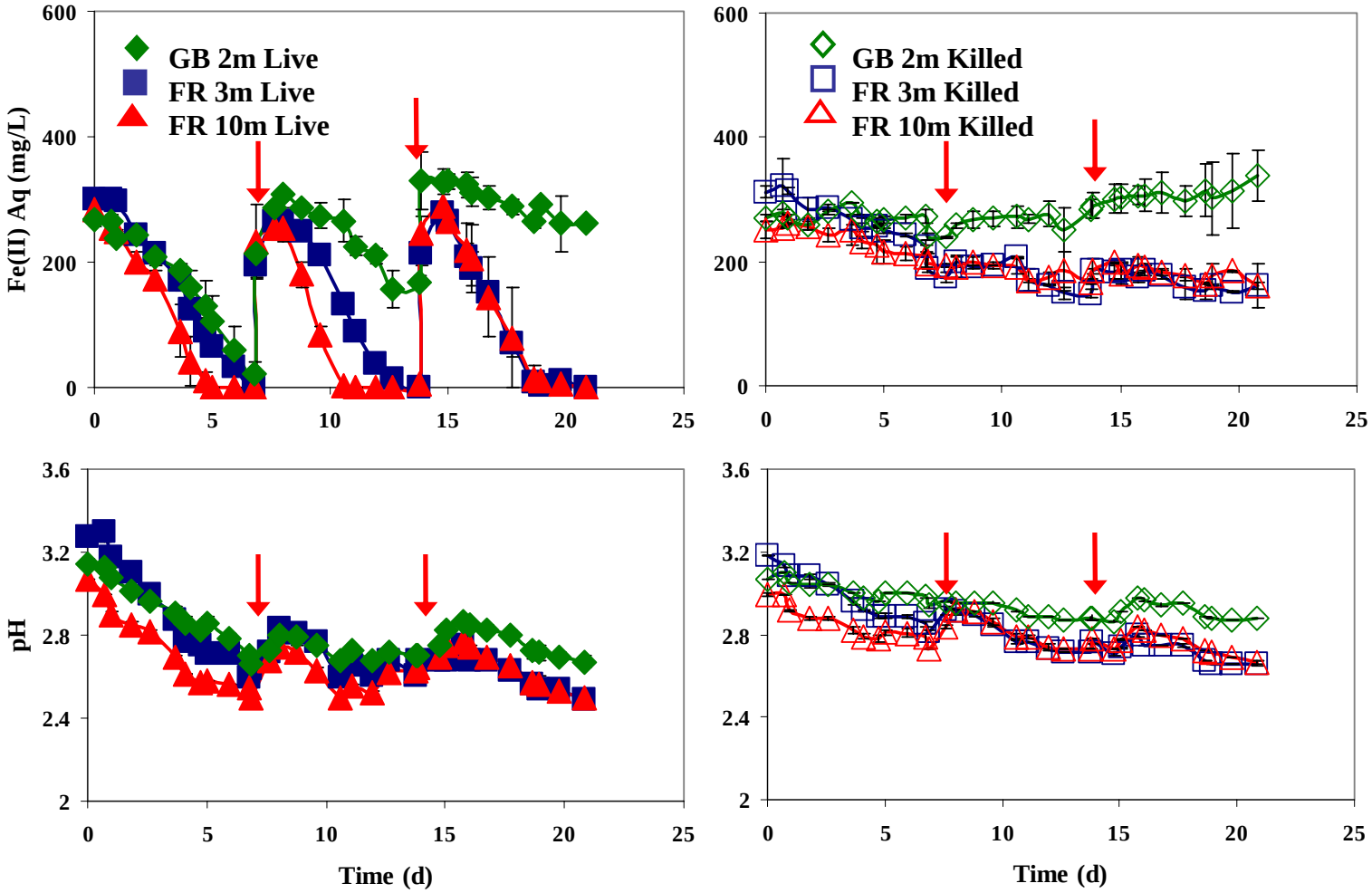

Figure 5-5: Soluble iron(II) concentrations and pH measurements for sediment batch reactors maintained under gas mix 1 comprised of 0.7% O_2, 1.1% CO_2, and 98.2% N_2. Red arrows indicate time when iron(II) was added to the reactors.

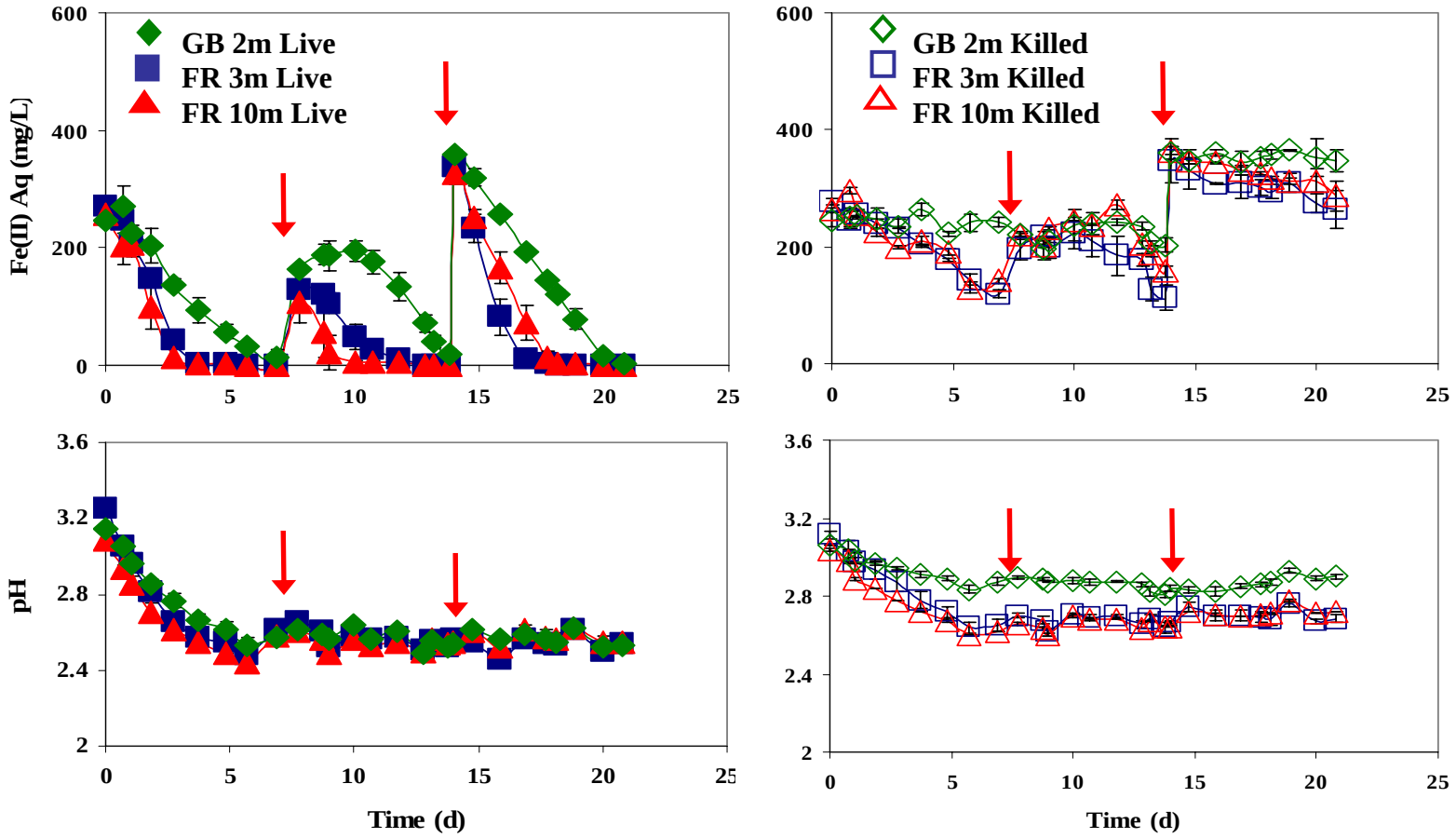

Figure **5-6**: Soluble iron(II) concentrations and pH measurements for sediment batch reactors maintained under gas mix 2 comprised of 1.5% O_2, 7.3% CO_2, and 91.2% N_2. Red arrows indicate time when iron(II) was added to the reactors.

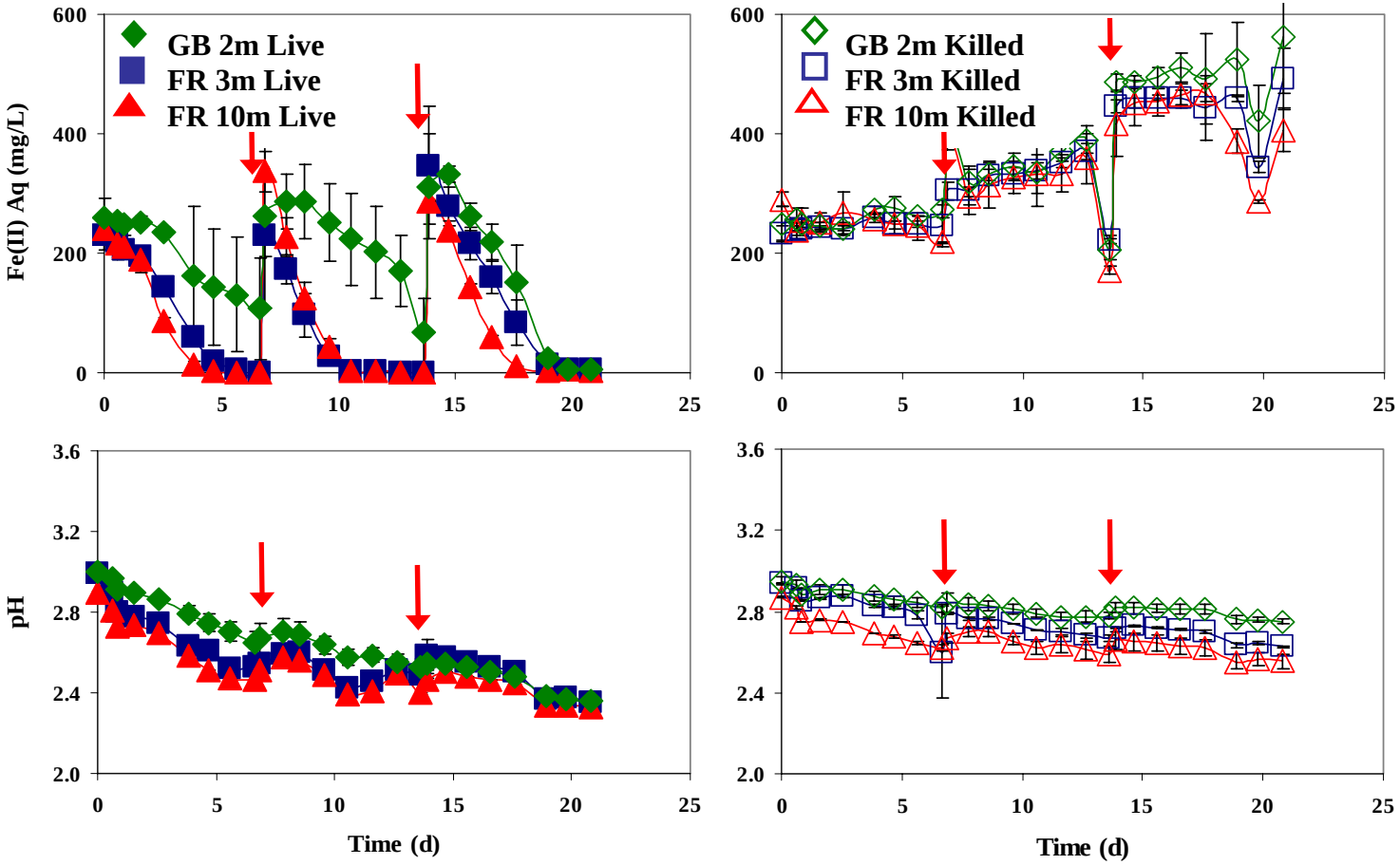

Figure **5-7**: Soluble iron(II) concentrations and pH measurements for sediment batch reactors maintained under gas mix 4 comprised of 10% O_2, 1% CO_2, and 89% N_2. Red arrows indicate time when iron(II) was added to the reactors.

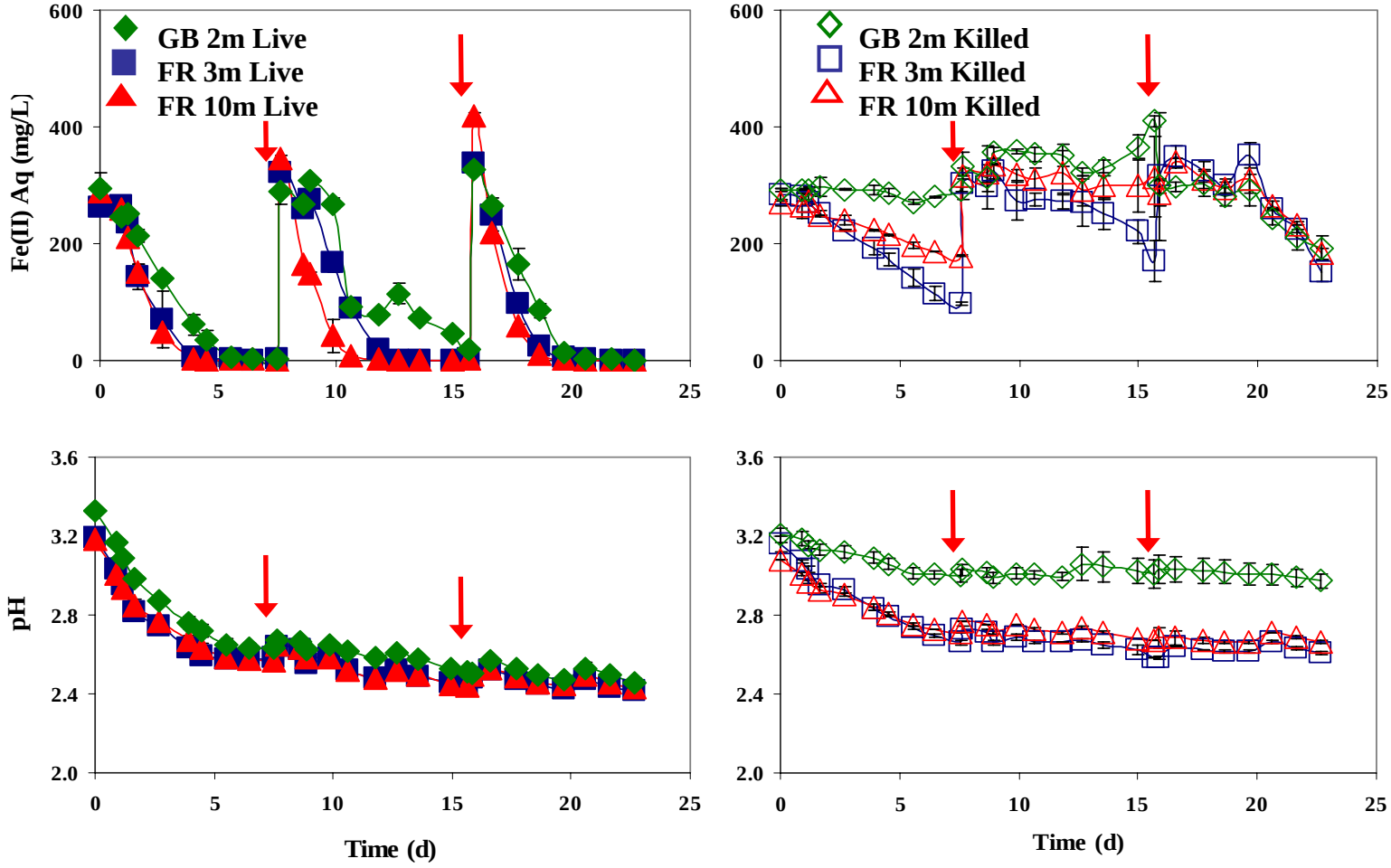

Figure **5-8**: Soluble iron(II) concentrations and pH measurements for sediment batch reactors maintained under gas mix 3 comprised of breathing air (21% O_2, 0.035% CO_2, and 78% N_2). Red arrows indicate time when iron(II) was added to the reactors.

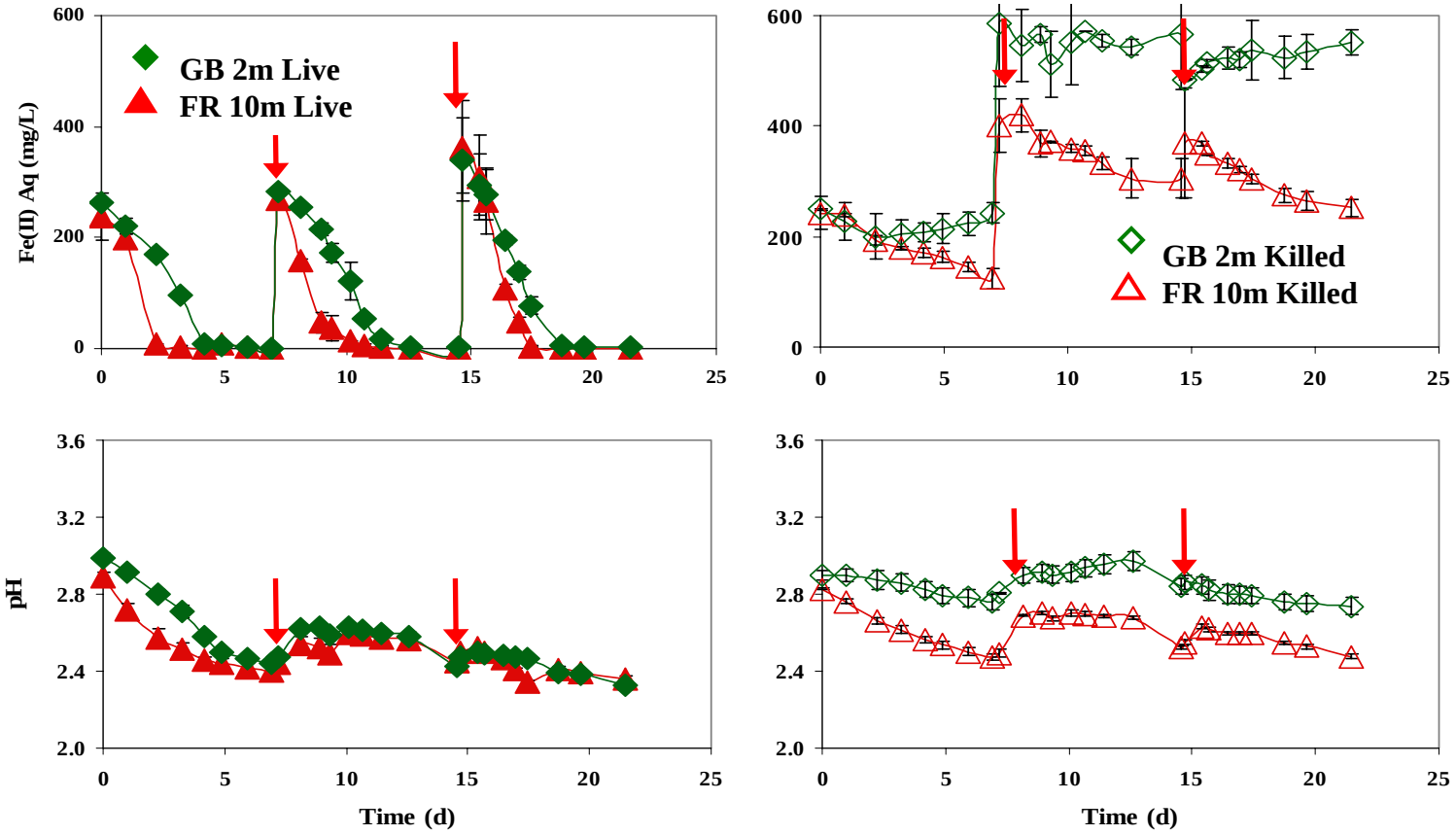

Figure **5-9**: Soluble iron(II) concentrations and pH measurements for sediment batch reactors maintained under gas mix 5 comprised of breathing air (21% O_2, 0.035% CO_2, and 78% N_2) and amended with 50 mg/L glucose. Red arrows indicate time when iron(II) was added to the reactors. Glucose was added to the batch reactors at time=0 and at subsequent iron(II) additions.

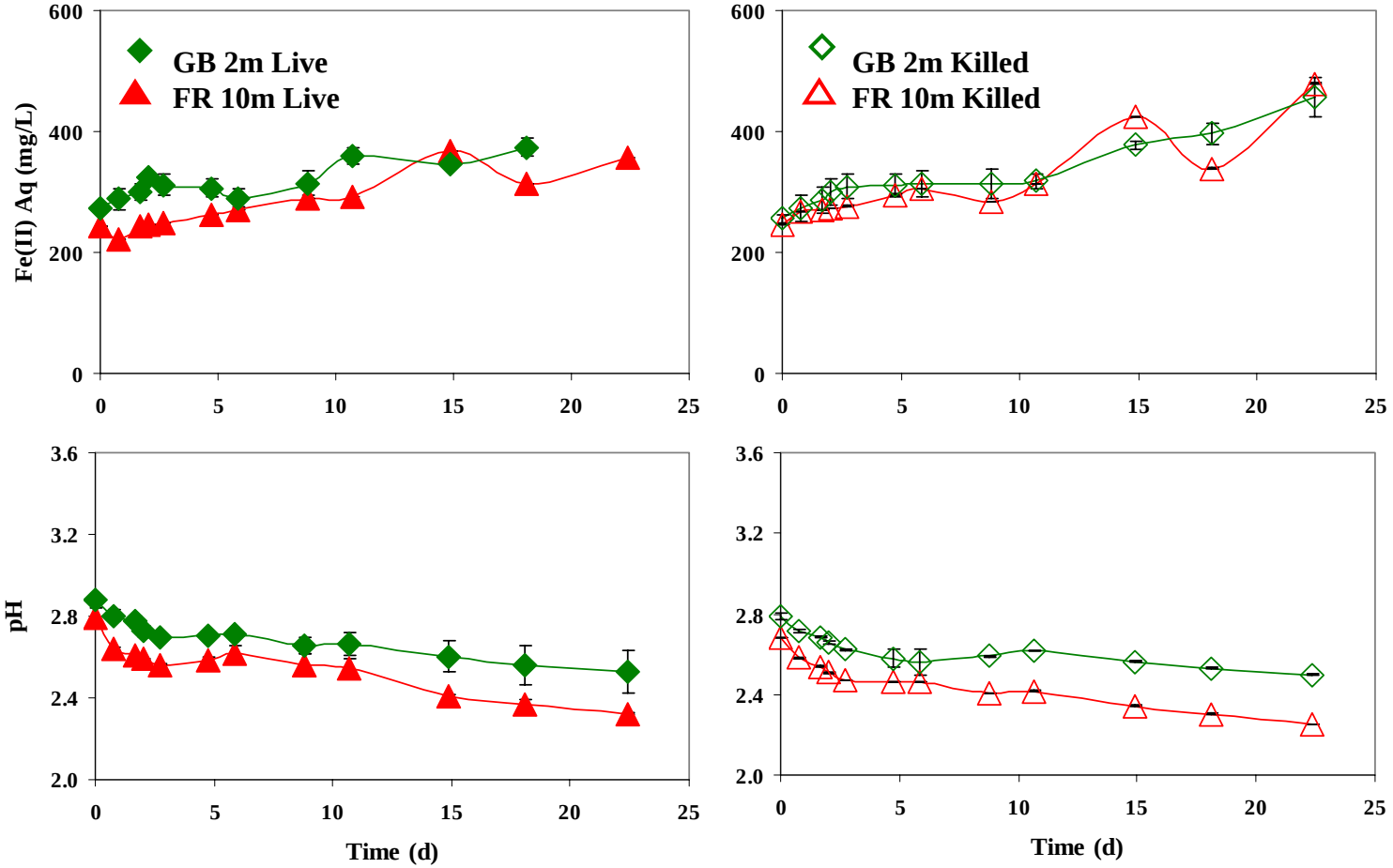

Figure **5-10**: Soluble iron(II) concentrations and pH measurements for sediment batch reactors maintained under gas mix 6 using 5% CO_2, and 95% N_2. This experiment did not involve 2nd and 3rd iron(II) additions.

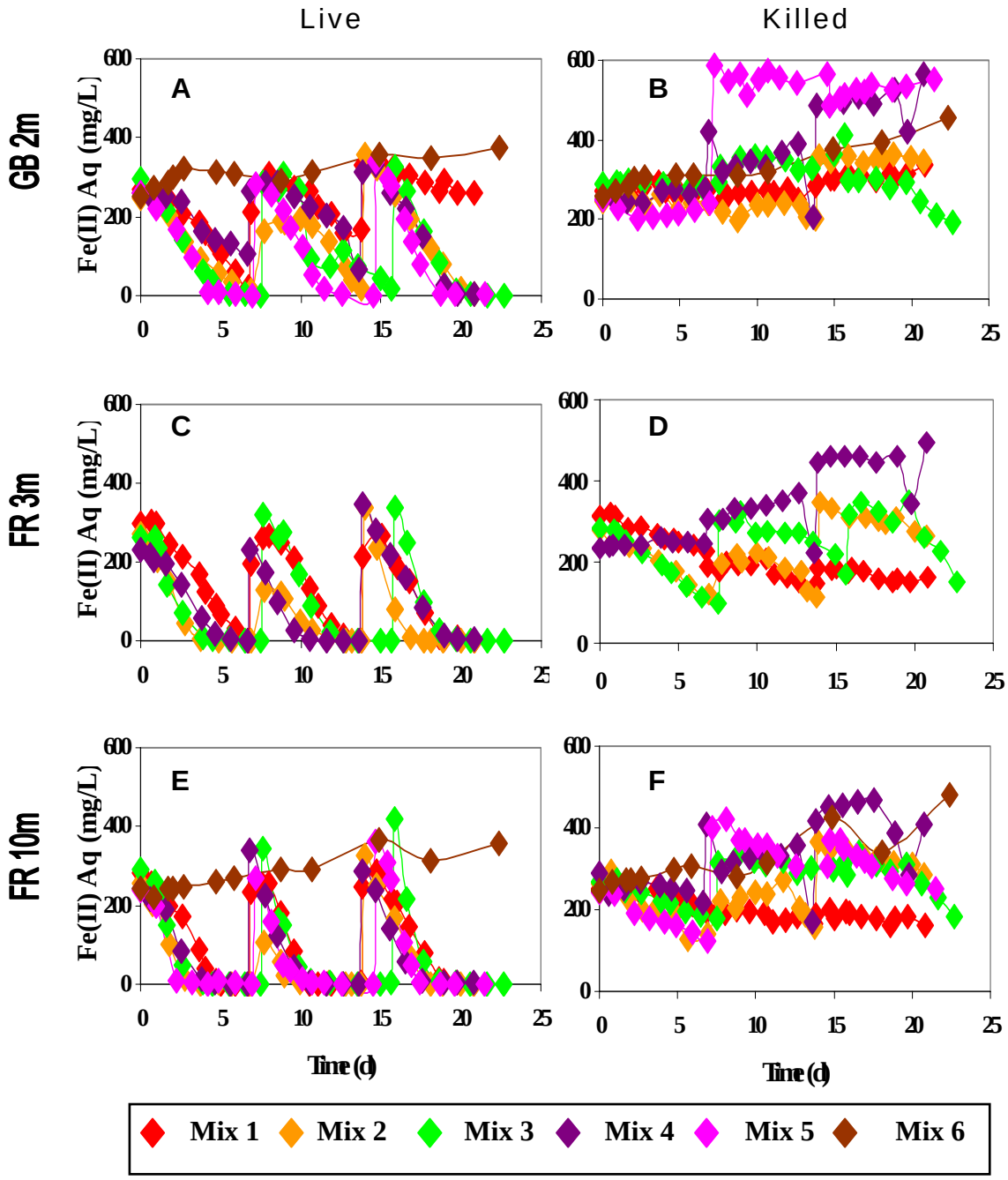

Figure **5-11**: Soluble iron(II) concentrations from all six gas mixes for live and killed reactors. Panels A and B represent GB 2m sediments. C and D represent FR 3m sediments and E and F represent FR 10m sediments. FR 3m sediments were not used in experiments with gas mixes 5 and 6. Legend: mix 1, 0.7% O_2; mix 2, 1.5% O_2; mix 3, breathing air; mix 4, 10% O_2; mix 5, breathing air + glucose; and mix 6, 0% O_2.

No strong differences in pH values were observed between the three sediments during each experiment. The pH values from the reactors' first iron(II) addition were used to compare each sediment across the gas mixes since pH adjustments were not made during the first addition. As O_2 increased from 0.7 to 1.5%, pH decreased faster and reached lower values during the first spike. However, no other differences were observed at higher O_2 concentrations.

The breathing air gas mix was duplicated in gas mixes 3 and 5 to look the possible contribution of heterotrophic activity to the iron(II) oxidation occurring at each mine site. Gas mix 5 incorporated additions of glucose (to maintain a concentration of about 50 mg/L) that were timed to occur immediately after the iron(II) additions (Figure **5-9**). No obvious differences in iron(II) concentrations or pH were observed between the sediments incubated with and without additional glucose.

The experiment conducted under gas mix 6 examined the loss of iron(II) from solution (presumably via oxidative precipitation) and/or the production of iron(II) into solution (presumably via reductive dissolution of iron(III) minerals) from the sediments under anaerobic conditions. Only microaerobic concentrations were obtained (see the following section); however, iron(II) concentrations increased and pH values decreased continuously from the start to the conclusion of the experiment (Figure **5-10**). In both the live and killed batch reactors, iron(II) and pH measurements were almost always higher in the GB2m reactors than in the FR 10m reactors.

Except for experiments conducted under gas mix 4 (10% O_2, 1% CO_2, and 89% N_2), both FR 3m and FR 10m killed reactors experienced more iron(II) removal from solution than the GB 2m killed reactors. The addition of formaldehyde to the killed

control reactors slightly lowered the initial pH values but this addition did not affect the overall trends observed. Throughout the duration of all 6 experiments, the pH measurements in the GB 2m killed batch reactors remained consistently higher than the pH values in the Fridays-2 killed batch reactors. All killed reactors showed a slight increase in iron(II) concentration from the start to the conclusion of each experiment, likely the result of evaporative water loss from the positive gas pressure maintained in the reactors. The pH of the killed batch reactors continued to drop consistently throughout the experiments. In the microaerobic environment under gas mix 6 (5% CO_2, 95% N_2), neither FR 10m nor GB 2m sediments showed any iron(II) oxidation (Figure **5-10**).

Control incubations were conducted on live sediments using iron(II)-free SAMD to determine the affects of sorption or desorption of iron(II) on the observed oxidation rates (Figure **5-12**). Any affect of desorption of iron(II) disappeared after 3 days for both FR 3m and FR 10m sediments. Soluble iron(II) remained in solution for GB 2m sediments for the duration of the experiment. Higher iron(II) concentrations for GB 2m suggests either higher dissolution rates or lower oxidation rates. However, for both mine sites, the maximum iron(II) measurements were about one order of magnitude less than the initial spiked concentrations used in the experimental batch reactors. The pH values of the three sediments were initially relatively similar and all declined throughout the course of the incubation.

To determine the possibility of phosphorus-limitation on the activity of the iron oxidizing bacteria, live GB 2m sediments were incubated with breathing air using SAMD both with (GB 2m reactors) and without phosphorus (PF reactors) (Figure **5-13**). There were no observable differences for either soluble iron(II) or pH between the two GB 2m

treatments. The slight variation in iron(II) concentration during the third spike was due to different iron(II) concentrations in the spike solutions; this difference was minimized quickly through oxidation. IOB population counts were performed on initial and final time samples from the gas mix 5 samples (Table **5-8**). CFU counts showed initial IOB numbers were similar between GB 2m and PF reactors, but GB 2m populations increased by an order of magnitude while PF counts decreased by an order of magnitude over the course of the experiment.

Table **5-8**: Microbial population counts for iron(II) oxidizing bacteria, reported as colony forming units (CFU) per g dry weight (DW). The gas mix 5 experiment (breathing air, glucose and iron(II) spikes) included reactors with GB 2m sediments and synthetic acid mine drainage either with (GB 2m) or without phosphorus (PF). Counts are for initial and final time samples for GB 2m and PF reactors, with standard deviations given in parentheses.

Reactor (treatment)	**Initial (CFU/g DW)**	**Final (CFU/g DW)**
GB 2m	2.8×10^6	2.6×10^7
(with phosphorus)	(1.2×10^5)	(6.4×10^6)
PF	1.2×10^6	1.2×10^5
(without phosphorus)	(3.6×10^5)	(3.6×10^4)

Control reactors were run using SAMD and no sediments (NS) to determine the effects of sediments on the killed reactor iron(II) concentrations (Figure **5-14**). FR 10m sediments appeared to have a larger rate of decline for both soluble iron(II) and pH compared to the other reactors; there were fewer differences between the GB 2m and no-sediment control reactors. Overall, little variation was observed between the formaldehyde-killed reactors and the no-sediment experiment control reactors. Counts conducted on killed and NS final slurries resulted in counts of zero CFU/g DW.

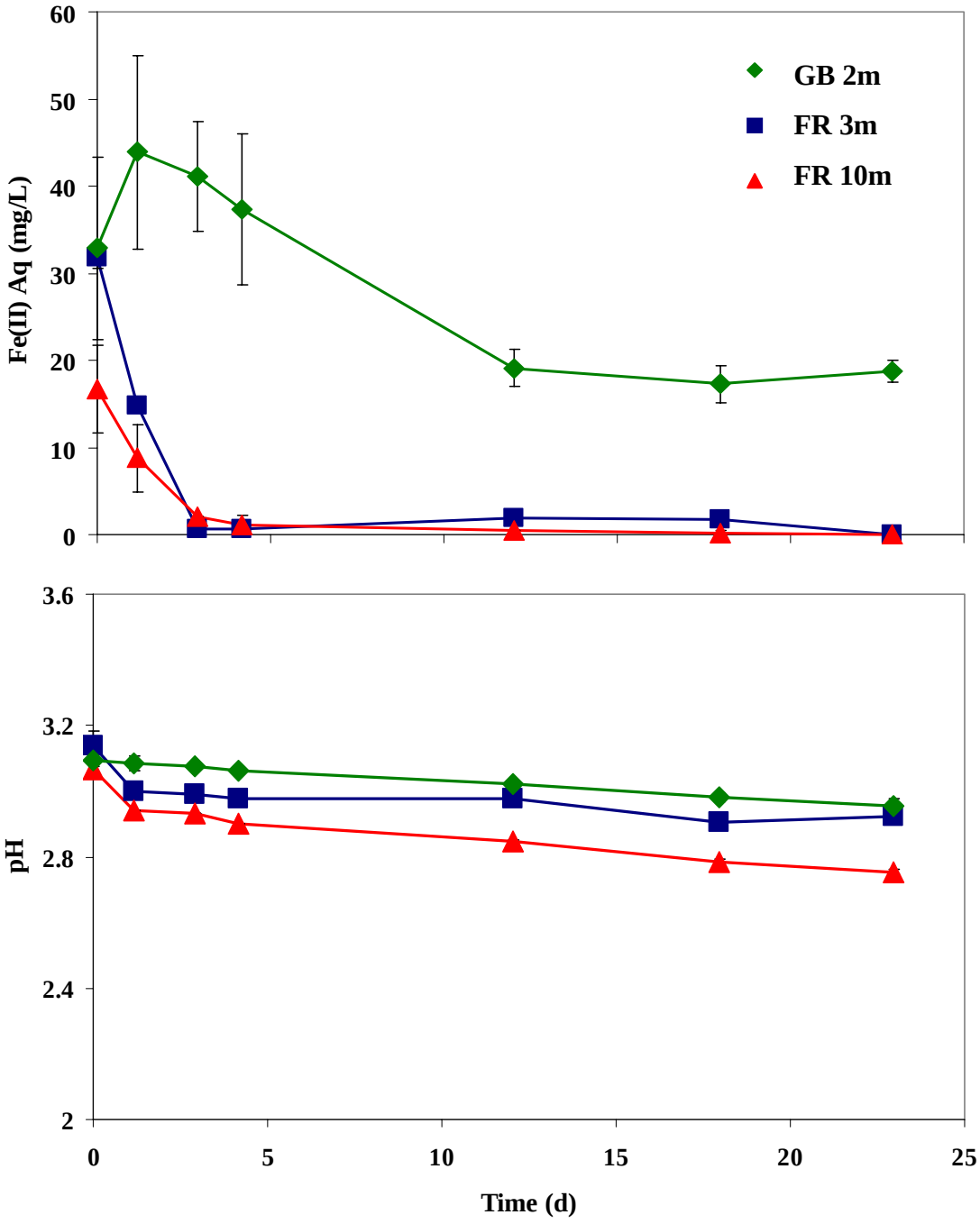

Figure **5-12**: Soluble iron(II) concentrations and pH measurements for live sediment incubations with iron(II)-free synthetic mine water. Green, blue, and red represent the GB 2m, FR 3m, and FR 10m sediments respectively. Reactors were 100 mL serum bottles left open to the ambient air and shaken by hand periodically.

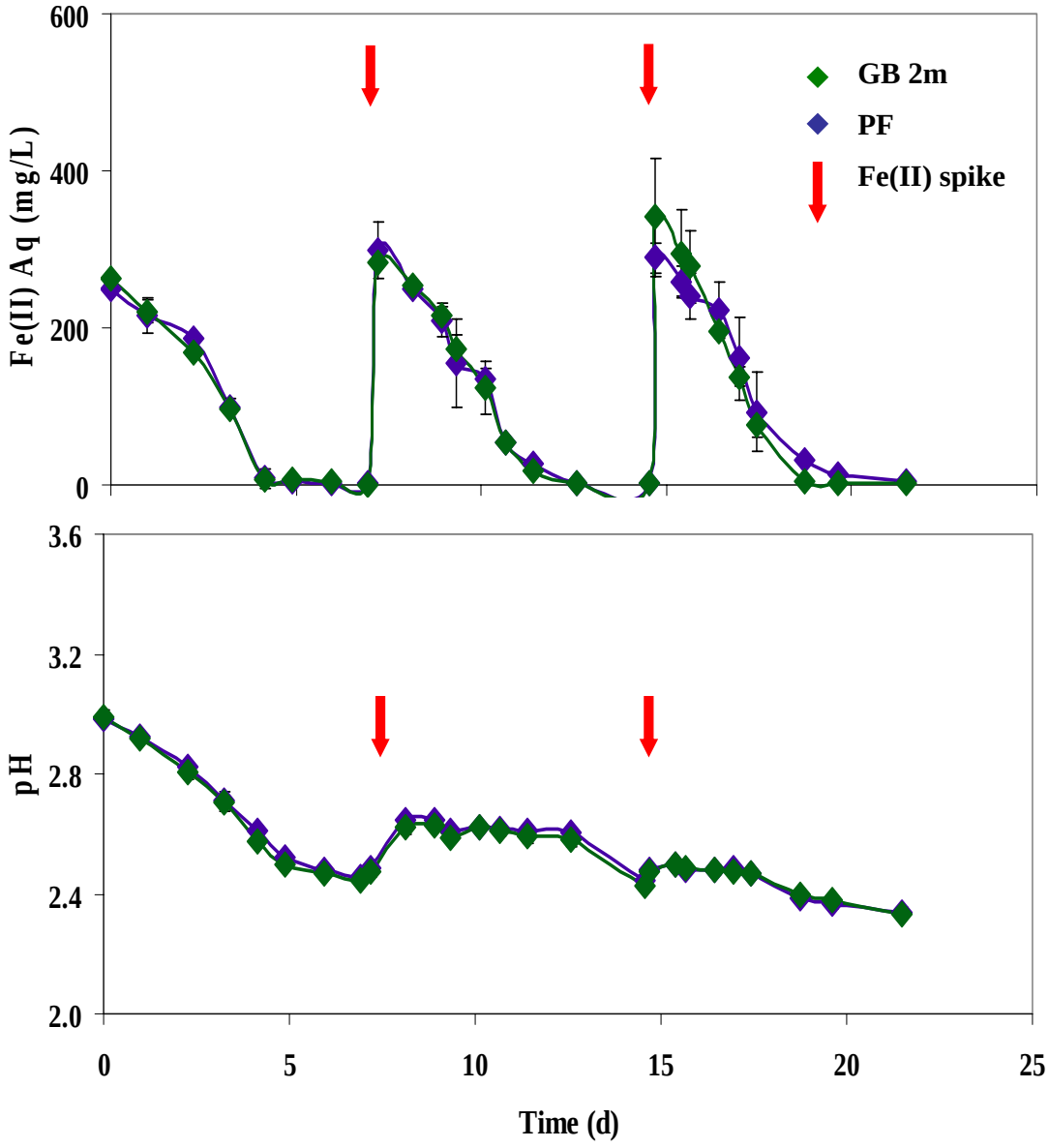

Figure **5-13**: Soluble iron(II) concentrations and pH measurements for GB 2m sediments for the experiment conducted under gas mix 5 (breathing air) + glucose. Green markers represent live sediments incubated in SAMD containing phosphorus while purple markers are live sediments that were incubated in phosphorus-free SAMD. Red arrows indicate iron(II) spikes. PF = Phosphorus-Free.

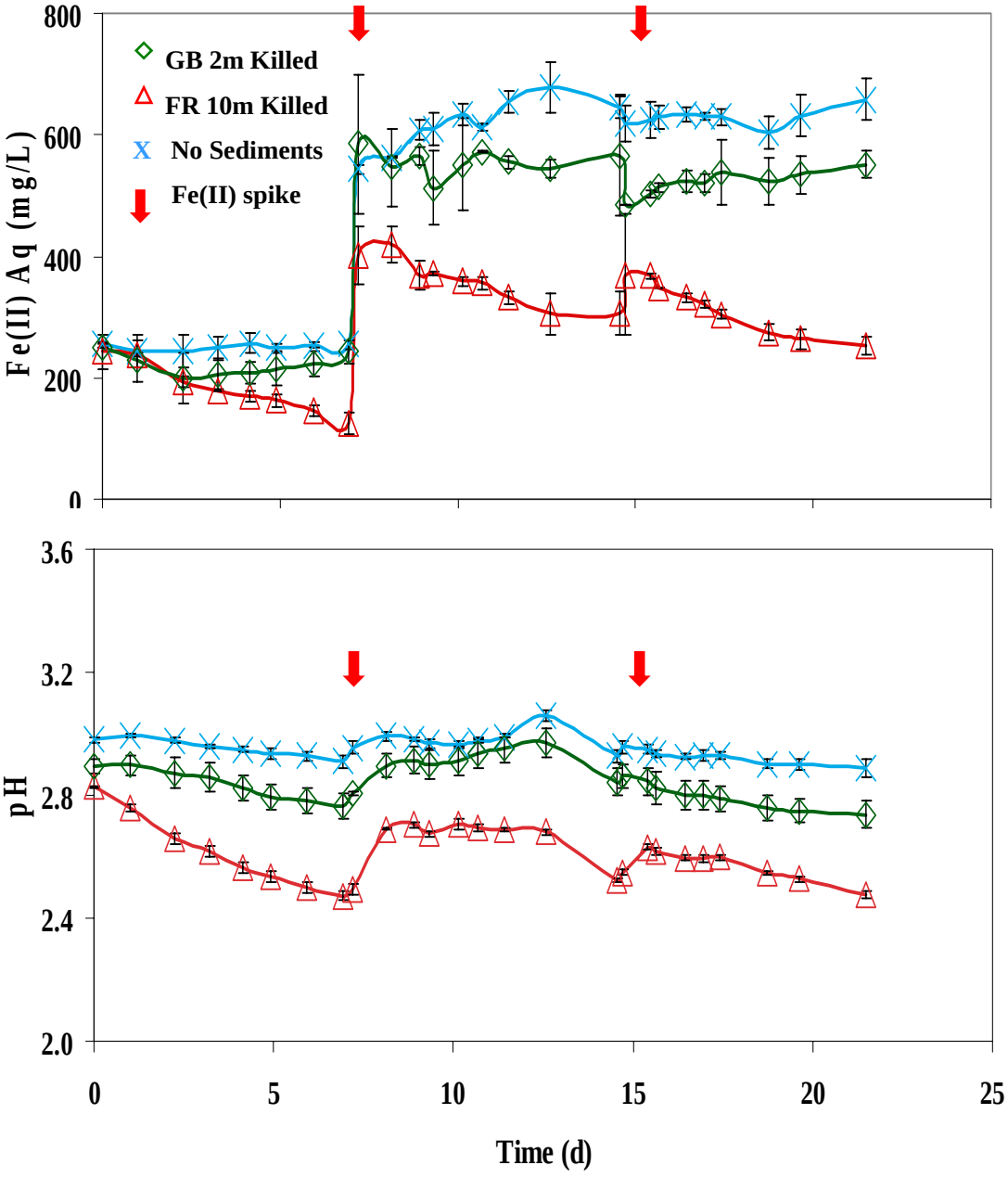

Figure **5-14**: Soluble iron(II) concentrations and pH measurements for killed and no-sediment control reactors for the experiment conducted under gas mix 5 (breathing air) + glucose. Red, green, and blue represent FR 10m, GB 2m, and no-sediment reactors respectively. Red arrows indicate iron(II) spikes. No-sediment reactors did not receive glucose additions.

5.3.2 Microbial Population Counts

Population counts of iron oxidizing bacteria (IOB) were conducted on live reactor slurries collected at the conclusion of each experiment (Figure **5-15**). CFU counts for the first two gas mixes with 0.7 and 1.5% O_2 did not differ much from the initial sediment values for all three sediments. At oxygen concentrations of 10% or higher, all three sediments experienced an increase in IOB numbers with the largest changes occurring in GB 2m reactors. All killed reactors yielded counts of zero CFU/g DW.

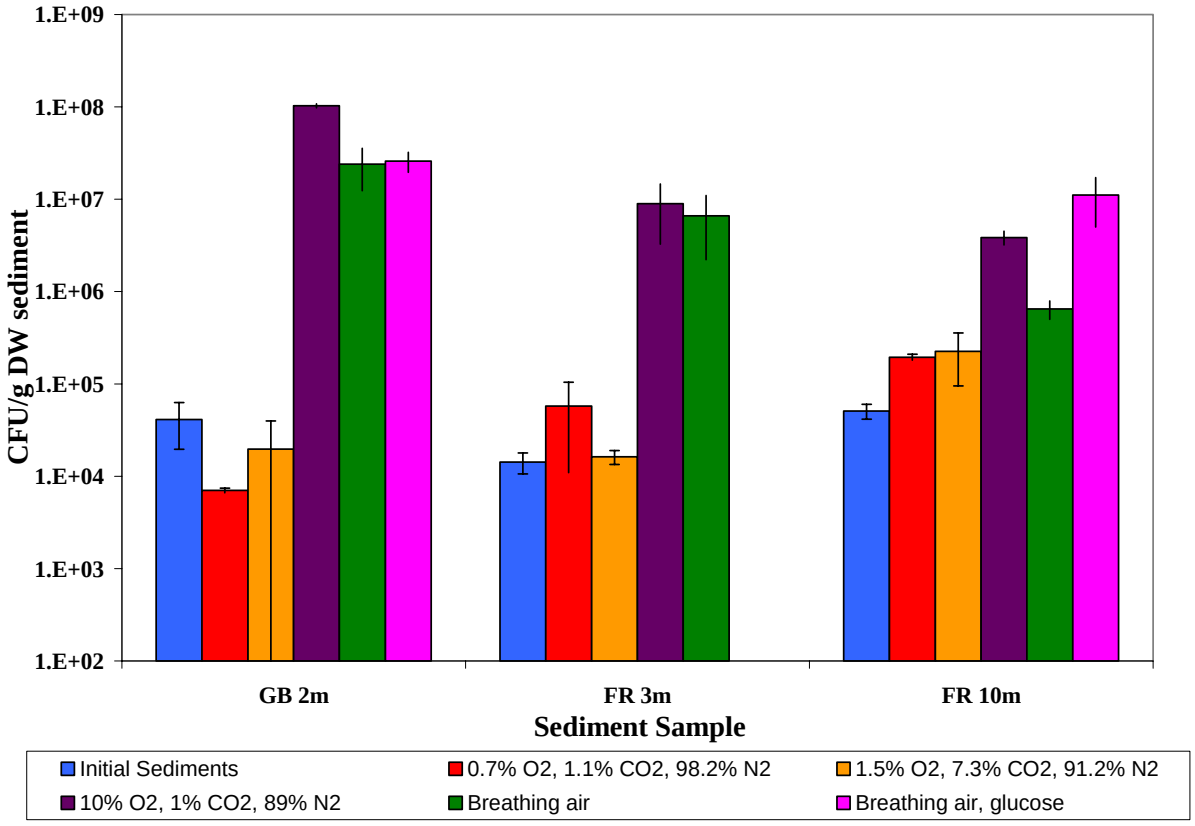

Figure **5-15**: Colony forming units (CFU/g DW) for iron(II)-oxidizing bacteria counts using initial sediments and live reactor slurry samples from the conclusion of each experiment. GB 2m refers to sediments collected 2 m downstream of AMD emergence at Gum Boot Mine. FR 3m and FR 10m refer to sediments collected 3 and 10 m downstream, respectively, of AMD emergence at Fridays-2 Mine. Legend identification: Blue, Initial Sediments; Red, 0.7% O_2; Orange, 1.5% O_2; Purple, 10% O_2; Green, 21% O_2; Pink, 21% O_2 + glucose.

5.3.3 Iron(II) Oxidation Rates

Iron(II) oxidation rates were calculated for the three sediments to compare performance of the mine sites under varying environmental conditions. Zero and first order rate laws were considered for the rate calculations. Biological and abiotic rates were then compared to examine the effects of different concentrations of oxygen and carbon dioxide on the ability of Gum Boot and Fridays-2 Mine sediments to remove iron(II) from solution.

5.3.3.1 Data Selection for Kinetic Analysis

To calculate the iron(II) oxidation rates of the different sediments, both zero order (Eq. **5.1**) and first order reaction rate laws (Eq. **5.2**) were applied to the plots of soluble iron(II) concentrations for the first and third iron spikes. A zero order reaction results in a linear graph when concentration is plotted with time; the slope of the line is the negative value of the rate constant, k. Multiple zero or near-zero points at the end of each iron spike were omitted from the zero order plot (Figure **5-16**); this omission was due to the likelihood that biological oxidation is not occuring to any great extent once soluble iron(II) concentrations have been depleted.

$$[Fe(II)] = -k * T + [Fe(II)]_0 \qquad \textbf{5.1}$$

$$\ln [Fe(II)] = -k * T + \ln [Fe(II)]_0 \qquad \textbf{5.2}$$

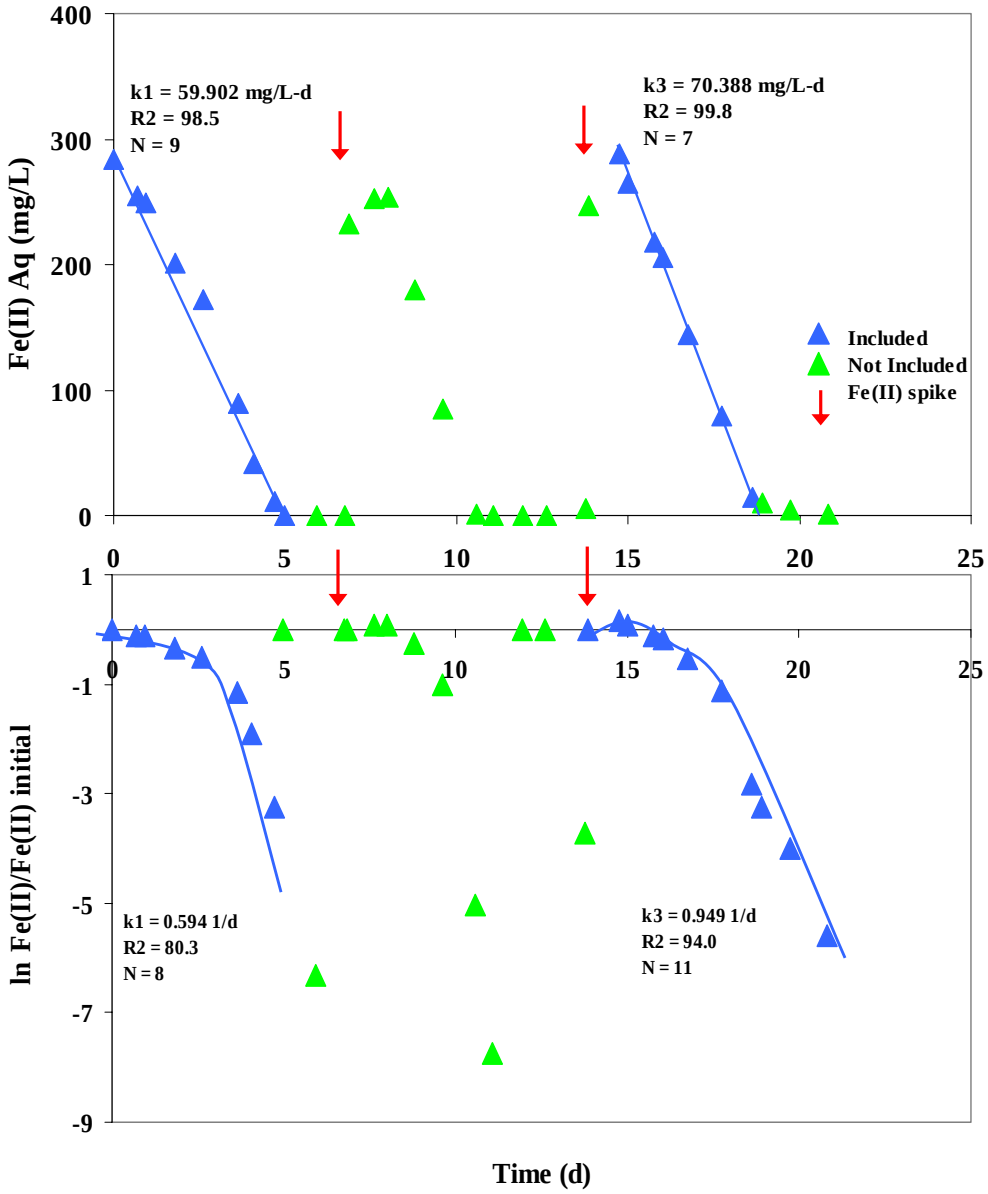

Figure **5-16**: Selection of data points for kinetic analysis of iron(II) oxidation rates from the first and third iron(II) additions, using zero and first order rate equations for each addition. Only FR 10m sediments for gas mix 1 (0.7% O_2) are shown here but similar selection methods were used for GB 2m and FR 3m sediments. Blue triangles represent data points included in the rate calculation while green triangles are data points not included. Multiple near-zero values were omitted from the zero order rate calculation; zero values were omitted from the first order rate calculation.

Iron(II) data was also plotted to calculate the first order reaction rates. A first order reaction results in a linear graph when the natural logarithm of the concentration is plotted with time; the slope of the line is the negative value of the rate constant, k. However, a first order reaction also has an exponential graph when the natural logarithm of concentration / initial concentration is plotted against time. Any zero points were omitted from the first order plot due to mathematical limitations of the rate equation.

5.3.3.2 Reaction Order Justification

Both zero and first order reaction equations were used to calculate the iron(II) oxidation rate constants for all three sediments under each gas mix. Published rates of iron(II) oxidation are frequently reported in units of concentration/time, which is consistent with the units of zero order k values (Nemati et al., 1998). However, other studies have reported oxidation rates as 1/time, the units for first order k values (Pesic et al., 1989). *Microsoft Excel* software was used to calculate the zero and first order rate constants and R^2 values for both. *Minitab* software was then used to calculate p values to determine the level of correlation, useful when multiple independent variables could explain variation in one dependent variable.

The zero order rate equation fit the experimental data very well (Table **5-9**). With the exception of gas mix 6 (5% CO_2, 95% N_2), all zero order R^2 values were equal to 0.900 or greater. All but one zero order p value suggested good correlation of the data, with values of 0.05 or less.

Table **5-9**: Comparison of zero order and first order rate models for the batch reactor sediment incubations, using the data from the first iron(II) spike. R^2, k_0, and k_1 were determined using Excel graphing features. P values were calculated with Minitab software.

		Zero Order			First Order	
Gas Mix	**Sediment**	**k_0 (mg/L-d)**	**p**	**R^2**	**k_1 (1/d)**	**R^2**
Mix 1#*	FR3m	49.3	0.000	0.982	0.420	0.641
(0.7% O_2, 1.1% CO_2, 98.2% N_2)		(N=11)			(N=11)	
	FR10m	59.9	0.000	0.985	0.594	0.803
		(N=9)			(N=8)	
	GB2m	36.5	0.000	0.955	0.301	0.774
		(N=11)			(N=11)	
Mix 2#*	FR3m	78.5	0.000	0.977	1.14	0.908
(1.5% O_2, 7.3% CO_2, 91.2% N_2)		(N=6)			(N=7)	
	FR10m	76.7	0.002	0.947	1.34	0.919
		(N=6)			(N=8)	
	GB2m	39.9	0.000	0.955	0.420	0.949
		(N=9)			(N=9)	
Mix 3#	FR3m	67.6	0.000	0.929	0.847	0.926
(21% O_2, 0.035% CO_2, 78% N_2)		(N=7)			(N=10)	
	FR10m	71.0	0.000	0.937	0.964	0.913
		(N=7)			(N=10)	
	GB2m	56.3	0.000	0.987	0.745	0.939
		(N=8)			(N=10)	
Mix 4#	FR3m	44.7	0.000	0.978	0.836	0.871
(10% O_2, 1% CO_2, 89% N_2)		(N=8)			(N=9)	
	FR10m	49.8	0.000	0.943	1.06	0.936
		(N=8)			(N=9)	
	GB2m	25.4	0.000	0.945	0.141	0.944
		(N=9)			(N=9)	
Mix 5#	FR3m	---	---	---	---	---
(21% O_2, 0.035% CO_2, 78% N_2,	FR10m	82.6	0.052	0.900	1.45	0.905
glucose)		(N=4)			(N=4)	
	GB2m	56.8	0.000	0.970	0.891	0.910
		(N=6)			(N=8)	
Mix 6	FR3m	---	---	---	---	---
(5% CO_2, 95% N_2)	FR10m	- 8.46	0.000	0.798	- 0.025	0.829
		(N=12)			(N=12)	
	GB2m	- 7.39	0.010	0.922	- 0.021	0.924
		(N=12)			(N=12)	

Multiple zero or near-zero values at the end of each spike were omitted from the calculation of the linear trend line.
* Values of zero were graphically omitted in order to calculate the exponential trend lines.

While the first order rate equation also fit the data well, the correlation was not as strong as with the zero order equation. Several first order R^2 values were below 0.900, with the lowest value of 0.641. Unfortunately, p values were not calculated due to software limitations. However the high zero order and lower first order R^2 values support the decision to focus our comparisons and discussion on zero order iron(II) oxidation rate constants in this study.

5.3.3.3 Batch Reactor Iron(II) Oxidation Rates

The rates of iron(II) oxidation in the live sediment batch reactors were considered the overall oxidation rates, comprised of both biological and abiotic processes. By simply assuming a direct additive contribution, the biological oxidation rates were obtained by subtracting the killed (or abiotic) rates from the overall rates. With all gas mixes except number 6 (5% CO_2, 95% N_2), the biological rate of iron(II) oxidation exceeded the abiotic rate (Figure **5-17**).

In the first iron(II) addition, the rates of iron(II) oxidation in the three sediments do not display large variations but FR 3m and FR 10m sediments have slightly higher overall rates than GB 2m sediments. However, the abiotic rates of Gum Boot sediments are much less than the Fridays-2 abiotic rates. Surprisingly, biological and abiotic iron(II) oxidation rates decreased with 10% O_2 in almost all batch reactors. Overall, Gum Boot sediments showed an increase in overall rate with 21% or greater O_2 concentrations while the overall rates for Fridays-2 sediments increased as O_2 concentrations were raised.

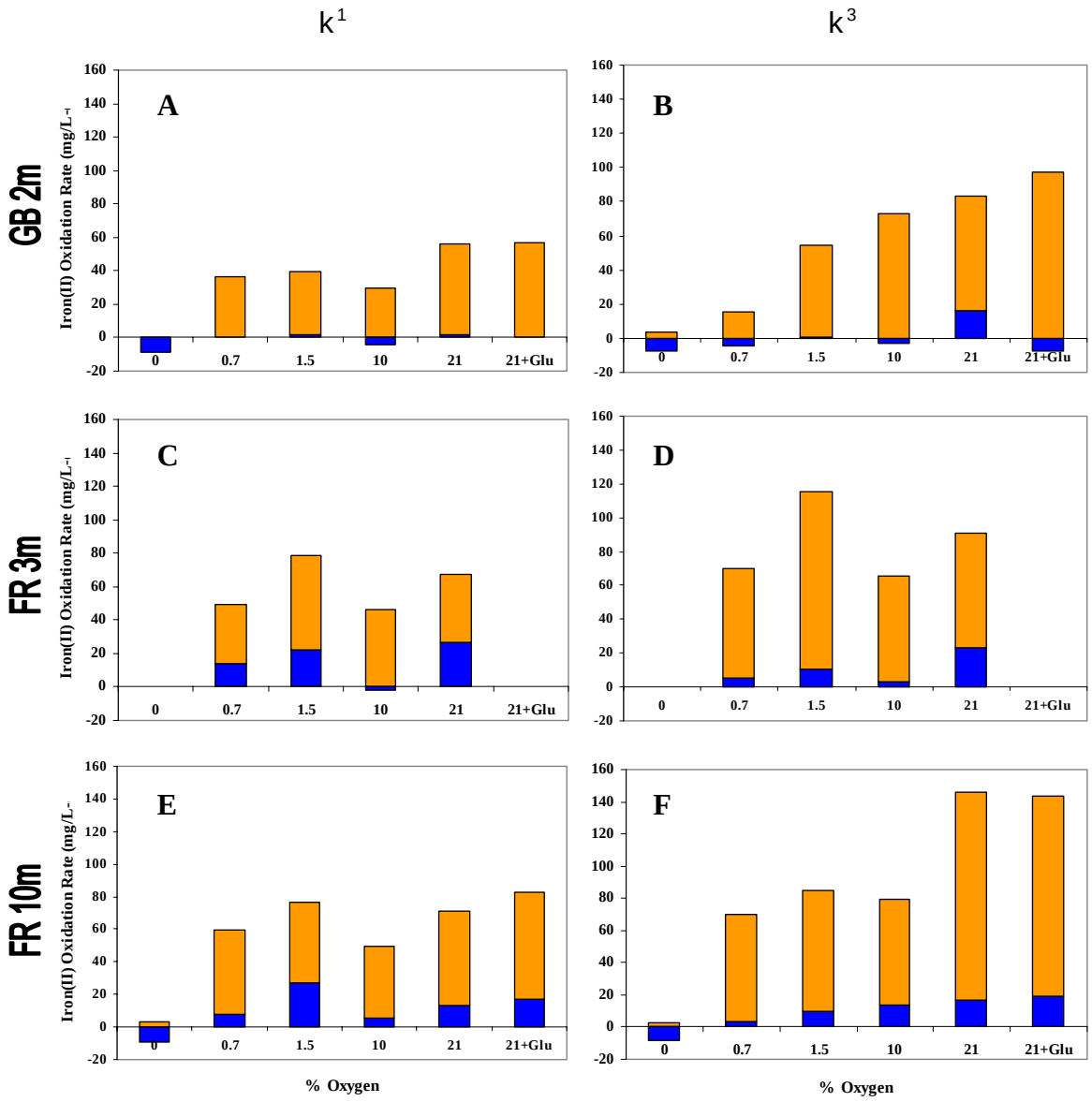

Figure **5-17**: Zero-order rates of iron(II) oxidation for GB 2m, FR 3m, and FR 10m sediments. Blue and orange represent the abiotic and biological contribution, respectively; biological values were obtained by subtracting the abiotic rate from the overall rate. Different batch experiments are designated by % O_2: 0, 0.7, 1.5, 10, 21, and 21% + glucose. The 21% + Glucose gas mix represents experiment 5 with breathing air and glucose spikes. FR 3m sediments were omitted from experiments 5 and 6 with 21% O_2 + glucose and 0% O_2. The labels of k^1 and k^3 represent the rates for the first and third iron(II) additions, respectively, during the batch reactor experiments.

While similar trends were observed for rates from the third iron(II) addition, the magnitude of the biological and overall rates were much larger than first addition rates. Biological iron(II) oxidation rates were much higher at 21% O2 than at lower concentrations for both GB 2m and FR 10m sediments. Additionally, FR 10m sediments achieved overall rates almost twice as fast as GB 2m sediments at oxygen concentrations of 21%. Lastly, though rates did increase during the third iron(II) addition, FR 3m sediments did not experience any noticeable changes in iron(II) oxidation removal with changes in oxygen concentration.

5.4 Modeling Results for Batch Reactor Iron(II) Oxidation Kinetics

The different modeling outputs from STELLA were plotted against the soluble iron(II) concentrations for live FR 10m sediments during the experiments conducted under gas mix 1 (0.7% O_2, 1.1% CO_2, and 98.2% N_2), mix 2 (1.5% O_2, 7.3% CO_2, and 91.2% N_2), and mix 3 (breathing air) (Figure **5-18**). For all three gas mix experiments, the Kirby et al. (1999) model over-predicted the observed rate of iron(II) oxidation. Variations in k_{bio} and C_{bact} resulted in noticeable changes in iron(II) oxidation and precipitation during each experiment. At lower O_2 concentrations, the model results using a lower kinetic rate constant of 1.02 x 10^8 L^3/mg-mol^2-s appeared to have the best fit to the batch reactor data. Model results for higher O_2 concentrations over-predicted the rate of iron(II) oxidation in the batch reactors except for the run using k_{bio} of 1.02 x 10^8 L^3/mg-mol^2-s and C_{bact} of 1.5 mg DW/L (Mix 3).

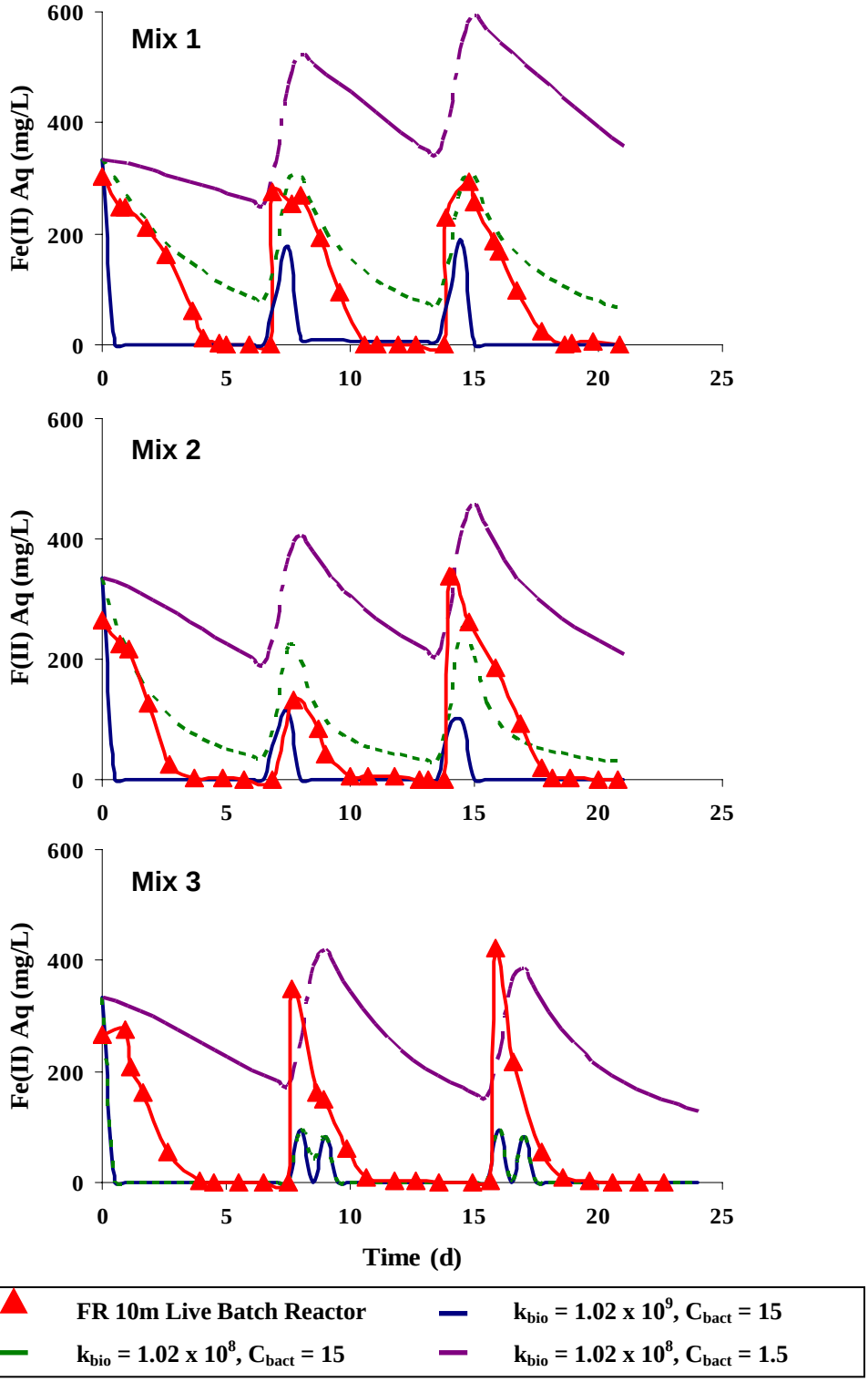

Figure **5-18**: Soluble iron(II) concentrations for the FR 10m live batch reactors under gas mix 1 (0.7% O2), mix 2 (1.7% O2), and mix 3 (breathing air). Modelled output is also included. k_{bio} is the biological kinetic rate constant (L^3/mg-mol^2-s) and C_{bact} is the bacterial concentration (mg DW/L). An iteration time of 0.5 d was used in STELLA.

6 DISCUSSION

While Gum Boot and Fridays-2 Mines have similar mine overburden, drainage characteristics, and emergent AMD chemistry, the rapid removal of iron(II) from the mine drainage is observed at Gum Boot but not at Fridays-2. The drop in pH at Gum Boot is indicative of the formation and precipitation of iron(III) (oxyhydr)oxides. Previous studies on the sediments of Gum Boot and Fridays-2 revealed the presence of iron(III)-minerals schwertmannite and goethite at the mine sites (data not shown; Figure E:1, Appendix E). These minerals are typically found at iron-rich, high sulfur mine drainage systems with a pH of 2.8 – 4.5 (Bigham et al., 1996). While the pH dropped slightly more at Gum Boot than Fridays-2 in the first 10 m, some decrease was observed at Fridays-2 for each sampling point. Thus, the formation of iron(III) precipitates from the oxidation of iron(II) was likely occurring at both Gum Boot and Fridays-2 Mines, despite the difference in observed removal of iron(II) along the mine drainage flow paths.

Temperature and DO increased at both mine sites through sheet flow over the hardened iron mounds. The cold groundwater at Gum Boot was quickly warmed by sunlight due to little canopy cover; however, any increase in temperature at Fridays-2 was much less since the iron mound was shaded for most of the day and the residence time across the iron mound was much shorter compared to Gum Boot. DO increased noticeably from AMD emergence to mixing with the creek at both mine sites. Closer comparison of DO changes reveals little difference in concentration or increase between

the two mine sites within the first 10 m of flow (Figure **6-1**); at Fridays-2, the AMD was near DO saturation before mixing with the creek. The difference in iron(II) removal at Gum Boot and Fridays-2 is probably not due to differences in oxygen diffusion as the AMD flows over the iron mounds.

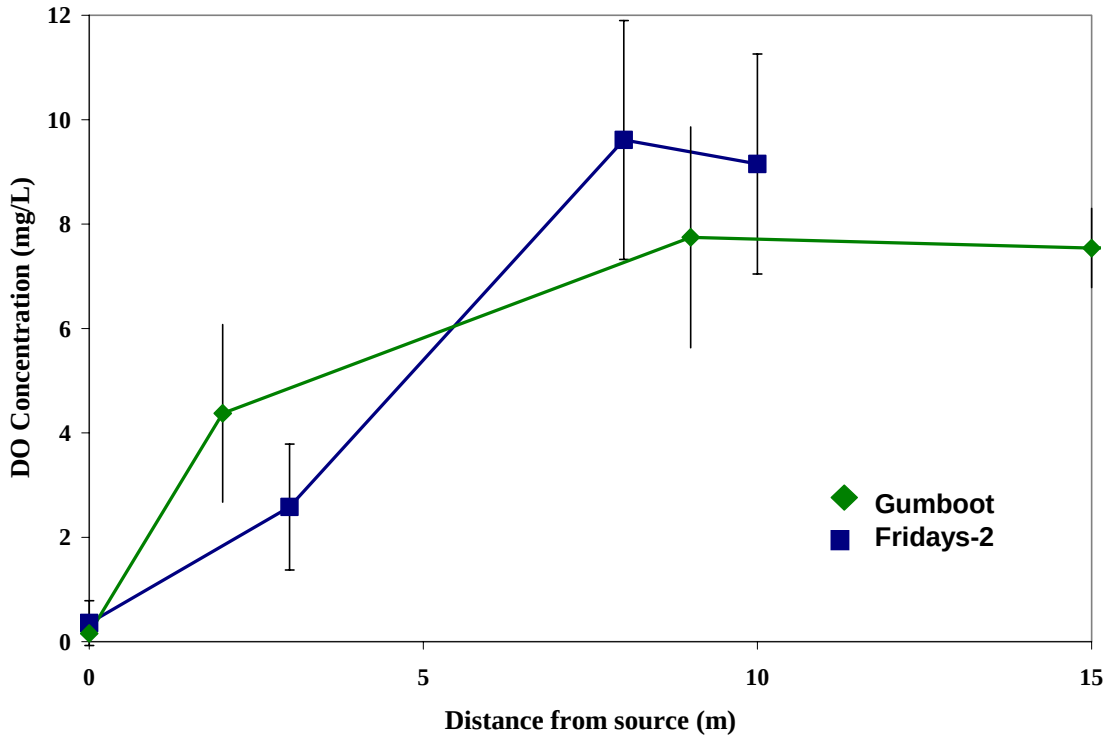

Figure **6-1**: Comparison of average DO concentration along the mine discharge flow paths. Blue represents Fridays-2 Mine (N=4 sampling events) and green represents Gum Boot Mine (N=4 sampling events).

Due to the annual leaf senescence each autumn, both Gum Boot and Fridays-2 Mines receive a large amount of organic matter (OM) that can be incorporated into the iron mounds and leach nutrients into the AMD over time. Additionally, dissolved OM

can drain from the mine overburden and contribute to the nutrient load of the AMD. However, microbial growth may decline under conditions of nutrient limitation which would result in a decrease in iron(II) removal capacity for a mine drainage system. Thus, the identification of nutrient limitation at either mine would suggest a less-than-optimal rate of biological iron(II) oxidation.

Previous work demonstrated that biological iron(II) oxidation can be uncoupled from cellular growth at limited CO_2 concentrations. (Kelly and Jones, 1978). Using the overall stoichiometric relationship for autotrophic biological iron(II) oxidation and biomass synthesis for IOB (Smith et al., 1988) (Eq. **3.7**), 0.0045 moles of CO_2 are utilized for every mole of iron(II) oxidized. Given the emergent iron(II) concentrations at Gum Boot (0.1-0.8 mM) and Fridays-2 (0.8-1.0 mM), inorganic carbon limitation could occur at CO_2 concentrations of 0.00045 mM to 0.0036 mM. However, measurements for total inorganic carbon (TIC) at Fridays-2 Mine have been as high as 2.39 mM TIC as C, or the equivalent of $pCO_2 = 0.043$ atm (personal communication, B. Means). Since Gum Boot and Fridays-2 Mines were likely developed along the same coal seam and have similar overburden (personal communication, J. Smoyer), emergent concentrations of TIC are probably similar between these two mines sites. As a result, autotrophic IOB at these mine sites are not likely CO_2-limited.

To identify potential nitrogen limitation, nitrogen demands can be calculated from the iron(II) and TN measurements of the emergent AMD at Gum Boot and Fridays-2 Mines (Eq. **3.7**). The commonly-used Redfield ratio of molecular C:N:P for oceanic bacteria is 106:16:1 (Redfield, 1958) with a C:N ratio of about 6.6:1, which is larger than the C:N ratio of 5.1:1 given by Smith et al. (1988) for the autotroph *A. ferrooxidans*; thus,

the Smith et al. (1988) C:N ratio was considered to be more N-limited and Eq. **3.7** was used to calculate nutrient demands for all iron(II) oxidizers. Emergent iron(II) concentrations at Gum Boot ranged from about 0.1-1.0 mM Fe^{2+}, or 5.6-56mg Fe^{2+} /L; this concentration of iron(II) would require 0.002-0.02 mg NH_4/L, which is much less than the measured values of 0.1 – 0.4 mg N/L for emergent Gum Boot AMD (see Figure **5-2**). Provided the dissolved nitrogen in the mine drainage is in a form accessible to IOB, the Gum Boot AMD system should not be nitrogen-limited for bacterial biomass synthesis.

Emergent iron(II) concentrations at Fridays-2 ranged from 0.8-1.0 mM Fe^{2+}, which would consume 0.016 mg NH_4/L according to Smith et al. (1988). TN measurements on Fridays emergent AMD resulted in concentrations of 0.4-0.6 mg N/L. Thus, with respect to biomass synthesis, the Fridays-2 AMD system is also probably not nitrogen-limited.

Field chemistry and laboratory results suggest that the highest activity of biological iron(II) oxidation at Gum Boot and Fridays-2 Mines occurs near GB 2m and FR 10m sampling locations. The largest changes in iron(II) concentration and pH occur at these two sampling locations. Microbial population counts revealed the highest IOB numbers (CFU/g DW sediment) at both GB 2m and FR 10m; initial experiments by Senko et al., (in press) indicate that these sediments also had high first-order rate constants for iron(II) oxidation. The Fridays-2 AMD system appears to be capable of efficient biological iron(II) oxidation within 10 meters from AMD emergence. However, due to a greater flow rate over a shorter distance, the Fridays-2 AMD system has a much shorter residence time. The majority of the biological oxidation is occuring near the

steep ledges and, as a result, iron(III) can not hydrolyze and precipitate out of solution before the AMD reaches Fridays Run.

To support the field site characterization, the results of batch reactor experiments were used to calculate the rates of iron(II) oxidation in the Gum Boot and Fridays-2 iron mound sediments. The abiotic zero order iron(II) oxidation rates in the killed reactors ranged over two orders of magnitude from 3.11×10^{-11} M/s to 5.67×10^{-9} M/s (see Figure **5-17**). All abiotic batch reactor zero-order iron(II) oxidation rates were less than the predicted rate of pyrite oxidation in AMD systems under similar conditions (Figure **6-2**). The iron-free-SAMD control reactors and the killed controls both demonstrated differences between the iron(II) oxidizing capacity of the sediments from Gum Boot and Fridays-2 Mines. Iron(III) hydroxides have been shown to catalyze the oxidation of sorbed iron(II) in the presence and absence of oxygen (Dempsey et al., 2001; Jeon et al., 2001); a greater amount of iron(III) accessible for oxidation reactions in the sediments at Fridays-2 may be increasing the abiotic rates of oxidation compared to sediments at Gum Boot.

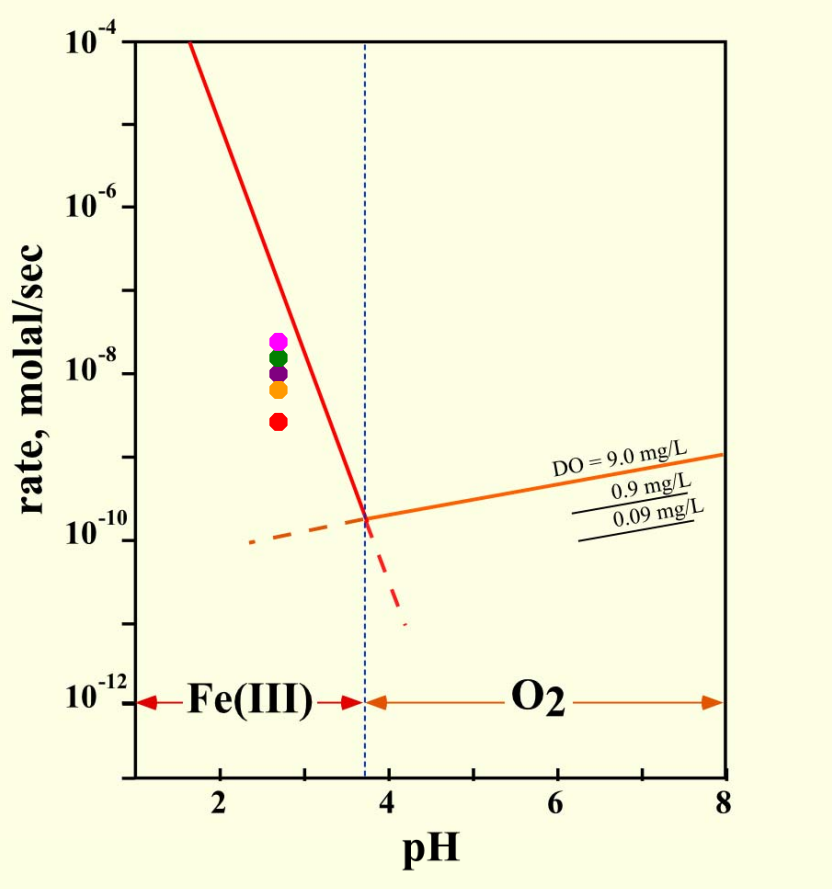

Figure **6-2**: Abiotic rates of pyrite oxidation by iron(III) and dissolved oxygen (DO) (Rimstidt, 2004). Colored circles represent the 3rd iron addition abiotic iron(II) oxidation rates for the FR 10m batch reactors in this study. Legend identification: Blue, Initial Sediments; Red, 0.7% O2; Orange, 1.5% O2; Purple, 10% O2; Green, 21% O2; Pink, 21% O2 + glucose.

Liang et al. (1993) reported different rates of abiotic iron(II) oxidation with different pO_2 values as well as increases in rate with increases in the concentration of natural organic matter (NOM). The Fridays-2 AMD system was observed to incorporate a much larger amount of annual leaf litter directly into the hardened iron mound sediment matrix, lending to a slightly rippled flow effect (personal observation). Additionally, organic carbon measurements conducted by drying (105 °C for 5 days) and ashing (400

°C for 24 hours) showed slightly higher carbon content per g of dry weight in the Fridays-2 sediment samples compared to the Gum Boot sediment samples.(data not shown; Table E:2, Appendix E). This leaf litter contributed NOM to the Fridays-2 sediments which could have increased the abiotic iron(II) oxidation rate in the Fridays-2 reactors relative to the Gum Boot reactors.

SEM images revealed the presence of bacterial microorganisms in both Gum Boot and Fridays-2 iron sediments (see Figure **5-3**). Panels c and e show cocci bacteria of similar size and morphology at sampling locations GB 9m and FR 3m. Additionally, similar bacteria were observed in sediments downhill from these sampling locations (panels d and f). However, bacteria in panels d and f were coated with what appeared to be iron(III) precipitates, suggesting biological iron(II) oxidation and immediate precipitation of iron(III) outside the cell membrane.

A difference between microorganisms at Gum Boot and Fridays-2 was the observed increase in morphological diversity at Gum Boot. Two sheath-forming iron(II) oxidizers, possibly indicative of *Gallionella* spp. and *Leptothrix* spp., were observed in Gum Boot sediments (see Figure **5-3**, panels a and b). These images suggest a greater morphological diversity of IOB at Gum Boot versus Fridays-2 Mine. Due to the lower temperatures and potential shear effect from higher flow at Fridays-2 Mine, fewer species of IOB may be capable of colonizing and efficiently oxidizing aqueous iron(II).

The presence of similar cocci bacteria at both Gum Boot and Fridays-2 Mines supports the findings from Senko et al. (in press) that similar IOB phyla are responsible for the biological oxidation of iron(II) in the AMD. However, the morphological diversity observed in this study does not appear to correlate with the phylogenetic

diversity patterns observed by Senko et al. (in press). Phylogenetic characterization reveals greater phylum-level diversity at emergence at Gum Boot than at Fridays-2 (Figure **5-4**), which agrees with the presence of different bacterial morphologies in the SEM images (Figure **5-3**). Though the bacterial communities at Gum Boot and Fridays-2 Mines are compositionally different, they appear to have similar phylum-level diversity at sampling locations experiencing biological iron(II) oxidation. In contrast, the SEM images in this study did not reveal any morphological diversity in the bacterial community at Fridays-2 Mine. This finding could be the consequence of preferential preservation of the bacteria during the preparation of the samples for SEM analysis.

The results from the live batch reactor experiments indicate biological rates of iron(II) oxidation increased with increasing oxygen concentrations for both mine sites. This trend was most easily observed with GB 2m and FR 10m sediments and at oxygen concentrations of 10% or greater. Noticeably higher IOB numbers in the final batch reactor samples at 10% O_2 or more suggest that batch reactors may have been O_2-limited with respect to biomass synthesis at 0.7 and 1.5% O_2 concentrations. However, the oxidation rates for the 0.7 and 1.5 % O_2 experiments were likely not affected by the rates of biomass growth due to uncoupling of iron(II) oxidation and biomass synthesis under nutrient-limiting conditions (Kelly and Jones, 1978). Similarly, iron(II) oxidation rates were not significantly different with the presence or absence of P, yet the final IOB numbers were noticably higher with P present. This contrast suggests that even a relatively small population of IOB may be capable of effective oxidative precipitation of iron from AMD. Contrary to field observations, at 21% O_2 FR 10m sediments oxidized iron(II) faster than the GB 2m sediments. These findings support the conclusion that the

difference in iron(II) removal at Gum Boot and Friday-2 is due to a shorter residence time instead of the lack of sufficient biological iron(II) oxidation activity at Fridays-2 Mine.

To look at the effects of oxygen concentration on the specific activity of the batch reactor IOB populations, the overall (abiotic + biological) iron(II) oxidation rates were normalized to the IOB numbers in the initial sediments as well as IOB numbers at the conclusion of each experiment (Figure **6-3**). The IOB specific activities of the first iron(II) addition displayed trends similar to those observed among the non-normalized iron(II) oidation rates (Figure **5-17**); Fridays-2 IOB specific activities were higher than Gum Boot specific activities and FR 10m activities increased with increasing oxygen concentration. However, the IOB specific activities of the third iron(II) addition displayed much different trends at all oxygen concentrations. Under microaerobic conditions, GB 2m sediments had the highest specific activity at 0.7% O_2 and FR 3m sediments showed the largest increase in specific activity between 0.7 and 1.5% O_2. FR 10m sediments had the highest specific activity at 10 and 21% O_2 concentrations, though the IOB specific activity of all three sediments decreased significantly at higher O_2 concentrations. These findings suggest that the IOB communities at both Gum Boot and Fridays-2 Mines are capable of adjusting their specific activities of iron(II) oxidation to compensate for changing environmental conditions. Under low O_2 conditions, the specific activity may be increased to maintain sufficient iron(II) oxidation to meet biological energy demands.

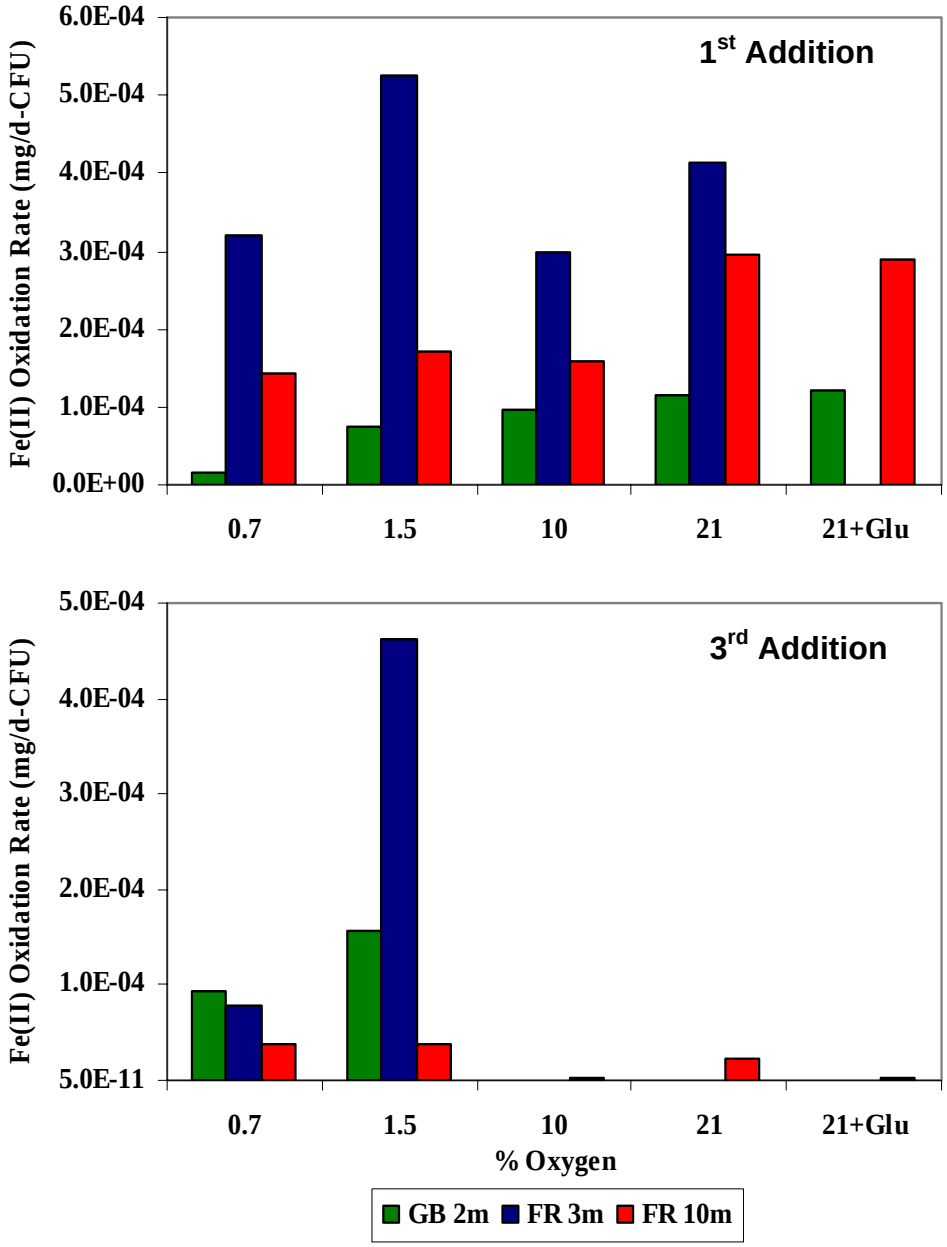

Figure **6-3**: Rates of iron(II) oxidation from the live batch reactors normalized to IOB numbers. First overall (abiotic + biological) iron(II) addition rates were normalized using the initial sediment CFU counts while third overall iron(II) addition rates were normalized using the final batch reactor IOB numbers.

The biological iron(II) oxidation rates from this study are similar to rates published by previous studies but are about one order of magnitude lower than predicted by Pesic et al. (1989) (Figure **6-4**). The application of the Kirby et al. (1999) iron(II) oxidation model demonstrated that observed overall iron(II) oxidation rates are lower than those predicted (see Figure **5-18**). Additionally, decreases in the biological rate constant, k_{bio}, resulted in noticable decreases in the predicted rates of iron(II) oxidation using the STELLA model. These findings suggest that the lower biological iron(II) oxidation rates in this study may be the result of a lower observed biological iron(II) oxidation rate constants for the IOB communities at Gum Boot and Fridays-2 Mines.

Biological rates ranged from 6.12×10^{-9} M/s to 1.36×10^{-8} M/s (see Figure **5-17**). Glucose concentrations decreased during the mix 5 experiment but the rate of biological iron(II) oxidation did not change noticeably, indicating little to no advantage of heterotrophs over autotrophs at either mine site. Iron(II) oxidation rates from this study were much lower to those reported for *A. ferrooxidans* in the presence of 0-100 mg/L glucose and heterotrophic IOB, *A. acidophilum* (Marchand and Silverstein, 2003); however, this difference could be due to the lower concentrations of 50 mg/L glucose used in this study versus 1500 mg/L in the study by Marchand and Silverstein (2003). In summary, iron(II) oxidizing bacteria are present in high enough concentrations for the removal of iron(II) from the AMD at both Gum Boot and Fridays-2 Mines. Additionally, both mine sites appear equally capable of efficient biological iron(II) oxidation given the field and laboratory conditions in this study.

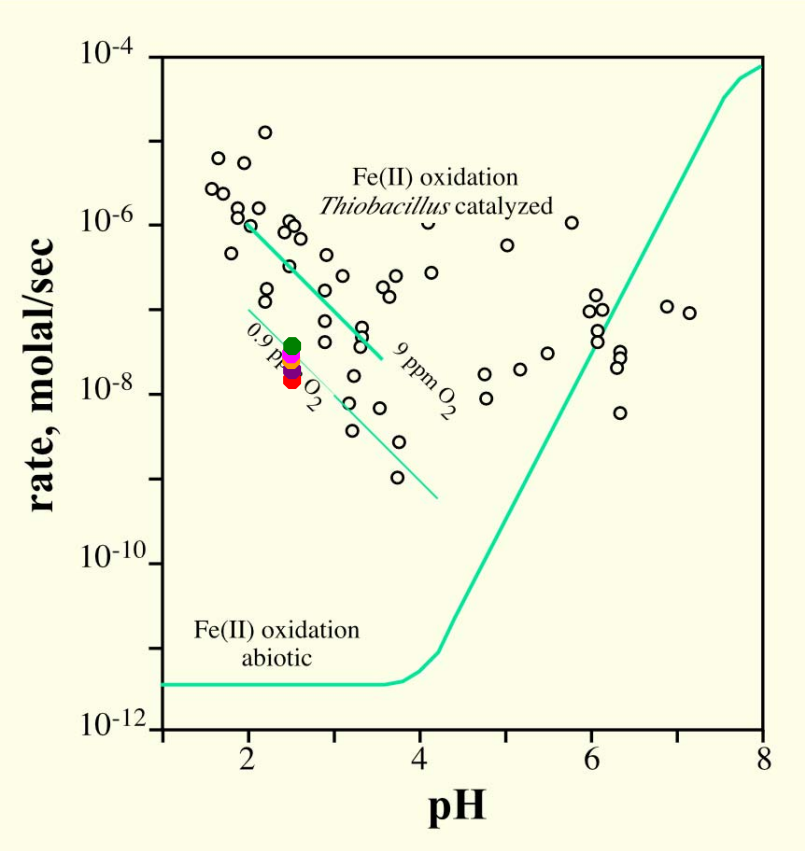

Figure **6-4**: Biological and abiotic rates of iron(II) oxidation of acid mine drainage (Rimstidt, 2004). Open circles represent observed in-situ rates of combined biological and abiotic iron(II) oxidation. Colored circles represent the 3rd iron addition overall iron(II) oxidation rates for the FR 10m batch reactors in this study. Legend identification: Blue, Initial Sediments; Red, 0.7% O2; Orange, 1.5% O2; Purple, 10% O2; Green, 21% O2; Pink, 21% O2 + glucose.

Collaborative studies have measured the effect of oxygen concentration on the composition of AMD microbial populations. The copy numbers of an iron(II) oxidizer gene were measured in initial, pre-iron(II) addition, and final batch reactor slurry samples at various DO concentrations. According to preliminary results, the number of iron(II) oxidizing bacteria in the batch reactor samples increased both with time and higher DO concentrations, agreeing with the CFU counts reported in this study (see Figure **5-15**).

Preliminary results also indicate *Acidothiobacillus* is not the dominant genus at either Gum Boot or Fridays-2 Mines (personal communication, P. Wanjugi). These findings agree with the results of Senko et al. (in press) that the dominant phyla on Gum Boot and Fridays-2 iron mounds are Actinobacteria and Gammaproteobacteria. The difference in the observed and predicted biological iron(II) oxidation rates could be explained by a slower iron(II) oxidation rate for the prevalent IOB at Gum Boot and Fridays-2 Mines than for pure cultures of *A. ferrooxidans*.

Nutrient limitations experienced by the bacteria within the batch reactors is another possible cause for the difference in observed and predicted rates of biological iron(II) oxidation. If the IOB were not capable of uncoupling biomass synthesis from iron(II) oxidation, limitation of particular nutrients could result in lower than expected biological oxidation rates. Nutrient limitation by IOB in Gum Boot sediments during the batch reactor experiments could also explain why laboratory biological iron(II) oxidation rates were higher in Fridays-2 batch reactors while observed field oxidation rates were higher at Gum Boot.

Several studies have examined the effects of CO_2 concentration on autotrophic IOB growth rates but little work has been directed at the effects of concentration on the biological rates of iron(II) oxidation. Under conditions of CO_2 limitation, autotrophic bacteria may be able to uncouple of growth from iron oxidation (Kelly and Jones, 1978), which would result in lower number of IOB and relatively unchanged rates of iron(II) oxidation. Unfortunately, the batch reactor experiments were not designed to examine the effect of CO_2 concentration under constant O_2 concentration. However at a concentration of ~ 1% CO_2, IOB counts increased between gas mixes 1 and 4 containing

0.7 and 10% O_2 respectively. Additionally, gas mixes 3 and 5 with ~ 0.035% CO_2 had the highest biological iron(II) oxidation rates for GB 2m and FR 10m batch reactors. These results suggest that under the experimental conditions of this study, CO_2 did not have a noticable affect on biomass synthesis or biological oxidation rates and the batch reactors were likely not nutrient limited with respect to autotrophic requirements for CO_2.

The experimental batch reactors should not have been N-limited due to leaf litter incorporated into the iron sediments; during the experiments, this organic matter could decay and leach nutrients into the reactors. However, disregarding possible nitrogen additions from allochthonous organic matter, nitrogen was added to each reactor in the form of 0.2 mM NH_4 (or 3.6 mg/L) in the SAMD. TN measurements on batch reactor samples (gas mix 4, data not shown; Table E:4, Appendix E) showed relatively stable concentrations of nitrogen over the duration of the experiment at an average of 3.454 mg N/L. Following the equation by Smith et al. (1988) (see Eq. **3.7**), 0.0011 moles of NH_4 are used per mole of Fe^{2+}. For about 400 mg Fe^{2+} in each batch reactor, 3.94 x 10^{-6} moles of NH_4 would be consumed; this mass of 0.071 mg NH_4 is much less than the 1.727 mg N mass measured in the batch reactor samples. Thus, none of the batch reactor experiments in this study should have been nitrogen-limited.

Magnesium is necessary for autotrophs as part of the Carbon Cycle to fix CO_2. Malhotra et al. (2002) showed adequate growth and oxidation with Mg^{2+} at concentrations as low as 2.8 mg/L. Metals analysis (ICP-AES) of final slurry samples from the batch reactor experiments (data not shown; Table E:5, Appendix E) reported concentrations of about 100 mg Mg^{2+}/L in all reactors for both gas mixes 2 and 3. These results agree with concentration of 4 mM magnesium sulfate added to the batch reactor

SAMD. Additionally, both field sites had dissolved Mg concentrations of at least 5.0 mg/L at Gum Boot and about 20 mg/L at Fridays-2. Microbial populations should not have been magnesium-limited in the batch reactor experiments or at either field site.

Because phosphorus was not measured along the mine drainage flow path at either mine site, conclusions can not be made regarding possible IOB nutrient limitation of phosphorus at either mine site. However, the inclusion of phosphorus in the batch reactor SAMD did not noticably alter the oxidation rates or the pH of GB 2m live reactors (see Figure **5-13**). Population counts performed on initial and final reactor samples showed an increase in IOB numbers for reactors with phosphorus and a decrease in numbers with phosphorus-free reactors (see Table **5-8**). The decreased biomass synthesis suggest the reactors in gas mixes 1-4 and 6 may have been phosphorus-limited; additionally, similarity between the observed rates of iron(II) oxidation for GB 2m and PF reactors could be the result of an uncoupling of biological oxidation from cellular growth under conditions of nutrient limitation in the PF batch reactors (Kelly and Jones, 1978). The IOB populations at Gum Boot and Fridays-2 Mines may be phosphorus-limited. If so, prolonged nutrient limitation could result in an observed biological iron(II) oxidation rate that is lower than the potential maximum rate for either field site under optimal growth conditions.

In summary, the Fridays-2 Mine AMD system appears capable of achieving rates of biological iron(II) oxidation similar to those observed at the Gum Boot Mine. Though nutrient limitation may have resulted in observed biological oxidation rates lower than rates predicted by previous studies, it is probably not the explanation for the observed differences between Gum Boot and Fridays-2 Mines. The main conclusion of this study

is that iron(II) in both Gum Boot and Fridays-2 AMD is oxidized by both autotrophic and heterotrophic iron(II) oxidizing bacteria on the iron mound. However, a shorter residence time at the Fridays-2 AMD system does not allow for the hydrolysis and precipitation of iron(III) hydroxides before the AMD mixes with Fridays Run.

7 CONCLUSION

The major conclusions from the research presented in this thesis are summarized in the following list:

- Field chemistry and microbial characterization of Gum Boot and Fridays-2 Mines indicate that biological iron(II) oxidation is occurring at both mine sites, with the highest microbial activity found in the first 10 meters of flow from acid mine drainage (AMD) emergence at either site.
- A shorter residence time at the Fridays-2 AMD system does not allow for the hydrolysis and precipitation of iron(III) hydroxides from solution before the mine drainage mixes with Fridays Run. The greatest activity of IOB at Fridays-2 is 10 meters from AMD emergence, which is where the AMD drops over steep ledges and immediately joins with the creek. An engineered AMD treatment system to increase the residence time at Fridays-2 Mine would promote the precipitation of iron(III) hydroxides on the iron mound instead of in surface waters.
- While microbial characterizations identified heterotrophic IOB on both iron mounds, batch reactor results suggest that autotrophic IOB are responsible for the oxidation and removal of iron at both Gum Boot and Fridays-2 AMD systems. Additionally, flow characteristics and environmental conditions of the mine drainage may be driving community

structure at the two sites, leading to morphological and compositional differences between the IOB communities at Gum Boot and Fridays-2 Mines.

- Nutrient limitations were not observed to affect the biological iron(II) oxidation rates at either Gum Boot or Friday-2 Mines. Field and laboratory results indicate adequate concentrations of CO_2, nitrogen, and Mg in the AMD at both sites. However, the IOB populations may be P-limited (see Discussion). While nutrient limitations are not likely at Gum Boot or Fridays-2 given the results of this study, prolonged limitation could result in observed biological iron(II) oxidation rates lower than the rates predicted under optimal growth conditions.
- Sediments from Gum Boot and Fridays-2 AMD sites displayed variation between the rates of abiotic iron(II) oxidation during the batch reactor experiments. Both NOM and iron(III) have been shown to increase the rate of abiotic oxidation independent of DO concentrations (Liang et al., 1993; Dempsey et al., 2001; Jeon et al., 2001). The larger abiotic rates in the Fridays-2 batch reactors may have been caused by greater amounts of labile NOM or iron(III) in the Fridays-2 sediments relative to the Gum Boot sediments.
- Batch reactor experimental results suggest that both Gum Boot and Fridays-2 AMD systems are equally capable of biological iron(II) oxidation and subsequent iron(III) precipitation under a range of environmental conditions. This conclusion is promising for AMD

remediation as it suggests that efficient and adequate biological oxidation can occur at most AMD sites given the appropriate environmental conditions.

- The iron(II) oxidation model proposed by Kirby et al. (1999) was effectively modified from a flow-through system to a batch reactor system. This finding suggests the model is broad enough to be applied to a variety of AMD systems for iron(II) oxidation modeling. Further results revealed that observed biological iron(II) rate constants may be different from those published by previous studies. In conclusion, all parameters must be considered when evaluating the iron(II) oxidation kinetics of an AMD system for remediation purposes.

Future Research

In-depth field experiments are required to confirm that the Fridays-2 AMD system is capable of sufficient iron(II) removal given a longer residence time. Subsequent studies should examine the best treatment method to maintain the biological iron(II) oxidation while increasing the residence time of the AMD. Further work is also required to evaluate the differences in abiotic iron(II) oxidation rates, looking specifically at the effects of NOM as well as the autocatalytic properties of the iron(III) minerals present in the iron sediment mounds at the two mines. Additional studies should continue the microbial characterization of the IOB populations at Gum Boot and Fridays-2 Mines to determine if differences in community composition could affect the observed rates of iron(II) oxidation. Lastly, future research should focus on more detailed kinetic

modeling to determine if 1) the Kirby model can be applied to the iron mound AMD systems seen at Gum Boot and Fridays-2 Mines and 2) if biological kinetic rates constants vary with bacterial community composition or environmental factors.

Bibliography

Baker B. and Banfield J. (2003) Microbial communities in acid mine drainage. *FEMS Microbiology Ecology*, **44**(2): 139-152.

Bigham J.M., Schwertmann U., Traina S.J., Winland R.L., and Wolf M. (1996). Schwertmannite and the chemical modeling of iron in acid sulfate waters. *Geochmica et Cosmochimica Acta*, **60**(12): 2111-2121.

Cherry D.S., Currie R.J., Soucek D.J., Latimer H.A., and Trent G.C. (2001) An integrative assessment of a watershed impacted by abandoned mined land discharges. *Environmental Pollution*, **111**(3): 377-388.

Civil & Environmental Consultants, Inc. 2006. Bennett Branch Water Quality and Flow Assessment Acid Mine Drainage Abatement Project, Hollywood, Huston Township, Clearfield County, Pennsylvania. Prepared for the Pennsylania Department of Environmental Protection.

Cravotta C.A. and Trahan M.K. (1999). Limestone drains to increase pH and remove dissolved metals from acidic mine drainage. *Applied Geochemistry*, **14**: 581-606.

Cravotta III C.A. (2008b). Dissolved metals and associated constituents in abandoned coal-mine discharges, Pennsylvania, USA. Part 2: Geochemical controls on constituent concentrations. *Applied Geochemistry*, **23**: 203-226.

Dellamea C. (2006) Bituminous Coalfields of the Appalachian Basin. www.coalcampusa.com

Dempsey B.A., Roscoe H.C., Ames R., Hedin R., and Jeon B. (2001) Ferrous oxidation chemistry in passive abiotic systems for the treatment of mine drainage. *Geochemistry: Exploration, Environment, Analysis*, **1**: 81-88.

DeNicola D.M. and Stapleton M.G. (2002) Impact of acid mine drainage on benthic communities in streams: the relative roles of substratum vs. aqueous effects. *Environmental Pollution*, **119**(3): 303-315.

Department of Conservation and Natural Resources (DCNR), Bureau of Topographic and Geologic Survey. (1992) http://www.dcnr.state.pa.us/topogeo/gismaps/index.aspx

Encyclopaedia Britannica (2006) Coal Mining. In *Encyclopaedia Britannica Online*. Retrieved February 15, 2008, from www.britannica.com.

Gazea B., Adam K., and Kontopoulos A. (1996) A Review of Passive Systems for the Treatment of Acid Mine Drainage. *Minerals Engineering*, **9**(1): 23-42.

Grishin S.I. and Tuovinen O.H. (1988). Fast kinetics of Fe2+ oxidation in packed-bed reactors. *Applied Environmental Microbiology*, **54**(12): 3092-3100.

Grishin S.I. and Tuovinen O.H. (1989). Scanning electron microscopic examination of *Thiobacillus ferrooxidans* on different support matrix materials in packed bed and fluidized bed bioreactors. *Applied Microbiology and Biotechnology*, **31**(5-6): 505-511.

Growing Greener (2003) Bennett Branch Watershed Assessment and Restoration Plan: Final Report. Pennsylvania Growing Greener Program, Round 1.

Halfmeier H., Schafer-Treffenfeldt W., and Ressus M. (1993a). Potential of *Thiobacillus ferrooxidans* for waste gas purification: Part 1, Kinetics of continuous ferrous iron oxidation. *Applied Microbiology and Biotechnology*, **40**: 416-420.

Halfmeier H., Schafer-Treffenfeldt W., and Reuss M. (1993b). Potential of *Thiobacillus ferrooxidans* for waste gas purification: Part 2, Increase in continuous ferrous iron oxidation kinetics using immobilized cells. *Applied Microbiology and Biotechnology*, **40**: 582-587.

Hallberg K.B. and Johnson D.B. (2005) Microbiology of a wetland ecosystem constructed to remediate mine drainage from a heavy metal mine. *Science of the Total Environment*, **338**: 53-66.

Hashimoto H., Yokoyama S., Asoaka H., Kusano Y., Ikeda Y., Seno M., Takada J., Fujii T., Nakanishi M., and Murakami R. (2007). Characteristics of hollow microtubes consisting of amorphous iron oxide nanoparticles produced by iron oxidixing bacteria, *Leptothrix ochracea*. *Journal of Magnetism and Magnetic Materials*, **310**: 2405-2407.

Herlihy A.T., Kaufmann P.R., and Mitch M.E. (1990). Regional estimates of acid mine drainage impact on streams in the Mid-Atlantic and Southeastern United States. *Water, Air, and Soil Pollution*, **50**: 91-107.

Hippe H. (2000) *Leptospirillum* gen. nov. (*ex* Markosyan 1972), nom. rev., including *Leptospirillum ferrooxidans* sp. nov. (*ex* Markosyan 1972), nom. rev. and *Leptospirillum thermoferrooxidans* sp. nov. (Golovacheva et al. 1992). *International Journal of Systematic and Evolutionary Microbiology*, **50**: 501-503.

Huang L. and Forsberg C.W. (1990) Cellulose digestion and cellulose regulation and distribution in *Fibrobacter succinogenes* subsp. *succinogenes* S85. *Applied Environmental Microbiology* **56:** 1221-1228.

Jensen A. and Webb C. (1994). A trickle-bed reactor for ferrous sulfate oxidation using *Thiobacillus ferrooxidans*. *Biotech. Tech.*, **8**(2): 87-92.

Jeon B., Dempsey B.A., Burgos W.D., and Royer R.A. (2001). Reactions of ferrous iron with hematite. *Colloids and Surfaces A: Physicochemical and Engineering Aspects*, **191**: 41-55.

Johnson D.B. (1995) Selective solid media for isolating and enumerating acidophilic bacteria. *Journal of Microbiological Methods*, **23**: 205-218.

Johnson D.B. (1998) Biodiversity and ecology of acidophilic microorganisms. FEMS Microbiol. Ecol., 27: 307-317.

Johnson D.B., Rolfe S., Hallberg K.B., and Iversen E. (2001) Isolation and phylogenetic characterization of acidophilic microorganisms indigenous to acidic drainage waters at an abandoned Norwegian copper mine. *Environmental Microbiology*, **3**(10): 630-637.

Johnson D.B., Okibe N., and Hallberg K.B. (2005) Differentiation and identification of iron-oxidizing acidophilic bacteria using cultivation techniques and amplified ribosomal DNA restriction enzyme analysis. *Journal of Microbiological Methods*, **60**: 299-313.

Kelly D.P. and Jones C.A. (1978). Factors affecting metabolism and ferrous iron oxidation in suspensions and batch culture of *Thiobacillus ferrooxidans*: relevance to ferric iron leach solution regeneration. In: L.E. Murr, A.E. Torma, J.A Bierly (Eds.), *Metallurgical Applications of Bacterial Leaching and Related Microbiological Phenomena*, 19-43. New York, Academic press.

Kelly D.P. and Wood A.P. (2000) Reclassification of some species of *Thiobacillus* to the newly designated genera *Acidithiobacillus* gen. nov., *Halothiobacillus* gen. nov. and *Thermithiobacillus* gen. nov. *International Journal of Systematic and Evolutionary Microbiology*, **50**: 511-516.

Kirby C.S., Thomas H.M., Southam G., and Donald R. (1999). Relative contributions of abiotic and biological factors in Fe(II) oxidation in mine drainage. *Applied Geochemistry*, **14**: 511-530.

Lehigh Earth Observatory (2008). Abandoned Mine Reclamation Problems: Successes, Problems, and Lessons Learned.
http://www.leo.lehigh.edu/envirosci/enviroissue/amd/links/bamr1.html

Liang L., McNabb J.A., Paulk J.M., Gu B., and McCarthy J.F. (1993) Kinetics of Fe(II) Oxygenation at Low Partial Pressure of Oxygen in the Presence of natural Organic Matter. *Environmental Science and Technology*, **27**: 1864-1870.

Lovley D.R. and Phillips E.J.P. (1987). Rapid assay for microbially reducible ferric iron in aquatic sediments. *Applied Enviromental Microbiology*, **53**: 1536-1540.

MacDonald D.G. and Clark R.H. (1970). The oxidation of aqueous ferrous sulphate by *Thiobacillus ferrooxidans*. *Canadian Journal of Chemical Engineering*, **48**: 669-676.

Madigan M.T. and Martinko J.M. (2006). *Brock Biology of Microorganisms*, 11th edition. Prentice Hall, New Jersey.

Morgan B. and Lahav O. (2007) The effect of pH on the kinetics of spontaneous Fe(II) oxidation by O2 in aqueous solution – basic principles and a simple heuristic description. *Chemosphere*, **68**(11): 2080-2084.

Nakamura K., Noike T., and Matsumoto J. (1986). Effect of operation conditions on biological Fe2+ oxidation with rotating biological contactors. *Water Res.*, **20**(1): 73-77.

National Mine Land Reclamation Center (2008). West Virginia Water Research Institute, West Virginia University. http://wvwri.nrcce.wvu.edu/programs/nmlrc/

Nemati M. and Webb C. (1996). Effect of ferrous iron concentration on the catalytic activity of immobilized *Thiobacillus ferrooxidans*. *Applied Microbiology and Biotechnology*, **46**: 250-255.

Nemati M., Harrison S.T.L., Hansford G.S., and Webb C. (1998) Biological oxidation of ferrous sulphate by *Thiobacillus ferrooxidans*: a review on the kinetic aspects. *Biochemical Engineering Journal*, **1**: 171-190.

Olem H. and Unz R.F. (1977). Acid mine drainage treatment with rotating biological contactors. *Biotechnology and Bioengineering*, **19**: 1475-1491.

Pennsylania Department of Environmental Protection 2003. Status Report: The environmental legacy of coal mining in Pennsylvania.

Pennsylania Department of Environmental Protection 2005. Gumboot Run Biological Assessment, McKean County, Pennsylvania.

Pennsylania Department of Environmental Protection 2006. The Development of a Mine Drainage Restoration Plan for Bennett Branch, Sinnemahoning Creek: Clearfield, Elk, and Cameron Counties, Pennsylvania.

Pesic B., Oliver D.J., and Wichlacz P. (1989) An Electrochemical Method of Measuring the Oxidation Rate of Ferrous to Ferric Iron with Oxygen in the Presence of *Thiobacillus ferrooxidans*. *Biotechnology and Bioengineering*, **33**: 428-439.

Planet Smethport (2008). *Gum Boot Mines*. www.smethporthistory.org/clermont/gum.boot.mine/gum.boot.mine.htm.

Redfield A.C. (1958). The Biological Controls of Chemical Factors in the Environment. *American Scientist*, **46**(3): 205-221.

Rimstidt J.D. (December 2004). Factors controlling rates of pyrite weathering.

Rossman W., Wytovich E., and Seif J.M. (1997). Abandoned Mines – Pennsylvania's single biggest water pollution problem. Pennsylvania Department of Environmental Protection.

Senko J.M., Bruns M.A., and Burgos W.D. (in press). Characterization of Fe(II) oxidizing bacterial communities at two acidic Appalachian coal mine drainage impacted sites. *International Society of Microbial Ecology*.

Silverman M.P. and Lundgren D.G. (1959) Studies on the chemoautotrophic iron bacterium Ferrobacillus ferrooxidans – I: An improved medium and a harvesting procedure for securing high cell yields. *Journal of Bacteriology*, **77**: 642-647.

Singer P. and Stumm W. (1970) Acidic Mine Drainage: The Rate-Determining Step. *Science*, **167** (3921): 1121-1123.

Skousen, J. (1995) Overview of Passive Systems for Treating Acid Mine Drainage. West Virginia University Extension Service. http://www.wvu.edu/~Agexten/landrec/passtrt/passtrt.htm.

Smith J.R., Luthy G.R., and Middleton A.C. (1988) Microbial ferrous iron oxidation in acidic solution. *Journal of Water Pollution Control Fed*. **60**(4): 518-530.

Sogaard E.G., Aruna R., Abraham-Peskir J., and Koch C.B. (2001) Conditions for biological precipitation of iron by *Gallionella ferruginea* in a slightly polluted ground water. *Applied Geochemistry,* **16**: 1129-1137.

Spring S., Kampfer P., Ludwig W., and Schleifer K.-H. (1996). Polyphasic characterization of the genus *Leptothrix*: New descriptions of *Leptothrix mobilis* sp. nov. and *Leptothrix discophora* sp. nov. nom. rev. and emended description of *Leptothrix cholodnii* emend. *Systematic and Applied Microbiology*, **19**(4): 634-643.

Stookey L.L. (1970) Ferrozine – a new spectrophotometric reagent for iron. *Analytical Chemistry* **42**: 779-781.

Stumm W. and Lee G.F. (1961) Oxygenation of Ferrous Iron. *Industrial Engineering Chemistry*, **53**: 143-146.

Stumm W. and Morgan J.J. (1981) *Aquatic Chemistry*, 2nd edition. John Wiley & Sons, New York.

Stumm W. and Morgan J.J. (1996) *Aquatic Chemistry*, 3rd edition. John Wiley & Sons, New York, 683-691.

Sung W. and Morgan J.J. (1980) Kinetics and Product of Ferrous Iron Oxygenation in Aqueous Systems. *Environmental Science and Technology*, **14**(5): 561-568.

Tamura H., Goto K., Yotsuynagi T., and Nagayama M. (1974). Spectrophotometric determination of iron(II) with 1,10-phenanthroline in the presence of large amounts of iron(III). *Talanta*, **21**: 314-318.

Tamura H. and Nagayama M. (1976) Effect of Anions on the Oxygenation of Ferrous Iron in Neutral Solutions. *Journal of Inorganic and Nuclear Chemistry*, **38**: 113-117.

Taylor W., Dunn M., and Busler S. (2003) *Accepting the Challenge: A primer about the history, cause, and solutions to abandoned mine drainage*, 2nd edition. Stream Restoration Incorporated, Pennsylvania.

Vatter A.E. and Wolfe R.S. (1956). Electron Microscopy of *Gallionella ferruginea*. *Journal of Bacteriology*, **72**(2): 248-.252.

Wiersma C.L. and Rimstidt J.D. (1984). Rates of reaction with pyrite and marcasite with ferric iron at pH 2. *Geochimica et Cosmochimica Acta*, **48**: 85-92.

Zhang, G., Dong H., Kim J., and Eberl D.D. (2007). Microbial reduction of structural Fe^{3+} in nontronite by a thermophilic bacterium and its role in promoting the smectite to illite reaction. *American Mineralogist*, **92**: 1411-1419.

Ziemkiewicz P.F., Skousen J.G., and Simmons J. (2003). Long-term Performance of Passive Acid Mine Drainage Treatment Systems. *Mine Water and the Environment*, **22**: 118-129.

Zinc T., Wolfe A., and Curley K. (2005) *Restoring the Wealth of the Mountains: Cleaning up Appalachia's Abandoned Mines*. Trout Unlimited.

Appendix A

Tabulated Data for Materials and Methods

Table A:1 – Data corresponding to Figure 4.5

Gum Boot Mine		
Distance (m)	**Fe(II)OB (CFU/g dry wt.)**	**k (1/day)**
0	1.0×10^4	3.1
2	2.0×10^5	5.8
9	6.0×10^4	6.2
15	5.0×10^4	1.5
60	3.0×10^3	1.4
127	2.0×10^4	2.7
Fridays-2 Mine		
Distance (m)	**Fe(II)OB (CFU/g dry wt.)**	**k (1/day)**
0	8.0×10^3	0.2
3	7.0×10^2	0.8
8	5.0×10^4	7.4
10	1.0×10^5	7.0
13	3.0×10^3	1.3

Table A:2 – Data corresponding to Figure 4.6

Treatment	Time (d)	Fe(II) Conc. (mg/L)	S.D. (mg/L)	pH	S.D.
Live	0	349	70.8	3.43	0
	0.10	323	49.3	---	---
	0.21	283	29.1	3.23	0.04
	0.31	257	15.2	---	---
	0.44	206	22.7	3.10	0.01
	0.60	131	13.9	---	---
	1.0	35.7	12.6	2.99	0.04
	1.3	15.2	8.85	---	---
	1.9	7.15	0	2.95	0.02
Azide	0	356	17.7	4.58	0.02
	0.10	317	44.2	---	---
	0.21	336	20.2	4.03	0.05
	0.31	344	13.9	---	---
	0.44	376	21.5	3.85	0.06
	0.60	368	10.1	---	---
	1.0	345	53.1	3.77	0.04
	1.3	353	24.0	---	---
	1.9	339	3.79	3.69	0.01
Formaldehyde	0	364	21.5	3.22	0.06
	0.10	334	43.0	---	---
	0.21	316	2.53	3.21	0
	0.31	340	5.05	---	---
	0.44	331	10.1	3.17	0.04
	0.60	355	1.26	---	---
	1.0	358	21.5	3.14	0.02
	1.3	306	0	---	---
	1.9	269	2.65	3.15	0.01
Autoclave	0	961	74.6	2.21	0.08
	0.10	1050	13.9	---	---
	0.21	939	128	2.14	0.04
	0.31	976	80.9	---	---
	0.44	920	6.32	2.16	0.08
	0.60	882	211	---	---
	1.0	954	192	2.15	0.06
	1.3	884	19.0	---	---
	1.9	931	3.16	2.13	0.06

Appendix B

Tabulated Data for Field Chemistry Analyses

Table B:1 – Data corresponding to Figure 5.1

Gum Boot Mine

		Distance (m)						
Analyte	**Sample Date**	**0**	**2**	**9**	**15**	**60**	**95**	**127**
Fe(II) Aq (mM)	Oct. 05	0.87	0.80	0.04	0.00	0.00	0.00	0.10
	Feb. 06	0.60	0.41	0.42	0.23	0.09	0.05	0.04
	May 06	0.55	0.56	0.24	0.00	0.02	0.00	0.06
	Jul. 06	0.11	0.09	0.03	0.00	0.00	0.00	0.01
	Oct. 06	0.19	0.14	0.02	0.00	0.00	---	0.01
	May 07	0.46	0.45	0.44	0.02	0.02	0.01	0.00
pH	Oct. 05	4.10	3.62	3.12	2.99	2.90	2.93	3.89
	Feb. 06	4.05	3.64	3.43	3.28	3.12	3.14	3.57
	May 06	3.90	3.17	3.17	3.01	3.26	3.73	3.95
	Jul. 06	3.85	3.60	3.29	3.13	3.12	3.12	5.55
	Oct. 06	4.05	3.86	3.16	3.07	3.05	---	7.30
	May 07	3.80	3.80	3.60	3.20	3.10	3.10	5.20
Temp. (C)	May 06	15	16	15	24	26	16	11
	Jul. 06	9	13	27	19	24	26	18
	Oct. 06	9	9	8	13	14	---	10
	May 07	12	10	17	21	17	20	15
DO (mg/L)	Oct. 05	0.06	5.48	6.78	8.40	8.10	8.66	6.33
	Jul. 06	0.10	4.87	6.00	7.50	7.73	6.32	7.15
	Oct. 06	0.30	5.30	7.40	7.70	7.91	---	7.3
	May 07	0.16	1.85	10.80	6.56	10.7	10.4	8.6

Fridays-2 Mine

		Distance (m)				
Analyte	**Sample Date**	**0**	**3**	**8**	**10**	**20**
Fe(II) Aq (mM)	Feb. 06	1.15	1.11	1.13	0.93	0.29
	May 06	0.90	0.69	0.76	0.70	0.21
	Jul. 06	0.84	0.82	0.72	0.63	0.39
	May 07	0.92	0.84	0.84	0.56	---
	Jul. 07	1.05	0.90	0.66	0.10	---
pH	Feb. 06	4.36	4.34	4.09	3.75	4.56
	Jul. 06	3.98	3.93	3.69	3.64	3.62
	May 07	4.10	4.10	3.90	3.50	---
	Jul. 07	3.86	3.65	3.32	3.18	---
Temp. (C)	Feb. 06	10	10	9	10	9
	Jul. 06	10	10	10	11	12
	May 07	10	11	13	16	---
	Jul. 07	10	10	11	11	---
DO (mg/L)	Feb. 06	0.00	1.23	10.80	11.75	9.96
	Jul. 06	0.03	1.91	11.04	8.95	6.86
	May 07	0.15	3.43	10.40	9.30	---
	Jul. 07	0.97	3.75	6.20	6.60	---

Table B:2 – Data corresponding to Figure 5.2

Gum Boot Mine

		Distance (m)						
Analyte	**Sample Date**	**0**	**2**	**9**	**15**	**60**	**95**	**127**
TOC (mg/L)	May 06	2.4	0.89	1.5	1.0	0.73	0.71	0.92
	Oct. 06	4.5	4.6	3.2	3.8	3.6	---	4.0
	May 07	1.7	2.2	1.6	2.4	1.8	1.7	2.3
TN (mg/L)	May 06	0.37	0.23	0.36	0.27	0.26	0.24	0.23
	Jul. 06	0.07	0.10	0.06	0.06	0.07	0.09	0.06
	Oct. 06	0.09	0.11	0.22	0.18	0.10	---	0.44
	May 07	0.02	0.02	0.18	0.18	0.15	0.17	0.16

Fridays-2 Mine

		Distance (m)				
Analyte	**Sample Date**	**0**	**3**	**8**	**10**	**20**
TOC (mg/L)	May 06	0.65	0.55	0.81	0.53	3.3
	Oct. 06	2.2	2.2	1.7	1.9	3.6
	May 07	3.1	1.7	1.5	0.93	---
TN (mg/L)	May. 06	0.53	0.50	0.54	0.49	0.29
	Jul. 06	0.38	0.40	0.36	0.38	0.31
	Oct. 06	0.34	0.37	0.43	0.39	1.2
	May 07	0.57	0.42	0.41	0.38	---

Appendix C

Tabulated Data for Batch Reactor Experiments

Table C:1 – Data corresponding to Figure 5.5

		Live				Killed			
Reactor Sediment	**Time (d)**	**Fe(II) (mg/L)**	**Fe(II) S.D. (mg/L)**	**pH**	**pH S.D.**	**Fe(II) (mg/L)**	**Fe(II) S.D. (mg/L)**	**pH**	**pH S.D.**
GB 2m	0	268	1.07	3.15	0.02	270	5.00	3.07	0.00
	0.698	264	11.1	3.13	0.01	278	4.65	3.10	0.00
	0.958	238	5.36	3.08	0.02	269	7.51	3.05	0.00
	1.81	243	3.22	3.02	0.02	260	10.7	3.05	0.02
	2.60	207	12.2	2.97	0.01	280	4.65	3.04	0.00
	3.65	186	11.1	2.91	0.04	294	0	3.00	0.00
	4.07	158	26.8	2.86	0.03	273	3.93	2.98	0.00
	4.71	130	40.7	2.83	0.04	264	5.72	2.96	0.00
	4.98	106	40.0	2.86	0.03	267	5.00	3.00	0.00
	5.94	60.7	35.5	2.78	0.03	269	6.79	3.00	0.00
	6.75	21.8	19.2	2.70	0.03	272	11.4	2.99	0.01
	6.85	214	6.43	2.66	0.03	241	5.36	2.94	0.01
	7.62	286	5.36	2.73	0.01	239	0.71	2.96	0.00
	8.02	308	8.22	2.80	0.01	258	4.29	2.95	0.00
	8.79	287	9.29	2.80	0.01	267	13.2	2.95	0.00
	9.60	274	20.4	2.75	0.01	269	11.1	2.96	0.01
	10.6	266	34.7	2.68	0.01	272	16.8	2.92	0.01
	11.1	225	15.0	2.73	0.01	268	6.08	2.89	0.00
	11.9	210	11.8	2.68	0.01	276	21.4	2.89	0.00
	12.6	158	29.7	2.72	0.01	251	36.1	2.87	0.00
	13.8	169	9.15	2.71	0.01	285	15.7	2.88	0.01
	13.8	330	46.5	2.70	0.01	290	20.0	2.88	0.01
	14.8	328	20.7	2.76	0.02	301	22.2	2.87	0.01
	15.0	330	12.2	2.83	0.04	302	23.6	2.91	0.00
	15.8	324	20.4	2.87	0.02	307	13.9	2.98	0.00
	16.0	312	21.8	2.85	0.02	306	25.4	2.97	0.01
	16.7	302	19.3	2.83	0.02	311	33.2	2.95	0.01
	17.7	288	12.5	2.80	0.03	297	24.0	2.95	0.00
	18.6	265	10.7	2.73	0.04	314	42.9	2.89	0.00
	18.9	293	1.43	2.72	0.04	302	59.0	2.88	0.00
	19.7	262	44.3	2.70	0.02	315	60.0	2.87	0.00
	20.8	262	3.57	2.67	0.03	338	40.7	2.88	0.00

FR 3m	0	299	1.79	3.28	0.04	312	10.4	3.18	0.00
	0.698	301	15.0	3.30	0.05	322	43.3	3.14	0.01
	0.958	297	4.29	3.18	0.02	314	6.79	3.08	0.00
	1.81	243	3.93	3.10	0.01	284	17.9	3.08	0.01
	2.60	213	11.4	3.00	0.00	286	5.72	3.05	0.01
	3.65	170	15.4	2.87	0.00	267	6.43	2.96	0.01
	4.07	123	11.8	2.77	0.02	255	7.15	2.92	0.01
	4.71	90.0	20.0	2.75	0.03	257	0.07	2.89	0.01
	4.98	65.7	16.4	2.71	0.00	249	4.65	2.89	0.01
	5.94	31.7	4.00	2.71	0.00	243	2.86	2.89	0.01
	6.75	0.81	1.14	2.60	0.01	225	8.58	2.85	0.01
	6.85	195	18.9	2.64	0.01	188	1.07	2.82	0.01
	7.62	264	3.93	2.72	0.00	176	8.22	2.92	0.02
	8.02	265	21.8	2.83	0.01	199	8.22	2.91	0.01
	8.79	248	9.29	2.81	0.02	191	3.57	2.90	0.01
	9.60	211	5.72	2.77	0.01	193	6.08	2.85	0.01
	10.6	134	2.50	2.60	0.01	207	0.00	2.77	0.01
	11.1	88.8	9.72	2.66	0.01	168	2.86	2.76	0.00
	11.9	38.5	8.43	2.61	0.01	162	1.79	2.73	0.00
	12.6	12.6	5.58	2.68	0.02	150	9.29	2.71	0.00
	13.8	0	0	2.61	0.01	149	5.72	2.71	0.00
	13.8	213	17.9	2.68	0.01	185	3.57	2.77	0.01
	14.8	278	1.79	2.68	0.00	182	11.4	2.71	0.01
	15.0	266	1.43	2.68	0.01	186	12.9	2.74	0.01
	15.8	208	22.2	2.76	0.01	175	7.86	2.80	0.01
	16.0	188	27.2	2.68	0.01	186	7.86	2.75	0.00
	16.7	151	0.715	2.68	0.00	178	6.79	2.75	0.00
	17.7	69.5	20.4	2.63	0.00	157	16.8	2.75	0.01
	18.6	7.48	10.6	2.57	0.01	152	12.9	2.67	0.00
	18.9	2.83	1.14	2.54	0.01	160	3.57	2.66	0.00
	19.7	10.9	14.3	2.54	0.01	151	2.14	2.66	0.00
	20.8	1.21	1.72	2.49	0.00	161	36.5	2.66	0.01
FR 10m	0	283	26.8	3.07	0.00	251	13.9	3.00	0.01
	0.698	255	11.4	3.00	0.00	254	1.43	2.99	0.00
	0.958	249	1.07	2.90	0.01	262	3.93	2.92	0.01
	1.81	201	14.3	2.85	0.02	256	3.57	2.88	0.01
	2.60	172	13.2	2.82	0.01	243	10.7	2.88	0.01
	3.65	89.7	41.8	2.70	0.01	251	24.7	2.82	0.01
	4.07	41.7	39.7	2.61	0.00	230	8.58	2.79	0.01
	4.71	11.0	13.0	2.57	0.00	225	29.7	2.78	0.01
	4.98	0	0	2.58	0.00	215	20.0	2.81	0.01
	5.94	0.51	0.71	2.56	0.00	213	11.4	2.81	0.02
	6.75	0	0	2.55	0.00	208	18.6	2.79	0.02
	6.85	232	59.7	2.50	0.00	197	14.7	2.73	0.00
	7.62	253	3.22	2.68	0.01	194	2.14	2.84	0.01

8.02	254	20.7	2.74	0.03	191	17.5	2.92	0.00
8.79	180	20.0	2.72	0.03	200	6.08	2.91	0.00
9.60	84.4	13.6	2.63	0.02	194	0.36	2.86	0.01
10.6	1.52	0.14	2.50	0.00	192	12.9	2.79	0.01
11.1	0.10	0.14	2.56	0.01	169	17.9	2.79	0.01
11.9	0	0	2.53	0.01	173	8.58	2.74	0.01
12.6	0	0	2.62	0.01	184	32.5	2.73	0.00
13.8	5.56	7.86	2.63	0.02	167	4.65	2.73	0.00
13.8	247	25.0	2.65	0.01	185	18.6	2.78	0.00
14.8	289	5.72	2.69	0.00	198	1.07	2.73	0.00
15.0	265	11.8	2.76	0.01	179	16.1	2.78	0.01
15.8	218	44.3	2.77	0.01	194	14.7	2.84	0.00
16.0	205	54.0	2.74	0.01	192	5.36	2.82	0.00
16.7	144	63.6	2.70	0.02	183	5.36	2.80	0.00
17.7	79.6	79.7	2.65	0.03	178	9.29	2.78	0.00
18.6	14.6	20.6	2.58	0.04	164	1.43	2.72	0.00
18.9	9.50	10.6	2.57	0.04	178	18.2	2.71	0.00
19.7	4.55	1.86	2.53	0.00	184	0.71	2.69	0.00
20.8	0.91	0.71	2.50	0.01	161	6.43	2.67	0.01

Table C:2 – Data corresponding to Figure 5.6

		Live				Killed			
Reactor Sediment	**Time (d)**	**Fe(II) (mg/L)**	**Fe(II) S.D. (mg/L)**	**pH**	**pH S.D.**	**Fe(II) (mg/L)**	**Fe(II) S.D. (mg/L)**	**pH**	**pH S.D.**
GB 2m	0	245	5.36	3.15	0.01	245	11.8	3.06	0.00
	0.729	271	34.0	3.06	0.02	251	16.4	3.04	0.00
	1.05	225	13.9	2.97	0.02	252	0	2.98	0.01
	1.83	204	29.7	2.86	0.02	248	16.8	2.97	0.01
	2.74	138	9.65	2.77	0.04	235	11.4	2.95	0.01
	3.71	93.7	21.0	2.67	0.04	264	11.8	2.91	0.01
	4.83	56.8	11.7	2.61	0.04	223	3.93	2.89	0.01
	5.69	33.5	4.15	2.53	0.04	242	14.7	2.84	0.02
	6.89	14.1	12.4	2.57	0.03	241	8.22	2.88	0.02
	7.74	163	4.65	2.61	0.01	221	3.93	2.90	0.01
	8.73	189	17.2	2.59	0.02	197	20.0	2.89	0.01
	8.98	187	25.7	2.56	0.03	211	3.57	2.88	0.01
	9.98	194	16.8	2.64	0.02	237	26.8	2.88	0.01
	10.7	176	20.0	2.56	0.01	238	18.9	2.87	0.01
	11.8	135	24.7	2.61	0.02	242	4.65	2.88	0.01
	12.8	71.5	14.7	2.49	0.00	235	6.43	2.86	0.01
	13.2	39.2	10.9	2.56	0.01	206	4.65	2.83	0.02
	13.8	18.9	7.29	2.52	0.00	203	12.2	2.81	0.01
	14.0	358	10.4	2.54	0.01	361	10.4	2.84	0.01
	14.8	320	15.0	2.62	0.01	346	5.36	2.83	0.01
	15.9	256	6.08	2.56	0.00	361	5.36	2.83	0.02
	16.9	193	0.36	2.59	0.00	343	20.7	2.85	0.01
	17.7	145	1.07	2.56	0.00	352	12.5	2.86	0.01
	18.1	121	8.94	2.55	0.00	357	7.86	2.87	0.01
	18.8	78.9	18.0	2.63	0.01	365	1.07	2.93	0.01
	20.0	16.8	4.86	2.52	0.00	353	32.2	2.89	0.01
	20.8	3.64	3.43	2.53	0.00	347	19.7	2.90	0.01
FR 3m	0	270	8.58	3.26	0.02	278	5.36	3.12	0.02
	0.729	245	20.4	3.06	0.01	246	15.0	3.03	0.06
	1.05	205	21.8	2.97	0.01	256	7.51	2.98	0.05
	1.83	147.	12.9	2.82	0.01	239	8.94	2.94	0.05
	2.74	44.1	7.15	2.66	0.01	233	0.71	2.88	0.05
	3.71	3.84	0.29	2.58	0.01	204	1.43	2.78	0.04
	4.83	2.02	0.86	2.55	0.01	177	2.14	2.72	0.03
	5.69	0	0	2.48	0.00	144	10.4	2.64	0.03
	6.89	0	0	2.61	0.00	119	6.79	2.65	0.03
	7.74	128	1.79	2.66	0.01	195	17.9	2.70	0.01
	8.73	122	8.22	2.61	0.01	217	8.58	2.68	0.02
	8.98	105	18.2	2.53	0.01	198	17.9	2.62	0.02
	9.98	47.9	21.2	2.58	0.01	223	26.8	2.71	0.01

	10.7	26.9	13.2	2.57	0.01	210	28.6	2.69	0.01
	11.8	9.40	4.72	2.57	0.01	185	34.0	2.70	0.01
	12.8	0.71	0.71	2.51	0.01	178	10.4	2.66	0.02
	13.2	0.00	0	2.56	0.01	128	19.7	2.69	0.02
	13.8	0.00	0	2.52	0.01	113	22.5	2.64	0.03
	14.0	337	29.3	2.57	0.01	347	38.2	2.67	0.01
	14.8	234	24.3	2.55	0.03	332	33.6	2.75	0.02
	15.9	82.1	31.1	2.46	0.04	308	1.43	2.70	0.03
	16.9	9.50	8.86	2.56	0.01	309	25.7	2.70	0.03
	17.7	1.62	0.57	2.54	0.01	302	12.9	2.69	0.03
	18.1	0	0	2.53	0.01	294	11.1	2.68	0.03
	18.8	0.61	0.86	2.61	0.00	309	15.7	2.76	0.01
	20.0	0	0	2.50	0.01	275	16.8	2.67	0.01
	20.8	0	0	2.54	0.01	263	32.5	2.69	0.02
FR 10m	0	256	12.2	3.09	0.01	264	3.57	3.04	0.01
	0.729	204	31.5	2.94	0.02	295	4.65	2.98	0.01
	1.05	206	15.0	2.85	0.04	255	5.36	2.89	0.01
	1.83	100	37.2	2.71	0.05	225	6.43	2.84	0.00
	2.74	13.0	16.4	2.62	0.05	199	1.43	2.78	0.00
	3.71	1.62	0.86	2.55	0.04	209	9.29	2.72	0.00
	4.83	3.74	2.72	2.49	0.00	191	4.29	2.68	0.01
	5.69	0.10	0.14	2.44	0.00	130	8.94	2.60	0.00
	6.89	0	0	2.58	0.00	142	3.93	2.62	0.00
	7.74	108	365	2.61	0.02	220	2.50	2.66	0.01
	8.73	56.1	41.5	2.56	0.01	202	2.50	2.64	0.01
	8.98	20.9	29.6	2.49	0.01	232	1.79	2.61	0.01
	9.98	5.56	1.86	2.56	0.01	244	0.36	2.70	0.01
	10.7	5.26	2.00	2.53	0.00	238	1.43	2.69	0.01
	11.8	4.55	2.43	2.55	0.00	271	7.15	2.69	0.01
	12.8	0.81	0.29	2.50	0.00	203	6.43	2.63	0.00
	13.2	0	0	2.56	0.00	187	3.93	2.67	0.00
	13.8	0	0	2.54	0.00	158	10.0	2.65	0.01
	14.0	328	12.2	2.55	0.00	364	6.08	2.65	0.01
	14.8	251	13.6	2.61	0.02	346	3.93	2.72	0.00
	15.9	167	26.1	2.53	0.02	344	1.07	2.71	0.01
	16.9	72.7	29.3	2.62	0.02	331	8.22	2.70	0.00
	17.7	12.7	11.7	2.58	0.04	325	2.86	2.71	0.01
	18.1	1.92	0.71	2.57	0.04	318	2.50	2.71	0.00
	18.8	1.52	0.71	2.62	0.03	313	5.36	2.78	0.01
	20.0	0	0	2.55	0.03	312	21.1	2.71	0.00
	20.8	0	0	2.55	0.03	287	25.4	2.72	0.00

Table C:3 – Data corresponding to Figure 5.7

		Live				Killed			
Reactor Sediment	**Time (d)**	**Fe(II) (mg/L)**	**Fe(II) S.D. (mg/L)**	**pH**	**pH S.D.**	**Fe(II) (mg/L)**	**Fe(II) S.D. (mg/L)**	**pH**	**pH S.D.**
GB 2m	0	259	33.6	3.00	0.01	249	27.9	2.95	0.02
	0.594	253	0.36	2.97	0.00	257	18.2	2.93	0.03
	0.844	249	1.07	2.91	0.01	249	6.08	2.89	0.03
	1.55	252	9.29	2.89	0.01	246	5.72	2.91	0.02
	2.57	236	7.86	2.87	0.02	241	4.65	2.91	0.02
	3.83	163	115	2.80	0.03	273	6.08	2.88	0.02
	4.65	143	98.2	2.75	0.05	275	19.7	2.86	0.02
	5.61	131	96.5	2.70	0.05	263	0	2.84	0.02
	6.64	107	86.1	2.65	0.06	274	15.7	2.82	0.02
	6.84	263	156	2.67	0.07	418	36.1	2.84	0.05
	7.79	287	45.0	2.70	0.06	318	22.9	2.83	0.03
	8.55	286	61.1	2.69	0.06	334	20.0	2.83	0.03
	9.58	251	65.1	2.64	0.05	345	22.2	2.81	0.03
	10.6	223	76.5	2.58	0.04	335	55.4	2.79	0.02
	11.6	202	77.9	2.59	0.04	369	14.7	2.78	0.02
	12.6	171	59.7	2.56	0.04	390	23.2	2.78	0.03
	13.6	67.2	55.8	2.53	0.04	206	17.9	2.78	0.01
	13.9	312	87.9	2.54	0.05	485	14.7	2.82	0.02
	14.7	332	14.7	2.54	0.03	488	8.58	2.82	0.03
	15.6	261	23.2	2.53	0.02	493	18.6	2.81	0.02
	16.5	219	29.0	2.50	0.01	509	26.4	2.82	0.02
	17.6	152	61.1	2.48	0.01	491	75.8	2.81	0.02
	18.9	25.5	3.43	2.39	0.00	524	62.2	2.76	0.02
	19.8	5.86	0.57	2.37	0.01	421	61.3	2.76	0.01
	20.8	5.16	1.29	2.36	0.01	563	95.2	2.75	0.01
FR 3m	0	230	23.2	2.99	0.01	233	13.9	2.94	0.00
	0.594	218	5.36	2.90	0.00	238	13.2	2.91	0.00
	0.844	207	6.08	2.80	0.01	241	11.1	2.85	0.00
	1.55	194	2.50	2.77	0.01	242	3.22	2.86	0.00
	2.57	143	6.43	2.74	0.00	240	11.1	2.88	0.00
	3.83	58.8	5.15	2.63	0.02	259	0.36	2.83	0.01
	4.65	19.9	6.72	2.61	0.01	248	6.79	2.82	0.01
	5.61	4.65	2.29	2.52	0.01	248	5.36	2.78	0.02
	6.64	0.61	0.57	2.52	0.01	246	35.4	2.60	0.23
	6.84	230	35.7	2.55	0.01	305	14.7	2.79	0.00
	7.79	172	23.6	2.59	0.04	307	40.4	2.76	0.00
	8.55	96.8	36.8	2.60	0.02	331	9.65	2.77	0.01
	9.58	28.2	11.9	2.52	0.02	333	10.4	2.74	0.00
	10.6	2.22	0.29	2.42	0.01	338	13.2	2.71	0.00
	11.6	1.42	0	2.45	0.01	352	7.86	2.70	0.02

	12.6	1.01	0.29	2.51	0.05	370	13.6	2.68	0.01
	13.6	0	0	2.49	0.05	223	6.08	2.67	0.01
	13.9	347	99.0	2.59	0.08	447	10.7	2.72	0.00
	14.7	279	31.8	2.58	0.04	460	15.4	2.73	0.01
	15.6	216	27.2	2.56	0.02	461	3.93	2.72	0.00
	16.5	159	27.2	2.53	0.01	460	11.4	2.71	0.00
	17.6	84.1	38.0	2.51	0.00	444	53.6	2.70	0.01
	18.9	12.5	3.43	2.36	0.01	459	5.15	2.64	0.01
	19.8	4.14	2.14	2.37	0.02	343	9.44	2.64	0.01
	20.8	5.66	3.15	2.35	0.03	493	51.5	2.63	0.00
FR 10m	0	242	1.43	2.90	0.00	290	11.1	2.87	0.00
	0.594	216	26.5	2.81	0.00	238	8.94	2.82	0.01
	0.844	212	18.2	2.73	0.00	253	22.9	2.75	0.00
	1.55	189	21.4	2.74	0.00	251	15.7	2.76	0.00
	2.57	85.4	7.15	2.70	0.01	267	35.4	2.75	0.00
	3.83	13.5	6.22	2.58	0.02	258	7.15	2.70	0.00
	4.65	2.33	1.57	2.51	0.00	250	17.2	2.68	0.01
	5.61	0.51	0.14	2.47	0.01	245	23.9	2.65	0.01
	6.64	0.71	0.14	2.46	0.01	218	0.36	2.62	0.01
	6.84	338	33.6	2.52	0.01	408	33.6	2.67	0.02
	7.79	227	31.1	2.58	0.00	295	14.3	2.70	0.02
	8.55	125	26.5	2.56	0.01	314	37.9	2.70	0.02
	9.58	42.0	13.6	2.49	0.02	327	27.2	2.66	0.02
	10.6	2.53	2.72	2.39	0.02	332	31.8	2.62	0.03
	11.6	1.62	0	2.41	0.01	333	31.1	2.64	0.04
	12.6	0.71	0.14	2.50	0.02	359	42.5	2.61	0.04
	13.6	0	0	2.40	0.00	171	5.72	2.59	0.04
	13.9	287	0	2.46	0.01	417	55.4	2.66	0.04
	14.7	239	14.3	2.50	0.00	452	37.5	2.65	0.04
	15.6	143	5.72	2.48	0.00	454	24.3	2.64	0.04
	16.5	58.1	5.00	2.46	0.00	465	21.8	2.63	0.04
	17.6	9.50	2.00	2.45	0.01	468	14.7	2.62	0.04
	18.9	3.03	0.29	2.33	0.03	387	20.4	2.55	0.03
	19.8	4.55	2.14	2.34	0.02	286	2.50	2.56	0.03
	20.8	3.23	0.57	2.33	0.02	407	35.4	2.55	0.04

Table C:4 – Data corresponding to Figure 5.8

		Live				Killed			
Reactor Sediment	**Time (d)**	**Fe(II) (mg/L)**	**Fe(II) S.D. (mg/L)**	**pH**	**pH S.D.**	**Fe(II) (mg/L)**	**Fe(II) S.D. (mg/L)**	**pH**	**pH S.D.**
GB 2m	0	293	8.94	3.33	0.01	291	2.86	3.21	0.04
	0.896	246	1.43	3.17	0.01	292	1.79	3.19	0.04
	1.15	250	7.51	3.09	0.00	291	6.08	3.16	0.02
	1.63	214	10.4	2.99	0.01	298	15.7	3.13	0.03
	2.66	141	7.51	2.87	0.01	293	1.07	3.12	0.03
	3.93	61.0	16.7	2.76	0.03	291	8.22	3.09	0.03
	4.51	34.8	16.0	2.72	0.03	288	6.43	3.06	0.03
	5.53	5.76	8.15	2.65	0.03	271	4.29	3.01	0.03
	6.48	2.73	2.72	2.64	0.02	280	1.79	3.01	0.02
	7.52	2.02	2.86	2.63	0.01	293	3.57	3.00	0.03
	7.63	288	20.4	2.67	0.00	333	23.2	3.03	0.03
	8.64	267	10.0	2.67	0.01	314	54.3	3.02	0.02
	8.91	307	7.15	2.62	0.00	356	9.29	2.99	0.03
	9.88	269	8.94	2.65	0.01	358	3.57	3.01	0.03
	10.6	92.3	3.00	2.62	0.01	353	12.9	3.01	0.02
	11.8	77.1	3.00	2.58	0.01	351	18.6	3.00	0.02
	12.7	115	16.6	2.61	0.01	322	6.43	3.06	0.08
	13.5	74.2	0.57	2.58	0.01	330	12.9	3.05	0.08
	14.9	45.6	3.57	2.53	0.01	365	21.4	3.03	0.06
	15.6	18.9	6.43	2.51	0.01	410	9.29	3.01	0.07
	15.9	327	8.22	2.51	0.01	299	11.4	3.03	0.07
	16.6	265	13.9	2.57	0.01	298	7.86	3.04	0.06
	17.7	165	27.2	2.53	0.01	303	21.8	3.03	0.06
	18.6	85.2	13.2	2.50	0.01	281	16.4	3.02	0.06
	19.7	14.5	5.58	2.48	0.02	292	27.5	3.01	0.06
	20.6	3.74	0.71	2.53	0.03	244	12.9	3.01	0.05
	21.6	1.72	1.29	2.50	0.02	211	20.7	2.99	0.04
	22.7	0.20	0.29	2.46	0.02	193	19.3	2.98	0.04
FR 3m	0	263	1.43	3.20	0.02	284	10.0	3.16	0.04
	0.896	264	10.0	3.03	0.01	280	6.43	3.08	0.01
	1.15	236	11.1	2.95	0.01	270	3.93	3.03	0.01
	1.63	144	21.4	2.82	0.02	251	6.43	2.96	0.01
	2.66	71.0	49.0	2.74	0.01	222	1.43	2.93	0.01
	3.93	6.67	5.72	2.64	0.01	193	11.4	2.84	0.01
	4.51	3.94	2.72	2.60	0.01	172	11.4	2.79	0.00
	5.53	2.53	0.14	2.58	0.01	141	14.7	2.74	0.01
	6.48	1.31	0.43	2.58	0.01	115	11.4	2.70	0.01
	7.52	1.92	2.72	2.58	0.01	98	2.14	2.66	0.01
	7.63	320	15.0	2.64	0.00	304	26.8	2.73	0.01
	8.64	261	3.93	2.62	0.01	297	8.22	2.71	0.01

	8.91	276	0.71	2.55	0.00	324	12.5	2.66	0.01
	9.88	168	16.1	2.58	0.01	273	33.2	2.69	0.01
	10.6	88.0	4.00	2.52	0.01	276	10.4	2.67	0.01
	11.8	20.1	6.15	2.48	0.01	273	14.3	2.66	0.00
	12.7	0.91	0.14	2.52	0.01	271	40.7	2.68	0.01
	13.5	0.30	0.14	2.49	0.01	251	25.7	2.65	0.01
	14.9	0	0	2.46	0.02	221	20.4	2.63	0.02
	15.6	2.12	1.29	2.45	0.02	170	35.7	2.58	0.00
	15.9	338	15.7	2.48	0.03	316	110	2.59	0.01
	16.6	248	10.7	2.52	0.01	349	19.7	2.64	0.00
	17.7	97.0	0.71	2.48	0.02	323	18.6	2.62	0.00
	18.6	25.0	11.1	2.45	0.01	300	12.2	2.62	0.01
	19.7	6.47	6.86	2.43	0.01	352	21.1	2.62	0.01
	20.6	2.02	1.43	2.47	0.00	261	2.14	2.67	0.01
	21.6	0	0	2.44	0.01	225	6.43	2.64	0.01
	22.7	0	0	2.42	0.01	150	15.0	2.61	0.01
FR 10m	0	289	31.1	3.18	0.03	269	5.00	3.08	0.00
	0.896	261	21.8	3.01	0.03	265	22.5	3.01	0.01
	1.15	212	3.22	2.94	0.02	273	19.7	2.97	0.01
	1.63	151	14.3	2.85	0.04	248	0.71	2.93	0.01
	2.66	48.0	12.2	2.77	0.02	242	7.86	2.91	0.01
	3.93	2.63	0.29	2.67	0.03	223	1.07	2.84	0.01
	4.51	1.31	0.14	2.64	0.02	216	1.43	2.81	0.01
	5.53	2.12	3.00	2.59	0.02	197	5.00	2.76	0.01
	6.48	1.52	1.29	2.58	0.01	187	0.71	2.73	0.00
	7.52	0.51	0.71	2.57	0.00	180	2.50	2.71	0.00
	7.63	345	6.43	2.65	0.01	316	0.71	2.77	0.00
	8.64	165	1.07	2.63	0.00	321	14.3	2.75	0.00
	8.91	148	3.22	2.59	0.01	336	1.79	2.72	0.01
	9.88	42.2	27.5	2.59	0.01	319	9.65	2.75	0.00
	10.6	7.28	2.00	2.52	0.00	312	17.5	2.73	0.01
	11.8	2.22	0.86	2.48	0.00	320	37.9	2.72	0.01
	12.7	1.31	0.43	2.52	0.00	291	25.7	2.74	0.01
	13.5	0.81	0.29	2.50	0.00	301	22.2	2.72	0.01
	14.9	0.10	0.14	2.45	0.01	299	45.4	2.68	0.00
	15.6	3.54	2.43	2.44	0.00	315	69.0	2.67	0.00
	15.9	419	4.29	2.50	0.00	287	21.4	2.69	0.05
	16.6	218	2.86	2.53	0.00	340	7.15	2.69	0.04
	17.7	58.6	2.86	2.49	0.00	311	16.1	2.67	0.01
	18.6	10.4	1.07	2.46	0.01	295	9.65	2.67	0.01
	19.7	2.22	0.29	2.45	0.01	311	23.6	2.67	0.01
	20.6	0.91	0.43	2.50	0.01	266	6.79	2.71	0.00
	21.6	0.51	0.71	2.46	0.00	232	6.08	2.69	0.01
	22.7	0.51	0.71	2.44	0.01	182	9.29	2.67	0.01

Table C:5 – Data corresponding to Figure 5.9

		Live				Killed			
Reactor Sediment	**Time (d)**	**Fe(II) (mg/L)**	**Fe(II) S.D. (mg/L)**	**pH**	**pH S.D.**	**Fe(II) (mg/L)**	**Fe(II) S.D. (mg/L)**	**pH**	**pH S.D.**
GB 2m	0	262	0.86	2.99	0.02	249	0.86	2.90	0.02
	0.990	221	13.7	2.92	0.01	228	34.6	2.90	0.03
	2.25	169	0	2.80	0.02	200	40.9	2.87	0.05
	3.23	97.3	2.57	2.71	0.03	204	27.2	2.86	0.05
	4.16	7.68	5.15	2.58	0.00	209	17.2	2.82	0.04
	4.90	6.87	4.86	2.50	0.00	215	26.6	2.79	0.04
	5.94	3.74	2.72	2.47	0.00	224	20.9	2.78	0.04
	6.93	0.71	1.00	2.44	0.00	243	18.3	2.76	0.04
	7.20	283	5.43	2.47	0.02	586	115	2.81	0.01
	8.14	255	2.29	2.62	0.02	546	64.6	2.90	0.04
	8.92	215	12.6	2.63	0.02	565	14.5	2.91	0.04
	9.32	174	16.6	2.59	0.02	512	60.5	2.90	0.05
	10.1	123	33.7	2.62	0.02	551	75.6	2.91	0.05
	10.7	54.2	2.29	2.61	0.02	572	1.00	2.94	0.04
	11.4	18.3	2.14	2.59	0.02	555	11.0	2.95	0.05
	12.6	3.13	0.43	2.58	0.02	543	15.0	2.97	0.05
	14.6	1.82	0.86	2.43	0.01	565	99.1	2.84	0.04
	14.7	340	74.3	2.47	0.01	485	1.00	2.86	0.04
	15.4	295	54.6	2.50	0.01	503	5.50	2.85	0.04
	15.6	278	46.0	2.49	0.01	514	8.01	2.82	0.05
	16.4	195	7.43	2.48	0.02	524	19.0	2.80	0.05
	16.9	138	12.3	2.47	0.01	520	13.5	2.80	0.05
	17.4	77.4	15.7	2.47	0.01	538	53.0	2.79	0.04
	18.7	4.55	0.43	2.40	0.00	524	38.0	2.76	0.04
	19.6	3.34	0.71	2.38	0.00	534	31.5	2.75	0.04
	21.5	2.22	1.14	2.33	0.00	551	22.0	2.74	0.05
FR 10m	0	237	1.43	2.89	0.03	242	29.5	2.83	0.00
	0.990	197	10.0	2.72	0.03	238	3.72	2.76	0.01
	2.25	7.18	11.1	2.57	0.05	193	8.29	2.66	0.02
	3.23	3.94	21.4	2.52	0.03	179	1.72	2.62	0.02
	4.16	0	49.0	2.46	0.02	170	8.86	2.57	0.02
	4.90	8.19	5.72	2.44	0.02	163	10.6	2.54	0.02
	5.94	2.83	2.72	2.42	0.03	146	8.01	2.50	0.02
	6.93	0.81	0.14	2.40	0.03	124	18.3	2.47	0.01
	7.20	267	0.43	2.44	0.02	402	47.8	2.49	0.02
	8.14	157	2.72	2.54	0.04	420	30.0	2.69	0.00
	8.92	47.1	15.0	2.53	0.04	368	23.5	2.70	0.01
	9.32	36.8	3.93	2.49	0.04	371	2.50	2.67	0.01
	10.1	13.6	0.71	2.60	0.04	359	7.51	2.71	0.02
	10.7	6.57	16.1	2.59	0.04	356	9.51	2.70	0.01

	11.4	3.64	4.00	2.58	0.02	332	11.0	2.69	0.01
	12.6	1.11	6.15	2.56	0.01	305	34.5	2.68	0.01
	14.6	0.71	0.14	2.45	0.01	305	35.5	2.52	0.01
	14.7	363	0.14	2.50	0.01	369	100	2.55	0.01
	15.4	308	0	2.52	0.01	368	4.50	2.63	0.01
	15.6	266	1.29	2.50	0.01	349	0.50	2.62	0.01
	16.4	106	15.7	2.46	0.01	332	8.01	2.60	0.01
	16.9	48.1	10.7	2.41	0.01	321	6.00	2.60	0.01
	17.4	3.64	0.71	2.34	0.01	305	7.51	2.60	0.01
	18.7	1.01	11.1	2.41	0.01	275	14.0	2.55	0.00
	19.6	0.51	6.86	2.39	0.01	264	16.5	2.53	0.01
	21.5	0.51	1.43	2.36	0.01	253	15.5	2.48	0.01

Table C:6 – Data corresponding to Figure 5.10

		Live				**Killed**			
Reactor Sediment	**Time (d)**	**Fe(II) (mg/L)**	**Fe(II) S.D. (mg/L)**	**pH**	**pH S.D.**	**Fe(II) (mg/L)**	**Fe(II) S.D. (mg/L)**	**pH**	**pH S.D.**
GB 2m	0	254	4.57	2.88	0.01	257	6.58	2.79	0.02
	0.792	274	17.7	2.80	0.03	273	21.44	2.71	0.01
	1.69	288	12.9	2.77	0.03	286	21.44	2.69	0.01
	2.04	300	5.15	2.73	0.03	300	20.87	2.66	0.01
	2.70	323	16.6	2.70	0.02	309	20.87	2.63	0.00
	4.73	312	15.4	2.71	0.02	311	19.73	2.58	0.05
	5.86	307	14.0	2.71	0.02	313	21.73	2.56	0.06
	8.77	290	19.7	2.66	0.04	313	24.02	2.59	0.00
	10.7	315	13.7	2.66	0.05	318	12.01	2.61	0.00
	14.9	358	2.00	2.60	0.08	377	6.00	2.56	0.00
	18.1	347	14.7	2.56	0.09	396	17.16	2.53	0.00
	22.4	374	7.51	2.53	0.10	457	31.81	2.50	0.00
FR 10m	0	244	0.86	2.79	0.05	246	0.04	2.68	0.00
	0.792	222	13.7	2.64	0.01	267	0.34	2.58	0.01
	1.69	243	0	2.61	0.00	271	0.56	2.54	0.00
	2.04	245	2.57	2.59	0.01	273	0.79	2.51	0.00
	2.70	248	5.15	2.56	0.01	277	1.01	2.47	0.00
	4.73	261	4.86	2.59	0.02	296	0.40	2.47	0.00
	5.86	269	2.72	2.61	0.04	306	0.08	2.46	0.00
	8.77	290	1.00	2.56	0.05	283	0.19	2.41	0.00
	10.7	291	5.43	2.55	0.04	313	0.23	2.42	0.00
	14.9	366	2.29	2.41	0.01	425	0.31	2.34	0.00
	18.1	313	12.6	2.37	0.03	339	1.00	2.30	0.00
	22.4	357	16.6	2.32	0.00	480	1.99	2.25	0.00

Table C:7 – Data corresponding to Figure 5.12

Reactor Sediment	Time (d)	Fe(II) (mg/L)	Fe(II) S.D. (mg/L)	pH	pH S.D.
GB 2m	0	32.9	10.4	3.10	0.02
	1.15	43.9	11.2	3.09	0.02
	2.91	41.0	6.29	3.08	0.01
	4.18	37.4	8.65	3.06	0.00
	12.0	19.1	2.14	3.02	0.00
	18.0	17.3	2.14	2.98	0.01
	23.0	18.8	1.22	2.96	0.02
FR 3m	0	31.7	1.14	3.14	0.04
	1.15	14.9	0.43	3.00	0.01
	2.91	0.66	0.50	2.99	0.01
	4.18	0.61	0.86	2.98	0.02
	12.0	1.92	0.29	2.98	0.01
	18.0	1.77	0.50	2.91	0.01
	23.0	0	0	2.93	0.01
FR 10m	0	16.7	5.00	3.07	0.02
	1.15	8.79	3.86	2.94	0.00
	2.91	2.12	0.00	2.93	0.00
	4.18	1.06	1.22	2.90	0.00
	12.0	0.51	0	2.85	0.01
	18.0	0.20	0.29	2.79	0.01
	23.0	0	0	2.76	0.01

Table C:8 – Data corresponding to Figure 5.13

Reactor Sediment	Time (d)	Fe(II) (mg/L)	Fe(II) S.D. (mg/L)	pH	pH S.D.
GB 2m	0	262	0.86	2.99	0.02
	0.990	221	13.7	2.92	0.01
	2.25	169	0	2.80	0.02
	3.23	97.3	2.57	2.71	0.03
	4.16	7.68	5.15	2.58	0.00
	4.90	6.87	4.86	2.50	0.00
	5.94	3.74	2.72	2.47	0.00
	6.93	0.71	1.00	2.44	0.00
	7.20	283	5.43	2.47	0.02
	8.14	255	2.29	2.62	0.02
	8.92	215	12.6	2.63	0.02

	9.32	174	16.6	2.59	0.02
	10.1	123	33.7	2.62	0.02
	10.7	54.2	2.29	2.61	0.02
	11.4	18.3	2.14	2.59	0.02
	12.6	3.13	0.43	2.58	0.02
	14.6	1.82	0.86	2.43	0.01
	14.7	340	74.3	2.47	0.01
	15.4	295	54.6	2.50	0.01
	15.6	278	46.0	2.49	0.01
	16.4	195	7.43	2.48	0.02
	16.9	138	12.3	2.47	0.01
	17.4	77.4	15.7	2.47	0.01
	18.7	4.55	0.43	2.40	0.00
	19.6	3.34	0.71	2.38	0.00
	21.5	2.22	1.14	2.33	0.00
PF	0	250	0.57	2.98	0.01
	0.990	215	23.2	2.93	0.00
	2.25	187	0.86	2.83	0.01
	3.23	99.3	10.0	2.71	0.01
	4.16	8.49	12.0	2.61	0.00
	4.90	3.54	2.43	2.52	0.01
	5.94	2.63	2.29	2.48	0.01
	6.93	1.72	1.86	2.46	0.01
	7.20	299	35.5	2.49	0.01
	8.14	250	2.86	2.64	0.01
	8.92	210	20.9	2.64	0.00
	9.32	154	56.3	2.61	0.00
	10.1	134	12.9	2.62	0.01
	10.7	53.6	2.00	2.62	0.01
	11.4	27.2	2.43	2.61	0.01
	12.6	3.23	1.72	2.60	0.01
	14.6	2.02	0.57	2.45	0.01
	14.7	289	19.2	2.48	0.01
	15.4	259	20.3	2.50	0.01
	15.6	241	29.5	2.48	0.01
	16.4	223	36.3	2.48	0.02
	16.9	161	52.3	2.48	0.01
	17.4	92.8	50.0	2.47	0.01
	18.7	30.6	2.72	2.39	0.01
	19.6	14.0	1.14	2.37	0.02
	21.5	5.26	4.29	2.34	0.02

Table C:9 – Data corresponding to Figure 5.14

Reactor Sediment	Time (d)	Fe(II) (mg/L)	Fe(II) S.D. (mg/L)	pH	pH S.D.
GB 2m	0	249	0.86	2.90	0.02
	0.990	228	34.6	2.90	0.03
	2.25	200	40.9	2.87	0.05
	3.23	204	27.2	2.86	0.05
	4.16	209	17.2	2.82	0.04
	4.90	215	26.6	2.79	0.04
	5.94	224	20.9	2.78	0.04
	6.93	243	18.3	2.76	0.04
	7.20	586	115	2.81	0.01
	8.14	546	64.6	2.90	0.04
	8.92	565	14.5	2.91	0.04
	9.32	512	60.5	2.90	0.05
	10.1	551	75.6	2.91	0.05
	10.7	572	1.00	2.94	0.04
	11.4	555	11.0	2.95	0.05
	12.6	543	15.0	2.97	0.05
	14.6	565	99.1	2.84	0.04
	14.7	485	1.00	2.86	0.04
	15.4	503	5.50	2.85	0.04
	15.6	514	8.01	2.82	0.05
	16.4	524	19.0	2.80	0.05
	16.9	520	13.5	2.80	0.05
	17.4	538	53.0	2.79	0.04
	18.7	524	38.0	2.76	0.04
	19.6	534	31.5	2.75	0.04
	21.5	551	22.0	2.74	0.05
FR 10m	0	242	29.5	2.83	0.00
	0.990	238	3.72	2.76	0.01
	2.25	193	8.29	2.66	0.02
	3.23	179	1.72	2.62	0.02
	4.16	170	8.86	2.57	0.02
	4.90	163	10.6	2.54	0.02
	5.94	146	8.01	2.50	0.02
	6.93	124	18.3	2.47	0.01
	7.20	402	47.8	2.49	0.02
	8.14	420	30.0	2.69	0.00
	8.92	368	23.5	2.70	0.01
	9.32	371	2.50	2.67	0.01
	10.1	359	7.51	2.71	0.02
	10.7	356	9.51	2.70	0.01
	11.4	332	11.0	2.69	0.01
	12.6	305	34.5	2.68	0.01

	14.6	305	35.5	2.52	0.01
	14.7	369	100	2.55	0.01
	15.4	368	4.50	2.63	0.01
	15.6	349	0.50	2.62	0.01
	16.4	332	8.01	2.60	0.01
	16.9	321	6.00	2.60	0.01
	17.4	305	7.51	2.60	0.01
	18.7	275	14.0	2.55	0.00
	19.6	264	16.5	2.53	0.01
	21.5	253	15.5	2.48	0.01
NS	0	257	2.00	2.98	0.01
	0.990	244	28.0	2.99	0.01
	2.25	243	26.6	2.98	0.01
	3.23	249	19.4	2.96	0.00
	4.16	257	16.6	2.95	0.01
	4.90	250	5.15	2.94	0.02
	5.94	254	3.72	2.93	0.02
	6.93	254	7.43	2.91	0.02
	7.20	543	8.58	2.96	0.02
	8.14	563	1.00	2.99	0.02
	8.92	607	16.5	2.98	0.00
	9.32	609	26.5	2.97	0.01
	10.1	634	17.0	2.96	0.01
	10.7	613	5.50	2.98	0.01
	11.4	653	18.5	2.99	0.00
	12.6	678	41.5	3.06	0.02
	14.6	646	19.5	2.93	0.02
	14.7	618	30.0	2.96	0.02
	15.4	624	29.5	2.95	0.01
	15.6	629	19.5	2.93	0.01
	16.4	634	11.5	2.93	0.01
	16.9	630	5.50	2.93	0.02
	17.4	630	14.0	2.93	0.01
	18.7	603	26.5	2.90	0.01
	19.6	632	33.5	2.90	0.02
	21.5	658	35.0	2.89	0.03

Table C:10 – Data corresponding to Figure 5.15

	GB 2m		FR 3m		FR 10m	
Gas Mix	**CFU/g DW**	**S.D.**	**CFU/g DW**	**S.D.**	**CFU/g DW**	**S.D.**
Initial	4.1×10^4	2.2×10^4	1.4×10^4	3.7×10^3	5.1×10^4	9.4×10^3
1	7.0×10^3	4.0×10^2	5.8×10^4	4.7×10^4	2.0×10^5	1.5×10^4
2	2.0×10^4	2.0×10^4	1.6×10^4	2.8×10^3	2.3×10^5	1.3×10^5
3	2.4×10^7	1.2×10^7	6.6×10^6	4.4×10^6	6.5×10^5	1.5×10^5
4	1.0×10^8	5.2×10^6	8.9×10^6	5.7×10^6	3.9×10^6	6.5×10^5
5	2.6×10^7	6.4×10^6	---	---	1.1×10^7	6.1×10^6

Appendix D

Tabulated Data for Iron(II) Oxidation Rates

Table D:1 – Data corresponding to Figure 5.16

	Zero-order Rate Expression		First-order Rate Expression	
Time (d)	**FR 10m Fe(II) Conc. (mg/L) ***	**Kinetic Rate Data**	**ln Fe(II) / $Fe(II)_{initial}$***	**Kinetic Rate Data**
0	*283*	k_1 = 59.902	*0*	k_1 = 0.5941 1/d
0.698	*255*	mg/L-d	*-0.104*	
0.958	*249*		*-0.129*	R^2 = 0.803
1.81	*201*	R^2 = 98.5	*-0.345*	
2.60	*172*		*-0.498*	N=8
3.65	*90.0*	N=9	*-1.15*	
4.07	*41.7*		*-1.92*	
4.71	*11.0*		*-3.25*	
4.98	*0*		***	
5.94	0.505		-6.33	
6.75	0		***	
6.85	232		0	
7.62	253		0.085	
8.02	254		0.088	
8.79	180		-0.255	
9.60	84.4		-1.01	
10.6	1.52		-5.03	
11.1	0.101		-7.74	
11.9	0		***	
12.6	0		***	
13.8	5.56		-3.73	
13.8	247		*0*	
14.8	*289*	k_3 = 70.388	*0.157*	k_3 = 0.9491 1/d
15.0	*265*	mg/L-d	*0.070*	
15.8	*218*		*-0.122*	R^2 = 0.940
16.0	*205*	R^2 = 99.8	*-0.183*	
16.7	*144*		*-0.538*	N=11
17.7	*79.6*	N=7	*-1.13*	
18.6	*14.6*		*-2.83*	
18.9	9.50		*-3.26*	
19.8	4.55		*-3.99*	
20.8	0.910		*-5.60*	

* Italicized values were included in the rate expression.

Table D:2 – Data corresponding to Figure 5.17

First Iron(II) Addition (k^1)

		GB 2m (mg/L-d)			FR 3m (mg/L-d)			FR 10m (mg/L-d)		
Gas Mix	**% O2**	**Killed**	**Overall**	**Live**	**Killed**	**Overall**	**Live**	**Killed**	**Overall**	**Live**
6	0	-8.99	-8.60	0.393	---	---	---	-9.23	-6.10	3.13
1	0.7	0.150	36.5	36.3	13.9	49.3	35.4	7.93	59.9	52.0
2	1.5	1.73	39.9	38.1	22.2	78.5	56.3	27.4	76.7	49.3
4	10	-4.08	25.4	29.5	-1.83	44.7	46.5	5.11	49.8	44.7
3	21	1.49	56.3	54.8	27.0	67.6	40.6	13.4	71.0	57.7
5	21 + Glu	0.542	56.8	56.2	---	---	---	17.1	82.6	65.4

Third Iron(II) Addition (k^3)

		GB 2m (mg/L-d)			FR 3m (mg/L-d)			FR 10m (mg/L-d)		
Gas Mix	**% O2**	**Killed**	**Overall**	**Live**	**Killed**	**Overall**	**Live**	**Killed**	**Overall**	**Live**
6	0	-7.39	-4.13	3.27	---	---	---	-8.46	-5.81	2.65
1	0.7	-4.22	11.5	15.8	5.36	70.3	64.9	3.58	70.4	66.8
2	1.5	0.359	54.8	54.5	10.5	116	105	9.65	84.8	75.2
4	10	-3.36	69.3	72.6	3.36	65.9	62.5	13.6	79.1	65.5
3	21	16.3	83.2	66.9	23.4	91.0	67.6	17.1	146	129
5	21 + Glu	-7.74	89.2	97.0	---	---	---	19.4	144	124

Table D:3 – Data corresponding to Figure 5.18					
Batch Reactors		**Model Output: kbio (L^3/mg-mol^2-s) Cbact (mg DW/L)**			
Mix 1 (0.7% O_2, 1.1% CO_2, 98.2% N_2)					
Time (d)	**Fe(II) Aq (mg/L)**	**Time (d)**	**$1.02x10^9$ 15**	**$1.02x10^8$ 15**	**$1.02x10^8$ 1.5**
0	302	0	335	335	335
0.698	247	0.5	0	300	332
0.958	248	1	0	267	328
1.81	211	1.5	0	235	323
2.60	163	2	0	207	316
3.65	60.1	2.5	0	183	306
4.07	13.6	3	0	164	299
4.71	1.82	3.5	0	150	294
4.98	0	4	0	134	288
5.94	1.01	4.5	0	118	281
6.75	0	5	0	105	273
6.85	274	5.5	0	94.3	266
7.61	255	6	0	85.6	259
8.02	268	6.5	0	78.2	253
8.79	194	7	89.0	159	328
9.60	94.0	7.5	177	296	470
10.6	1.42	8	9.52	302	523
11.1	0.202	8.5	8.93	244	505
11.9	0	9	8.41	205	488
12.6	0	9.5	7.94	178	472
13.8	0	10	7.47	154	455
13.8	229	10.5	7.01	134	438
14.8	293	11	6.55	118	420
15.0	256	11.5	6.10	104	401
15.8	187	12	5.70	92.1	383
16.0	167	12.5	5.33	82.8	366
16.7	99.1	13	5.05	76.1	353
17.7	23.3	13.5	4.84	71.2	342
18.6	0	14	91	152	411
18.9	2.02	14.5	188	293	546
19.8	5.86	15	0	303	594
20.8	1.42	15.5	0	235	567
		16	0	196	545
		16.5	0	171	526
		17	0	151	506
		17.5	0	133	487

		18	0	119	467
		18.5	0	107	448
		19	0	95.8	428
		19.5	0	86.1	409
		20	0	78.2	391
		20.5	0	71.6	375
		21	0	65.9	359
Mix 2 (1.5% O_2, 7.3% CO_2, 91.2% N_2)					
0	265	0	335	335	335
0.729	226	0.5	0	268	328
1.05	216	1	0	214	320
1.83	126	1.5	0	170	310
2.74	24.7	2	0	137	299
3.71	2.22	2.5	0	112	287
4.83	1.82	3	0	93.4	275
5.69	0.202	3.5	0	79.1	263
6.89	0	4	0	67.8	250
7.74	133	4.5	0	58.8	238
8.73	85.4	5	0	51.3	226
8.98	41.9	5.5	0	45.0	214
9.98	6.87	6	0	39.9	202
10.7	6.67	6.5	0	35.6	191
11.8	6.27	7	74.2	106	252
12.8	1.01	7.5	112	222	369
13.2	0	8	0	198	405
13.8	0	8.5	0	129	376
14.0	337	9	0	97.9	349
14.8	261	9.5	0	78.7	324
15.9	185	10	0	66.4	303
16.9	93.4	10.5	0	57.7	285
17.7	21.0	11	0	50.8	268
18.1	1.42	11.5	0	45.2	253
18.8	2.02	12	0	40.9	239
20.0	0	12.5	0	37.5	227
20.8	0	13	0	34.4	216
		13.5	0	31.6	205
		14	87.1	115.7	278
		14.5	97.4	251	417
		15	0	205	456
		15.5	0	125	417
		16	0	92.7	380
		16.5	0	72.9	346
		17	0	61.9	321
		17.5	0	54.8	302
		18	0	49.0	284

		18.5	0	44.0	267
		19	0	40.2	253
		19.5	0	37.2	242
		20	0	34.4	230
		20.5	0	31.9	218
		21	0	29.7	208
Mix 3 (breathing air)					
0	267	0	335	335	335
0.896	276	0.5	0	0	328
1.15	209	1	0	0	320
1.63	161	1.5	0	0	310
2.66	56.6	2	0	0	300
3.93	2.43	2.5	0	0	288
4.51	1.42	3	0	0	275
5.53	0	3.5	0	0	263
6.48	0.607	4	0	0	250
7.52	1.01	4.5	0	0	238
7.63	350	5	0	0	226
8.64	164	5.5	0	0	214
8.91	150	6	0	0	203
9.88	61.7	6.5	0	0	193
10.6	8.69	7	0	0	184
11.8	2.83	7.5	0	0	175
12.7	1.62	8	94.9	94.9	253
13.5	1.01	8.5	0	41.8	389
14.9	0.202	9	84.1	84.1	420
15.6	1.82	9.5	0	0	379
15.9	422	10	0	0	344
16.6	216	10.5	0	0	313
17.7	56.6	11	0	0	286
18.6	9.60	11.5	0	0	261
		12	0	0	240
		12.5	0	0	220
		13	0	0	205
		13.5	0	0	192
		14	0	0	181
		14.5	0	0	170
		15	0	0	161
		15.5	0	0	152
		16	96.2	96.2	231
		16.5	0	0	362
		17	83.3	83.3	385
		17.5	0	0	342
		18	0	0	306
		18.5	0	0	276

	19	0	0	250
	19.5	0	0	228
	20	0	0	209
	20.5	0	0	193
	21	0	0	180
	21.5	0	0	170
	22	0	0	160
	22.5	0	0	151
	23	0	0	143
	23.5	0	0	136
	24	0	0	129

Appendix E

Supporting Data for Discussion

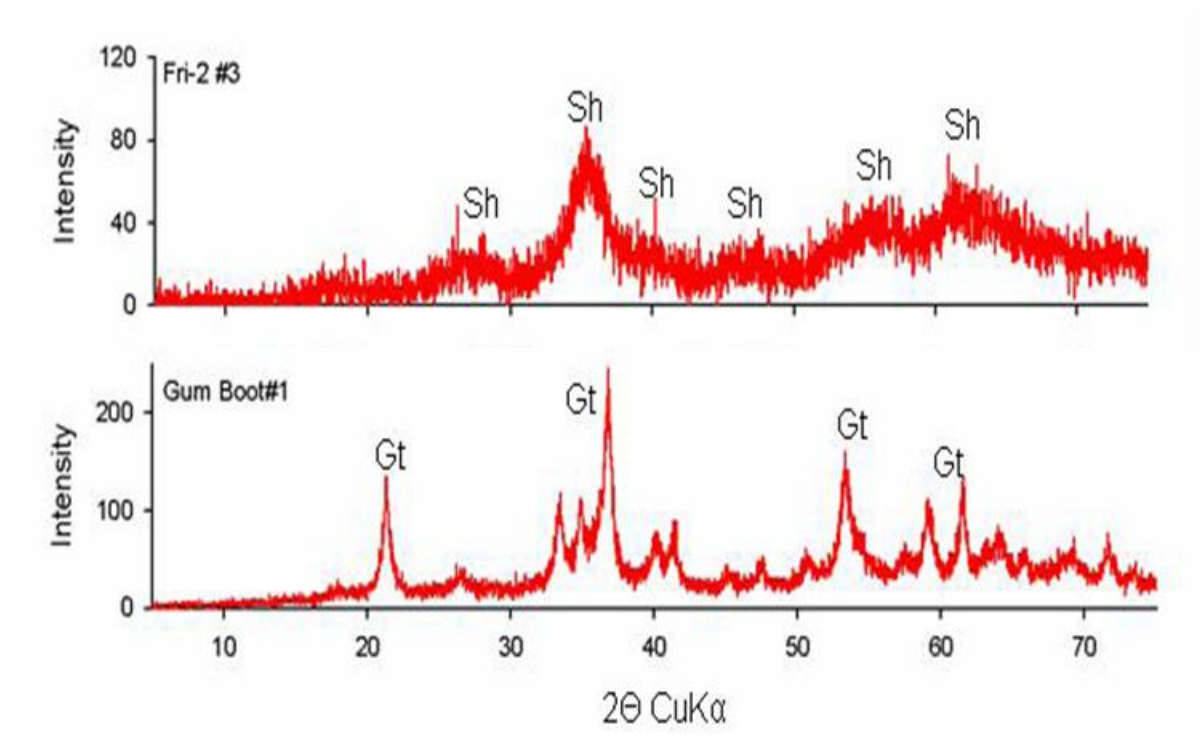

Figure E:1: X-ray diffraction patterns from sediments collected from the top 2 cm of the iron mounds at Gum Boot Run and Fridays-2. The upper pattern is from a sediment sample collected 3 m downstream of the Fridays-2 discharge. The lower panel is from a sediment sample collected immediately downstream of the Gum Boot Run discharge. Sh designates XRD peaks that correspond to schwertmannite, and Gt designates XRD peaks that correspond to goethite. Images courtesy of T. Peretyazhko.

Table E:1 – Data corresponding to Figure 6.1

Gum Boot Mine DO (mg/L)				
Distance (m)	**October 2005**	**July 2006**	**October 2006**	**May 2007**
0	0.06	0.10	0.3	0.16
2	5.5	4.9	5.3	1.9
9	6.8	6.0	7.4	11
15	8.4	7.5	7.7	6.6
60	8.1	7.7	7.9	11
95	8.7	6.3	---	10
127	6.3	7.2	7.3	8.6
Fridays-2 Mine DO (mg/L)				
Distance (m)	**February 2006**	**July 2006**	**May 2007**	**July 2007**
0	0	0.30	0.15	0.97
3	1.2	1.9	3.4	3.8
8	11	11	10	6.2
10	12	9.0	9.3	6.6
20	10	6.9	---	---

Table E:2 – TOC/TIC Data for iron mound sediments

Gum Boot Mine						
Sample Distance (m)	**WW (g)**	**DW (g) 105 °C, 5 days**	**AW (g) 400 °C, 24 hrs**	**AW (g) 550 °C, 24 hrs**	**TOC (mg $C_{400°C}$/kg $DW_{105°C}$)**	**TIC (mg $C_{550°C}$/kg $DW_{105°C}$)**
0	2.502	0.698	0.561	0.360	1.96×10^5	2.88×10^5
2	1.017	0.361	0.271	0.136	2.49×10^5	3.74×10^5
9	0.923	0.316	0.226	0.090	2.85×10^5	4.30×10^5
15	0.860	0.232	0.150	0.026	3.53×10^5	5.34×10^5
60	2.392	1.465	1.195	0.854	1.84×10^5	2.33×10^5
95	1.775	1.096	1.025	0.750	0.65×10^5	2.51×10^5
127	1.850	1.228	1.128	0.806	0.81×10^5	2.62×10^5
Fridays-2 Mine						
0	0.979	-0.027	-0.056	-0.123	-10.7×10^5	-24.8×10^5
3	1.059	0.327	0.250	0.114	2.35×10^5	4.16×10^5
8	1.053	0.174	0.115	0.027	3.39×10^5	5.06×10^5
10	0.978	0.191	0.126	0.010	3.40×10^5	6.07×10^5
20	1.069	0.388	0.307	0.147	2.09×10^5	4.12×10^5

Table E:3 – Data corresponding to Figure 6.3					
1st Fe(II) Addition (mg/d-CFU)					
Sediment	**Mix 1 (0.7% O_2)**	**Mix 2 (1.5% O_2)**	**Mix 4 (10% O_2)**	**Mix 3 (21% O_2)**	**Mix 5 (21% O_2 + glucose)**
GB 2m	1.6×10^{-5}	7.5×10^{-5}	9.5×10^{-5}	1.1×10^{-4}	1.2×10^{-4}
FR 3m	3.2×10^{-4}	5.3×10^{-4}	3.0×10^{-4}	4.1×10^{-4}	---
FR 10m	1.4×10^{-4}	1.7×10^{-4}	1.6×10^{-4}	3.0×10^{-4}	2.9×10^{-4}
3rd Fe(II) Addition (mg/d-CFU)					
GB 2m	9.2×10^{-5}	1.6×10^{-4}	3.8×10^{-8}	2.0×10^{-7}	1.9×10^{-7}
FR 3m	7.9×10^{-5}	4.6×10^{-4}	4.8×10^{-7}	8.9×10^{-7}	---
FR 10m	3.7×10^{-5}	3.9×10^{-5}	2.1×10^{-6}	2.3×10^{-5}	1.3×10^{-6}

Table E:4 – TOC/TN Data for gas mix 4 (10% O_2, 1% CO_2, 89% N_2)				
Reactor or Sample	**TOC (mg/L)**	**TOC S.D. (mg/L)**	**TN (mg/L)**	**TN S.D. (mg/L)**
SAMD	1.596	0.02	3.455	0.05
FR 3m – Live 1	5.416	0.02	3.765	0.03
FR 3m – Live 2	4.897	0.08	3.709	0.06
FR 3m – Killed 1	1470	20.2	3.322	0.05
FR 3m – Killed 2	1437	15.7	3.302	0.09
FR 10m – Live 1	3.98	0.08	2.995	0.05
FR 10m – Live 2	3.968	0.06	3.031	0.01
FR 10m – Killed 1	1359	17.0	3.354	0.07
FR 10m – Killed 2	1406	20.2	3.361	0.06
GB 2m – Live 1	6.679	0.07	4.072	0.19
GB 2m – Live 2	5.476	0.08	3.398	0.02
GB 2m – Killed 1	1432	7.30	3.712	0.01
GB 2m – Killed 2	1429	17.8	3.432	0.04

Table E:5 – ICP-AES Data for Field and Batch Reactor samples.

Sample	Al	Ba	Ca	Cr	Cu	K	Mg	Mn	Na	Si	Sr
					GB 2m						
Field	0.84	0.26	9.7	ND	ND	2.8	5.5	2.1	2	9.1	0.03
Mix 2 – Live	24.0	ND	223	ND	ND	0.5	104	24.0	295	9.6	0.03
Mix 2 – Killed	19.0	ND	218	ND	ND	0.45	102	23.5	48.0	8.0	0.02
Mix 3 – Live	24.5	0.41	225	ND	0.04	2.25	104	23.5	208	11.0	0.04
Mix 3 - Killed	17.5	0.69	223	ND	0.06	2.2	104	24.0	82.5	8.3	0.05
					FR 3m						
Initial	20.3	0.15	60.5	BDL	BDL	3.3	21.5	1.3	16	22.3	1.1
Mix 2 – Live	45.0	BDL	213	0.04	BDL	0.2	97.5	23.0	353	17.0	0.11
Mix 2 – Killed	44.0	BDL	233	0.03	0.03	0.75	108	23.0	183	14.5	0.10
Mix 3 – Live	53.0	0.45	223	0.08	0.06	2.25	103	25.5	255	20.0	0.13
Mix 3 - Killed	44.0	0.34	205	0.04	0.04	2.15	96.0	23.0	130	16.5	0.11
					FR 10m						
Initial	20.5	0.14	59.3	BDL	BDL	3.4	21.3	1.3	16.5	20.5	1.1
Mix 2 – Live	31.5	BDL	225	0.03	BDL	0.6	104	24.0	373	13.0	0.90
Mix 2 – Killed	26.0	BDL	213	BDL	BDL	0.35	99.5	21.0	170	9.55	0.80
Mix 3 – Live	33.0	0.61	235	0.04	0.06	2.3	106	25.0	240	14.0	0.11
Mix 3 - Killed	32.5	0.66	240	0.02	0.12	2.3	113	24.0	120	13.5	0.11

BDL = Below Detection Limit

The following description of methods (corresponding to Figure **5-4) is from the publication by Senko et al. (in press):

Nucleic Acid-Based Bacterial Community Characterization

All samples for nucleic acid-based microbial community analysis were stored at -80 °C until DNA was extracted. Direct extraction of DNA from Fe(III)-rich sediments proved difficult, so Fe(III) was removed from samples with 0.3 M ammonium oxalate (pH 3.0) as described by Nicormat et al. (2006a). Samples were incubated in ammonium oxalate solution for 1 hour at room temperature, centrifuged, the supernatant was decanted, and replaced with fresh ammonium oxalate. Complete removal of Fe(III) (indicated by a lack of orange color in the supernatant) was generally achieved after 6 washes. The remaining pellet (400 – 1000 mg (wet) recovered from 6 g of wet sediment) was then washed three times with TE buffer (10 mM trishydroxymethylaminomethane and 1 mM diaminetetraacetic acid, pH 8.0). Fe(III)-free samples were stored at -80 °C before further processing. DNA was extracted from Fe(III)-free sediments using the MoBio UltraClean Soil DNA extraction kit (MoBio Laboratories, Inc., Carlsbad, CA). Ribosomal intragenic spacer analysis (RISA)-polymerase chain reaction (PCR) was performed as described by Castillo-Gonzalez and Bruns (2005) using bacteria-specific primers based on *Escherichia coli* positions 16S-9266f (5'-AAAGTYAAAKGAATTGACGG-3') and 23S-115r (5'-GGGTTBCCCCATTCGG-3') (Lane, 1991) purchased from Invitrogen Corp. (Carlsbad, CA). PCR mixtures contained 2 µl of a 1:5 dilution of sediment-derived DNA, 5 µl of 10x HotMaster PCR buffer with 25 mM $MgCl_2$ (Eppendorf Corp., Westbury, NY), 1 µl of 10 mM dNTPs, 3 µl (each) of

10 mM primer, 0.5 µl of 50 mg/ml bovine serum albumin, 0.25 µl of 5 u/µl HotMaster Taq polymerase (Eppendorf Corp., city, state), and 35.25 µl of molecular biology grade water. PCR were performed using a 2400 Perkin-Elmer thermocycler with an initial denaturation step for 5 min at 94 °C and 30 cycles of 94 ^{o}C for 0.5 min, 54 ^{o}C for 0.5 min, and 72 ^{o}C for 1 min, followed by a final extension step at 72 ^{o}C for 7 min. RISA-PCR products were separated based on DNA fragment size by agarose gel electrophoresis (2% agarose in Tris-acetate-EDTA buffer (0.4 M tris-hydroxymethylaminomethane (Tris), 0.2 M acetic acid, and 0.01 M ethylenediamine tetraacetic acid (EDTA)), and 5 µg/ml ethidium bromide) at 85 V for 1.5 h. Ethidium bromide-stained DNA bands were visualized under UV illumination and photographed with EpiChemi II equipment (UVP Inc., Upland, CA).

To obtain 16S rDNA sequences from bands in the RISA gel, individual bands were excised from the gel, suspended in 50 µl of molecular biology grade water and macerated. The 16S rDNA portion of the RISA amplicons was amplified in 50 µl reaction mixtures as described above using bacteria-specific primers based on *E. coli* positions 16S-926f (5'-AAAGTYAAAKGAATTGACGG-3') and 16S-1492r (5'-TACGGYTACCTTGTTACGACTT-3'). Fresh PCR products were directly cloned into TOPO-TA vector (Invitrogen) following the manufacturer's instructions. Six PCR insert-containing clones were obtained per RISA band, grown to late log phase in Luria-Bertani broth (Atlas, 2004) that was supplemented with 75 µg ampicillin/ml, and stored in 12 % glycerol at -80 ^{o}C before further processing. PCR insert-containing TOPO-TA vectors were prepared for sequencing using TempliPhi rolling circle amplification (GE Healthcare Bio-Sciences Corp., Piscataway, NJ) in 96 well plate formats according to the

manufacturer's instructions. DNA sequencing was performed at The Pennsylvania State University's DNA sequencing facility using an ABI Hitachi 3730XL DNA Analyzer.

For phylogenetic placement of 16S rDNA sequences, they were initially checked using Basic Local Alignment Search Tool (BLAST) (Altschul et al., 1997). Sequences were checked for chimeras using the Ribosomal Database Project II's chimera detection function (Cole et al., 2003). Sequences with more than 90 % similarity were considered to be the same operational taxonomic unit (OTU). OTUs were assigned phylum-level classifications using the Ribosomal Database Project II's classifier function (Wang et al., 2007). Sequences obtained in this work and those obtained from GenBank were downloaded into a Geneious 3.0 software environment (Drummond et al., 2007). Sequences were aligned within the Geneious environment using the ClustalW algorithm (Thompson et al., 1994), and evolutionary distance trees (neighbor joining algorithm with Jukes-Cantor corrections) were produced using Geneious 3.0. We used the online application UniFrac (http://bmf2.colorado.edu/unifrac/; Lozupone et al., 2006) to assess evolutionary differences and similarities among the discrete environments within the GB and FR systems. Phyum-level evolutionary distance trees were produced as described above using 16S rDNA sequences from the GB and FR systems with *Aquifex pyrophilus* (GenBank accession number M83548) as an outgroup. This tree was annotated to indicate the environmental origin of each 16S rDNA sequence, and we produced descriptions of the GB or FR environments from which the sequences were obtained. The evolutionary distance tree and site descriptions were imported into the UniFrac environment and analyzed by principal coordinates analysis (PCoA) using the weighted UniFrac metric (Lozupone et al., 2007). To establish the phylogenetic affiliation of GB

and FR-derived 16S rDNA sequences that were represented by more than one OTU in our clone libraries, phylum-level evolutionary distance trees were produced using sequences obtained in this study and those obtained from GenBank as described above.